EFFECT OF RING SIZE ON BENZIMIDAZOLE ACCEPTOR UNIT ON THE PROPERTIES OF DONOR-ACCEPTOR-DONOR TYPE MONOMERS AND THEIR ELECTROCHROMIC POLYMERS

A THESIS SUBMITTED TO
THE GRADUATE SCHOOL OF NATURAL AND APPLIED SCIENCES
OF
MIDDLE EAST TECHNICAL UNIVERSITY

BY

EMİNE GÜL CANSU ERGÜN

IN PARTIAL FULLFILLMENT OF THE REQUIREMENTS
FOR
THE DEGREE OF DOCTOR OF PHILISOPHY
IN
POLYMER SCIENCE AND TECHNOLOGY

AUGUST 2015

Approval of the thesis:

EFFECT OF RING SIZE ON BENZIMIDAZOLE ACCEPTOR UNIT ON THE PROPERTIES OF DONOR-ACCEPTOR-DONOR TYPE MONOMERS AND THEIR ELECTROCHROMIC POLYMERS

submitted by **EMİNE GÜL CANSU ERGÜN** in partial fulfillment of the requirements for the degree of **Doctor of Philosophy in Polymer Science and Technology Department, Middle East Technical University** by,

Prof. Dr. Gülbin Dural Ünver
Dean, Graduate School of **Natural and Applied Sciences** _____

Prof. Dr. Necati Özkan
Head of Department, **Polymer Science and Technology** _____

Prof. Dr. Ahmet M. Önal
Supervisor, **Chemistry Dept., METU** _____

Prof. Dr. Atilla Cihaner
Co-Supervisor, **Chem. Eng. and Appl. Chem. Dept., Atılım University** _____

Examining Committee Members:

Assoc. Prof. Dr. Akın Akdağ _____
Chemistry Dept., METU

Prof. Dr. Ahmet M. Önal _____
Chemistry Dept., METU

Asst. Prof. Dr. Seha Tirkeş _____
Chem. Eng. and Appl. Chem. Dept., Atılım Univ.

Asst. Prof. Dr. Murat Kaya _____
Chem. Eng. and Appl. Chem. Dept., Atılım Univ.

Asst. Prof. Dr. İrem Erel Göktepe _____
Chemistry Dept., METU

Date: 21.08.2015

I hereby declare that all information in this document has been obtained and presented in accordance with academic rules and ethical conduct. I also declare that, as required by these rules and conduct, I have fully cited and referenced all material and results that are not original to this work.

Name, Last name : Emine Gül Cansu Ergün

Signature :

ABSTRACT

EFFECT OF RING SIZE ON BENZIMIDAZOLE ACCEPTOR UNIT ON THE PROPERTIES OF DONOR-ACCEPTOR-DONOR TYPE MONOMERS AND THEIR ELECTROCHROMIC POLYMERS

Cansu Ergün, Emine Gül

Ph. D., Department of Polymer Science and Technology

Supervisor: Prof. Dr. Ahmet M. Önal
Co-Supervisor: Prof. Dr. Atilla Cihaner

August 2015, 138 pages

In this thesis, a series of novel benzimidazole-type acceptor units were designed and synthesized. The target acceptors were benzimidazoles including cyclohexane, cycloheptane and cyclooctane rings. Each acceptor group was coupled with 3,4-ethylenedioxythiophene (EDOT) and dihexyl substituted 3,4-propylenedioxythiophene (PRODOT(C6)) donor groups separately and six donor-acceptor-donor (DAD) type monomers were obtained. The main aim of this thesis is to comperatively elucidate the electrochemical and optical properties of these six DAD type conjugated monomers and their polymers when the ring size in the selected acceptor unit is systematically changed.

In EDOT containing monomers, the monomer including cyclohexane ring (E6E) exhibited the strongest intramolecular charge transfer and the most red shifted absorption band (539 nm). The polymer films of the EDOT containing monomers showed similar optical absorption and the band gap values around 1.18 eV. Switching times of the polymers were quite fast and the fastest one was found to be for the polymer including cyclooctane ring (P(E8E)) (0.5 s). Coloration efficiencies were calculated as quite high for all polymers but the highest for P(E8E) (316 C/cm^2). All the polymer films exhibited ambipolar doping (both anodically and

cathodically dopable) properties (green in the neutral state, gray in the oxidized state and brick-red in the reduced state).

In PRODOT containing monomers, absorption maxima were found to be almost the same; 310 / 520 nm. The strongest intramolecular charge transfer were observed in the monomer including cyclooctane ring (P8P). For the polymer films, the lowest band gap value was obtained for the polymer including cylcohexane ring (P(P6P)) (1.29 eV). Switching times of the polymers were quite fast and the fastest response was found in P(P8P) (0.5 s). The coloration efficiencies of all the polymers were calculated as quite high but the highest for P(P8P) (572 cm^2/C at its longer wavelength absorption). All the polymer films exhibited ambipolar doping properties (green in the neutral state, gray in the oxidized state and brick-red in the reduced state).

After all these studies were finished, the monomers and polymers have been compared to each other in EDOT group and the PRODOT(C6) group, separately. At the end, one of the polymers from each two groups were selected to construct an electrochromic device with poly(3,4-ethylenedioxythiophene) (PEDOT). The device properties were revealed in terms of its switching ability, and color contrast ratio. Devices in both groups showed similar optical properties but the device constructed with PRODOT containing polymer exhibited higher coloration efficiency (189 C/cm^2 at its longer wavelength absorption).

Keywords: Conductive Polymers, Electron Donor-Acceptor Systems, Benzimidazoles, Electrochemical Properties, Optical Properties, Electrochromic Device

ÖZ

BENZİMİDAZOL ALICI BİRİM ÜZERİNDEKİ HALKA BOYUTUNUN ELEKTRON VERİCİ-ALICI-VERİCİ TİP MONOMERLER VE ONLARIN ELEKTROKROMİK POLİMERLERİ ÜZERİNE ETKİSİ

Cansu Ergün, Emine Gül

Doktora, Polimer Bilim ve Teknolojisi Bölümü

Tez Yöneticisi: Prof. Dr. Ahmet M. Önal
Eş Danışman: Prof. Dr. Atilla Cihaner

Ağustos 2015, 138 sayfa

Bu tezde, bir seri özgün benzimidazol türü elektron alıcı birim tasarlanmış ve sentezlenmiştir. Hedef elektron alıcı birimler; siklohekzan, sikloheptan ve siklooktan halkası içeren benzimidazollerdir. Her bir elektron alıcı birim, 3,4-etilendiyoksitiyofen (EDOT) ve dihekzil sübstitüyeli 3,4-propilendiyoksitiyofen (PRODOT(C6)) elektron verici grupları ile ayrı ayrı eşleştirilerek altı adet verici-alıcı verici (VAV) türünde monomer elde edilmiştir. Bu tezin ana amacı, seçilen elektron alıcı birim içerisinde bulunan halka boyutu sistematik olarak değiştiğinde, sentezlenen altı adet konjuge monomer ve onların polimerlerinin elektrokimyasal ve optiksel özelliklerinin değişiminin karşılaştırmalı olarak belirlenmesidir.

EDOT içeren monomerlerde, en güçlü molekül-içi elektron transferi ve kırmızı bölgeye en çok kayan optik soğurma bandı siklohekzan halkası içeren monomerde (E6E) (539 nm) gözlenmiştir. EDOT içeren monomerlerin polimer filmleri, benzer optik davranım ve bant aralığı değerleri göstermiştir (yaklaşık 1.18 eV). Polimerlerin yükseltgenme-indirgenme zamanları oldukça hızlı bulunmuş, en hızlı olan ise siklooktan halkası içeren polimer için P(E8E) rapor edilmiştir (0.5 s). Tüm polimerlerdeki renklenme verimliliği oldukça yüksek bulunmakla birlikte, en yüksek değer P(E8E) polimerine aittir. Tüm polimer filmler, ambipolar doplanma (anodik ve

katodik bölgede doplanabilme) özelliği göstermiştir (nötr halde yeşil, yükseltgenmiş halde gri ve indirgenmiş halde tuğla kırmızısı).

PRODOT içeren monomerlerde, maksimum soğurma bant değerleri neredeyse aynı bulunmuştur; 310 / 520 nm. En güçlü molekül-içi elektron transferi siklooktan halkası içeren monomerde (P8P) gözlenmiştir. Polimer filmleri için, en düşük bant aralığı değeri siklohekzan halkası içeren polimer filmine (P(P6P)) aittir (1.29 eV). Polimerlerin yükseltgenme-indirgenme zamanları oldukça hızlı bulunmuş, en hızlı olan ise siklooktan halkası içeren polimer için (P(P8P)) (0.5 s) rapor edilmiştir. Tüm polimerlerdeki renklenme verimliliği oldukça yüksek bulunmakla birlikte, en yüksek değer P(P8P) polimerine aittir (572 cm^2/C, daha uzun dalga boyundaki soğurma bandında). Tüm polimer filmler ambipolar doplanma davranışı göstermiştir (nötr halde yeşil, yükseltgenmiş halde gri ve indirgenmiş halde tuğla kırmızısı).

Tüm bu çalışmalardan sonra, EDOT grubundaki ve PRODOT(C6) grubundaki monomer ve polimerler ayrı ayrı birbirleri ile karşılaştırılmıştır. Son olarak, her iki gruptaki polimerlerden bir tanesi poli(3,4-etilendiyoksitiyofen) (PEDOT) ile elektrokromik cihaz yapımında kullanılmıştır. Cihaz özellikleri, yükseltgenme-indirgenme değişimi yeteneği, ve renk zıtlık oranı cinsinden açığa çıkarılmıştır. Her iki gruptaki cihazlar benzer optik özellikler göstermekle birlikte, PRODOT grubu içeren polimer ile yapılan cihazda renklenme verimliliği daha yüksek bulunmuştur 189 C/cm^2, daha uzun dalga boyundaki soğurma bandında).

Anahtar Kelimeler: İletken Polimerler, Elektron Alıcı-Verici Sistemler, Benzimidazoller, Elektrokimyasal Özellikler, Optiksel Özellikler, Elektrokromik Cihaz

ACKNOWLEDGMENTS

I express my gratitude to my supervisor Prof. Dr. Ahmet M. Önal for her guidance and excellent encauraging helps during this work. I also would like to thank him for not only his support throughout my PhD period but also treating me like a colleague and part of his family.

I would like to thank to my co-supervisor Prof. Dr. Atilla Cihaner for his academic guidance.

I wish to thank to my moms and dads (Hilmiye Cansu, Semiha Ergün, Şükrü Cansu, Ünal Ergün) for accepting my studentship after all these years and for their endless believes and supports.

My deepest thanks are to my husband Prof. Dr. İhsan Ergün for encauraging me and for making the life easy-going for us. His huge academic experience helped me to find my way at work. His big heart and patience helped me to find my way at home. I could not do anything without him.

Finally, my little princess Cansu; I send my smily thanks to you for just being in our life. In the beginning of this journey, you were just one year old, and now, you are eight. I wish a long, happy and healthy life for you my precious…

TABLE OF CONTENTS

LIST OF FIGURES

LIST OF SCHEMES

LIST OF TABLES

ABBREVIATIONS

ACN	Acetonitrile
Ar	Argon
BIm	Benzimidazole
BOx	Benzoxadiazole
BSe	Benzoselenadiazole
BTD	Benzothiadiazole
BTZ	Benzotriazole
C	Carbon
CB	Conducting band
$CDCl_3$	Deuterochloroform
CE	Coloration efficiency
CE	Counter electrode
CIE	Commission Internationale de I'Eclairge
CMYK	Cyan-magenta-yellow-key black
CP	Conducting polymer
CV	Cyclic voltammetry
DA	Donor-acceptor
DAD	Donor-acceptor-donor
DCM	Dichloromethane
ECD	Electrochromic device
EDOT	3,4-Ethylenedioxythiophene
E_g	Band gap
EtOH	Ethyl alcohol
FET	Field effect transistor
Ge	Germanium
H	Hydrogen
HOMO	Highest occupied molecular orbital
HRMS	High-resolution mass spectrometry
ICT	Intramolecular charge transfer

ITO	Indium tin oxide
LED	Light emitting diode
LUMO	Lowest unoccupied molecular orbital
N	Nitrogen
Na	Sodium
n-BuLi	n-butyl lithium
NMR	Nuclear Magnetic Resonance
OLED	Organic light emitting diode
OPV	Organic photovoltaic
PC	Propylene carbonate
PCE	Power conversion efficiency
Pd	Palladium
PEDOT	Poly(2,3-dihydrothieno[3,4-b][1,4]dioxine)
PMMA	Poly(methyl metacrylate)
PRODOT	3,4-propylenedioxythiophene
PRODOT(C6)	Dihexyl substituted 3,4-propylenedioxythiophene
Pt	Platinum
P3HT	Poly(3-hexylthiophene)
RE	Reference electrode
RGB	Red-green-blue
S	Sulfur
SC	Solar cell
Se	Selenium
Si	Silicon
Te	Tellurium
THF	Tetrahydrofuran
TLC	Thin layer chromatography
TMS	Tetramethylsilane
VB	Valence band
WE	Working electrode

CHAPTER 1

INTRODUCTION

1.1. Conducting Polymers

After the discovery of macromolecules in early 1930's, the term "plastics" became the most popular materials worldwide since they are lighter than wood, much more resistant to corrosives than metals, not brittle like ceramics and they are cheaper as well. When all the features are taken into account, it can be said that the discovery of macromolecules has opened up a new gate into a new age called the polymer age in the world of industry [1,2].

Beyond those superior properties, an exclusive feature of some polymers was discovered in 1977 by Shirakawa, Heeger and McDiarmid that they could also be conductive [3,4]. The conducting polymers (CPs) have been the most promising materials over the past decades [5,6]. They became competitive materials to inorganic semi-conductors for numerous reasons. First of all, they are low cost and processable materials. The second reason is that they are lightweight. The third advantage of organic-conductives is that they can be applied on flexible surfaces unlike their inorganic counterparts. Besides, their mechanical, electrical and optical properties can be improved by modifying their structures [7-16].

Because of these advantages, CPs fastly started to be developed and to be replaced to inorganics in technological areas such as smart windows [17,18], solar cells [19-46], light emitting diodes (LEDs) [47-56], television and mobile phone screens [57-60], field effect transistors (FETs) [61-66], camouflage materials [67-69], biosensors [70-73], etc.

It is obviously clear that the discovery of CPs has opened up another brand new gate inside the polymer age in the word of technology and they have already taken into attention by scientists who have been continuously developing these materials for having them better properties.

1.2. Concept of Band Theory

Electrical conductivity is a measure of material's ability to conduct electrical current via electron flow. This property of materials depends mainly on the energy difference between the valance band (Highest Occupied Molecular Orbital; HOMO) and conduction band (Lowest Unoccupied Molecular Orbital; LUMO) which is known as the band gap energy (E_g). High electrical conductivity of metals is due to either partially filled valance band or lack of energy difference between valence and conduction bands, which allows electron movement. In semi-conductors, on the other hand, it requires a little push to fill the conduction band because of the energy barrier which is less than 3.0 eV [74]. For insulators, the band gap is so large (higher than 3.0 eV) that makes those materials non-conductors (Figure 1.1).

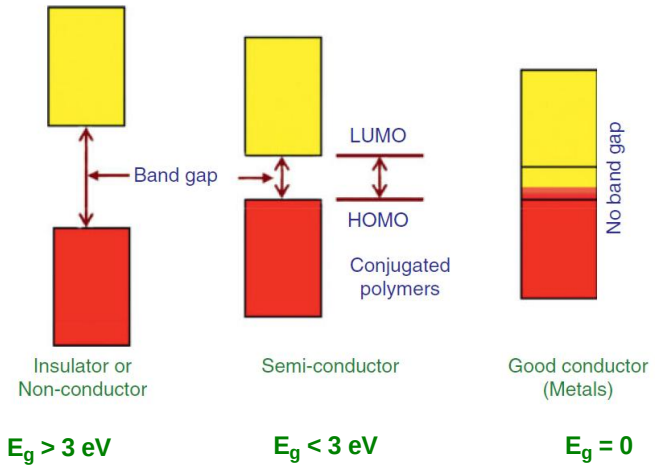

Figure 1.1. Simple band gap illustration for insulators, semi-conductors and conductors [75].

Chemical structures of the CPs are different from their ordinary plastic counterparts. They have alternating single-double bonds (conjugation) in the one-dimensional chain due to overlapping of p_z-orbitals. This π-conjugation imparts intrinsic conductivity to the polymer. The phenomena is similar to semi-conductors; both have low conductivities. However, this can be increased by creating defects (holes or extra electrons) on the polymer chain which is called as doping.

1.2.1. Doping

The pioneers of the area of conducting polymers are Shirakawa, Heeger and McDiarmid who firstly showed that conductivity of polyacetylene can be increased by 10^9 order of magnitude than undoped polyacetylene [76]. That was an important discovery and the Nobel Prize was awarded to this study in 2000. They doped trans-polyacetylene with iodine vapor and obtained a conductivity of 10^3 S/cm in the resulting polymer [77]. This was a remarkable value when compared with the conductivities of well-known metals like silver, iron or copper with conductivities of about 10^6 S/cm. On the other hand, the conductivity value for a typical insulator is 10^{-10} S/cm.

As it is mentioned before, alternating single and double bonds in the backbone are the major feature of CPs which is called as π-conjugation. Every single bond is strongly localized sigma bond, on the other hand, every double bond is weaker partially delocalized π- bond.

Doping is a process of charge injection or ejection. The dopants give extra electrons or make some holes on the chain which disturbs the structure and allows electron movement. CPs show semi-conductor-like band structures and their conductivities can be increased by doping process. If doping is made by injecting electrons into the material, it is called n-type doping. If the doping is occuring by removing electrons from the material, it is called p-type doping.

The basic optical transition of CPs lies between bonding and antibonding molecular orbitals (π-π* transition band). When an external energy is applied to the polymer structure, an exciton is created. Exciton can be defined as a new state of an electron and hole. For trans-polyacetylene, excitation results with the formation of a new quasi-particle (soliton) and this particle has an electronic state in the middle of the band gap. For aromatic structures, excitation results with different chain distortions (nondegenerated ground state) and excitation results with the formation of quasi-particle called polaron (Figure 1.2). A polaron can be defined as the moving electron (or hole) on defected structure [78].

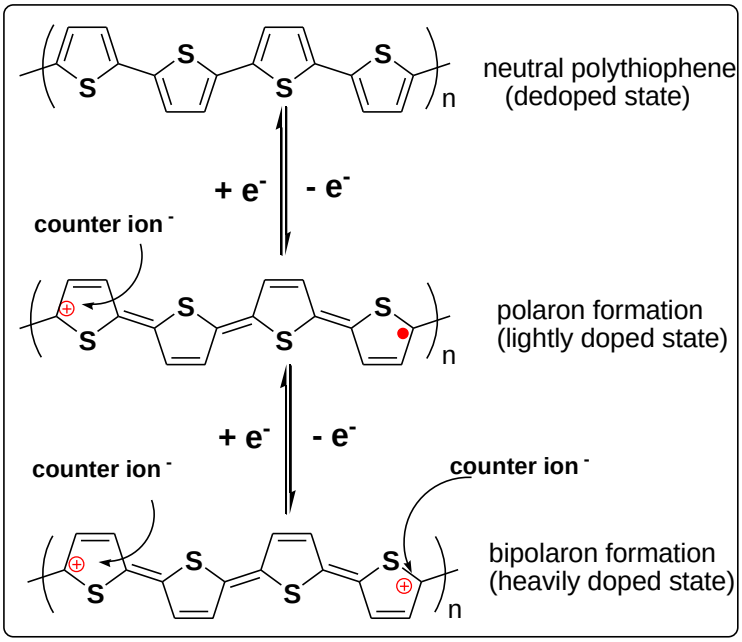

Figure 1.2. Illustration of polaron and bipolaron formation on polythiophene structure upon doping.

When a CP is oxidized, electrons are removed from the system resulting in the creation of holes (radical cation or polaron) and new energy levels are formed

between the valance and conduction bands. This is due to newly formed charge carriers. After further oxidation, two charge carriers are formed (radical dication or bipolaron) and energy levels come more closer to the mid energy gap [79].

Same process occurs when a CP is reduced. Addition of electrons results in the formation of negative polarons (radical anions) and bipolarons (radical dianions). In p-doping and n-doping processes, positive charges are counterbalanced with anions and negative charges are counterbalanced with cations, respectively. Doping process can be achieved reversibly in CPs, which is the major difference between CPs and inorganic semi-conductors [8], and it is possible to obtain doped-dedoped states either by chemical and electrochemical doping.

Chemical dopants play a convenient role in making the wide range of polymers conductive. Oxidizing or reducing compounds are used in chemical doping. Common p-type dopants (which are generally electron attracting substances or compounds) are Br_2, I_2, AsF_5, $SbCl_5$, PF_3, SF_6, $FeCl_3$, etc. The well-known n-type dopants (they are electron donating substances or compounds) are NH_3, N_2H_4, molten potassium, etc. In chemical doping, doping process is fixed by introducing the doping agent into the polymer structure. When polymer is p-doped, it is needed to introduce n-type dopant for dedoping process (reobtain the polymer in neutral state) or vice versa.

The polymers can also be doped (oxidized or reduced) easily by applying a potential with a direct current source (electrochemical doping). This method is widely used in doping CPs becasuse of variety uses of CPs in electronic applications. Electrochemically doping process has some advantages over chemical doping. First of all, amount of current passing through the system can be monitored and doping level can be controlled. Secondly, p- or n-type doping can be applied rapidly without any additional chemicals. Both in chemical and electrochemical doping, counter ions are needed to stabilize the charge on the polymer backbone. This may cause some structural distortions on the material and may affect conductivity.

There are some other types of doping methods which are also used in different applications. One of them is “photo-doping” which is defined as the irradiation of a conjugated polymer with a light beam of energy greater than its band gap energy. This method is used in organic photovoltaic (OPV) applications [33, 35]. Another type of doping is “charge-injection doping” where charge carriers are injected into the band gap by applying a suitable potential on a multilayer structure like metal-insulator-polymer. This method is used in FETs or LEDs [49]. Both in photo-doping and charge-injection doping, there is no counter ion generation so the structural distortion is minimized.

1.3. Synthesis of Conducting Polymers

1.3.1. Chemical Polymerization

Oxidative polymerization technique is suitable for chemical polymerization of unsubstituted monomers. For this purpose, suitable oxidizing agents such as ammonium peroxydisulfate ($(NH_4)_2S_2O_8$), ferric chloride ($FeCl_3$), potassium permanganate ($KMnO_4$) or hydrogen peroxide (H_2O_2) are commonly used [80].

However, if the monomer has any substitution like alkyl chains as in the case of 3-hexylthiophene, the planarity concept must be considered because oxidative technique results in regioirregular polymer. In the aim of synthesizing the planar or regioregular polymer chains, some specific reactions were developed. The metal catalysts are used in these reactions [81].

In the synthesis of electron donor-acceptor type polymers or copolymers, the various organometallic cross-coupling reactions are used depending on the types of functionalizing groups on the monomers. One of them is the Stille coupling reaction which is most widely used in chemical polymerization. In Stille coupling reaction, one of the monomer must be halogenated (mostly brominated) from both sides and

the other must be stannylated on both sides. Then, these two units come together alternatingly in the presence of a suitable catalyst, usually palladium compounds. The other well-known coupling reactions are Sonogashira Coupling, Suzuki Miyaura coupling, Kharash coupling, Negishi coupling, Himaya coupling and Kumuda coupling reactions.

1.3.2. Electrochemical Polymerization

CPs can be obtained as a thin film on a conducting substrate such as indium tin oxide (ITO) glass substrate or other suitable working electrode (WE) surfaces. The monomer is dissolved in a proper solvent including supporting electrolyte and electrochemicaly polymerized by applying external potential. There are various advantages of this method. One of them is small amount of monomer is enough to obtain polymer film. Another benefit is the ease of process which yields the required CP in relatively short time period. Furthermore, the polymer film thickness on the electrode surface can be easily controlled. However, the large scale production of CPs by this method is one of the main practical disadvantage.

Working principle of electrochemical polymerization starts with the oxidation of the monomer into a radical cation. This radical cation either attacks to a neutral monomer [82] or may couple with another radical cation [83]. Both of the routes yield an intermediate that produces a dimer unit after the loss of two protons. The repeating couplings go on until oligomeric particles become insoluble and precipitate onto the electrode surface.

The electropolymerization is generally performed by potentiostatic (constant potential), galvanostatic (constant current) or potentiodynamic (cyclic voltammetry) methods.

In electrochemical studies, it is important to choose a suitable electrolyte solution which includes the electrolyte and the solvent. To avoid any interference due to

oxidation of electrolytic solution, electrochemically inert solvent and electrolyte should be choosen for this purpose. Generally, high dielectric constant solvents such as acetonitrile (ACN), propylene carbonate (PC) and dichloromethane (DCM) are prefered since they allow high ionic conductivity for the electrolytic solution. The mostly used solvent is acetonitrile because of its wide potential window (i.e, potential window of acetonitrile extends from -1.8 V to +2.8 V in tetrabutyl ammonium tetrafluoroborate vs saturated calomel electrode) [84].

The examples of the well-known compounds used for supporting electrolyte can be given as in the following: tetrabutylammonium hexafluorophosphate ($N(Bu)_4PF_6$), tetrabutylammonium tetrafluoroborate ($N(Bu)_4BF_4$), lithium perchlorate ($LiClO_4$) and tetrabutylammonium perchlorate ($N(Bu)_4ClO_4$).

1.4. Donor-Acceptor Approach in Conjugated Polymers

After the discovery of conducting polyacetylene, molecular developments were accelerated in this field. The major aim was to obtain air-stable and processable materials due to air-instability and insolubility of polyacetylene. After these problems were overcome in time, conjugated systems were started to modify in many ways for various reasons:

i. to decrease the band gap,
ii. to obtain different colors,
iii. to get more chemically, optically or thermally stable materials for the desired applications.

In the scope of these aims, various conjugated systems have been designed and synthesized. During these developments, it was realized that if an acceptor molecule combines with a donor one, the resulting conjugated system reveals better properties in terms of reducing the band gap [85,86]. The studies about conjugated systems were focused on this approach since last decade. Hybridization of molecular orbitals

results in the narrower band gap as compared to their original counterparts (Figure 1.3). Also, by modifying the molecular structures, not only the band gap value can be altered but also solubility, stability and electrochromic properties can be enhanced. Since those properties are under the same roof, these systems are very popular in todays studies. The corresponding sytsems are called as "Donor-Acceptor-Donor" (DAD) systems.

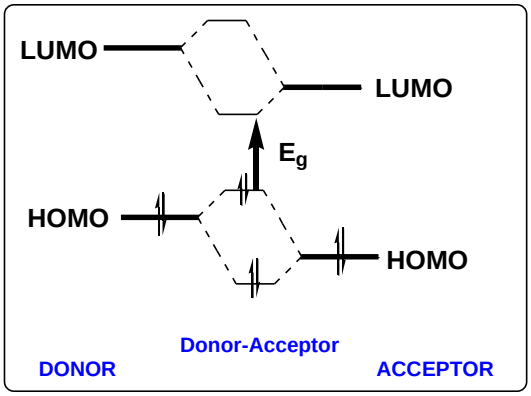

Figure 1.3. Illustration of resulting lower band gap energy for donor-acceptor type conjugated systems.

As shown in Figure 1.4, DAD systems allow to tune many properties of the resulting polymers. The difference between electron richness of the donor molecule and electron deficieny in the acceptor molecule determines the magnitude of the band gap. Also, it allows multiple redox states in low potentials; bringing the multicolor property with the ability of p- and n-type doping. Furthermore, solubility can be achieved via alkyl substituents [87,88]. Thus, DAD systems can be arranged as desired according to the application area. DAD type conjugated systems are desirable in electronic device applications such as electrochromic devices (ECDs), LEDs, SCs, FETs.

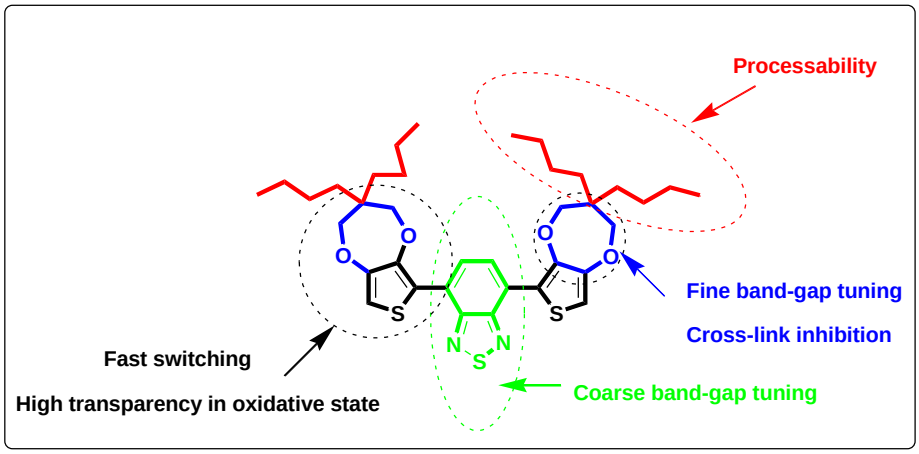

Figure 1.4. Tunable units on DAD type conjugated system

1.4.1. Electrochromism

Electrochromic property can be defined as the ability of changing color with an applied potential. Upon oxidation or reduction, electronic absorption spectra of the polymer film change due to the formation of intermediate states. Conjugated polymers have electrochromic property which allows them to be used in various electronic applications such as smart windows, electrochromic devices, car rear views [89], displays, light emitting diodes, etc.

For an effective electrochromic polymer, the following parameters must be achieved:

i. Redox potential window should be small. In other words, the polymer should be oxidized at low potentials (especially for the applications of OSCs or OLEDs).
ii. The optical absorption range should be broad (especially for OSCs in order to harvest more light).
iii. The band gap energy level (E_g) should be low (lower band gap polymers (< 1.8 eV) are suitable for OSC applications).
iv. The color switching ability should be fast (below seconds) and stable (fast response times are desired for smart windows).

v. The electrochromic contrast (transmittance difference between neutral and oxidized states) and the coloration efficiency (optical density property) should be high [90].

The new generation CPs have numerous advantages when they are compared to their inorganic counterparts such as tungsten oxide (WO_3). Conjugated polymers are low cost materials and can be applied on flexible and large surfaces. Also, they have high optical contrast ratio and they can exhibit multicolor properties. The electrochromic switching times of conjugated polymers are reversible and quite fast. With having all these advantages, design and synthesis of new electrochromic polymers have been taking attention during the last three decades. The studies are mainly focused on the design and synthesis of conjugated systems which can complete the scale of RGB (red-green-blue) and CMYK (cyan-magenta-yellow-key black) color systems for the availability in display applications.

Reynold's group reported the red and different hues of blue with the design and synthesis of corresponding conjugated polymers [91,92]. Basicly, poly(ethylenedioxythiophene)s (PEDOT) possesed the deep blue color in its neutral state and transmissive blue in its oxidized state. Poly(3-hexylthiophene)s (P3HT)s exhibited red color in its neutral form. Numerous polymer design and synthesis gave different colors and hues of a color.

In the case of green color, absorption spectrum of the polymer must have two peaks below 500 nm and beyond 600 nm in its neutral state. The pioneering study about the synthesis of neutrally green polymer was reported by Wudl et al. in 2004 (Scheme 1.1-a). The corresponding electrochromic polymer was in donor-acceptor-donor (DAD) pattern [93,94].

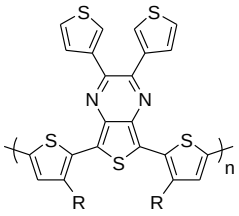

(a) (R = H, C_8H_{17})

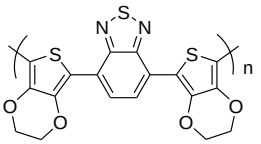

(b)

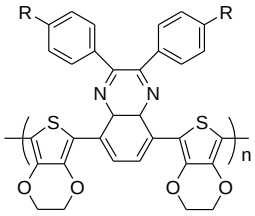

(c) (R=t-butyl, H)

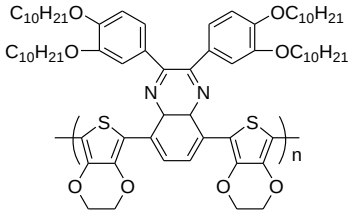

(d)

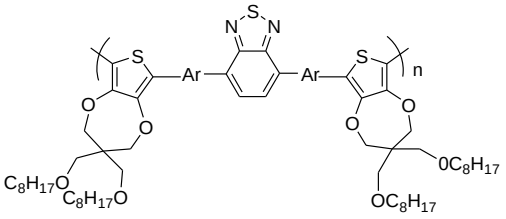

(e) (Ar= thiophene, EDOT)

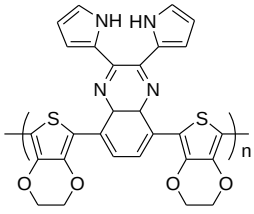

(f)

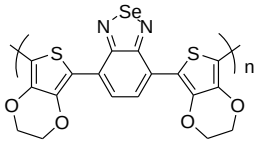

(g)

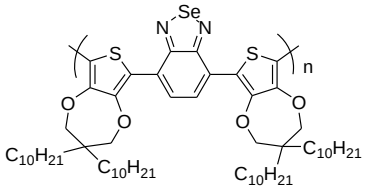

(h)

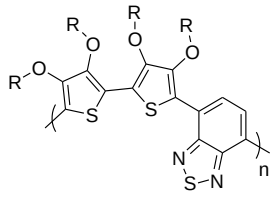

(i) (R=2-ethylhexyl)

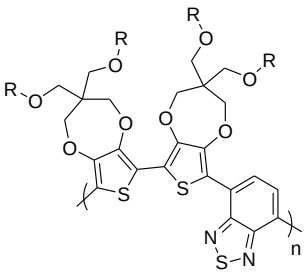

(j) (R=2-ethylhexyl, octyl)

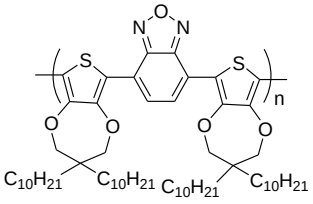

(k)

Scheme 1.1. Some electrochromic polymer structures in the literature.

Toppare's group (Scheme 1.1-b-c-d) [95-99], Reynold's group (Scheme 1.1-e) [100] and Cihaner's group (Scheme 1.1-f-g-h) [101-103] designed and synthesized other neutrally green DAD type conjugated polymers. The corresponding polymers were transparent in the oxidized state.

When it comes to CMYK color series, neutrally cyan color was achieved by Reynold's group in 2009 [104]. A series of alternating conjugated DA polymers containing 3,4-dioxythiophenes, 2,1,3-benzothiadiazole, and unsaturated spacers (either ethynylene or *trans*-ethylene) were obtained chemically and spray coated on ITO-glass in toluene for investigating the electro-optical features (Scheme 1.1-i-j). The different hues of cyan color were achieved by little modifications in the structure. Önal's group synthesized a DAD type electrochromic polymer in 2012, which revealed cyan color in its neutral state [105] (Scheme 1.1-k). The polymer was obtained via electrochemically and possesed good solubility and electro-optical stability. Oxidized color of the polymer was transparent.

The neutral state black colored polymer should absorb in the whole visible region and this was achieved by several groups [106-108].

As it is seen from the studies summarized above, DAD type conjugated polymers are promising candidates for advanced electrochromic applications.

1.5. Donor Materials

The early studies in 1980's was focused on the polyheterocycles such as polythiophene, polypyrrole, poly(phenylacetylene), poly(isothionaphthaline), polyfuran, polyaniline, poly(paraphenylene) and their derivatives [5,7,8]. These polymers possesed good conductivity but there were still some more problems to be resolved. For example, they all suffer from lack of solubility in common solvents. Furthermore, polythiophene and its close analogues may also polymerize via 3,4 carbon atoms leading to irregular structures.

These monomers also susceptible to oxygen attacks during polymerization. In order to bring a solution, alkyl chains were used as a substituent not only to close the oxygen susceptible carbon positions but also to enhance the solubilty of such polymers [106]. However, alkyl substitution causes a decrease in the planarity and also in regioregularity. Regio-irregularity increases the band gap because of decrease in effective conjugation length. Regioregular patterns can be obtained via special steps of reactions which need some special conditions and catalysts [109-112].

In 1980's, Bayer scientists in Germany developed a new polythiophene derivative, poly(3,4-ethylenedioxythiophene) (EDOT) in order to close the carbon atoms on 3rd and 4th position with alkoxy bridge [113]. Its polymer, PEDOT, possesed better conductivity and lower oxidation potential due to the presence of electron donating oxygen atoms. The obtained polymer film color was deep blue in the neutral state and very transparent blue in its oxidized form. However, PEDOT was still suffering from lack of solubility. In order to impart solubility, the ethylenedioxy bridge was replaced by alkyl chain substituted propylenedioxy bridge by Reynolds and his coworkers [114-120]. The first example of soluble PPRODOT derivative, PPRODOT-C4 was found to be soluble in common organic solvents and also was air-stable both in its neutral and oxidized states [121].

Then various PPRODOT derivatives bearing different alkyl sizes were synthesized and it was observed that solubity increases with increasing chain length [122].

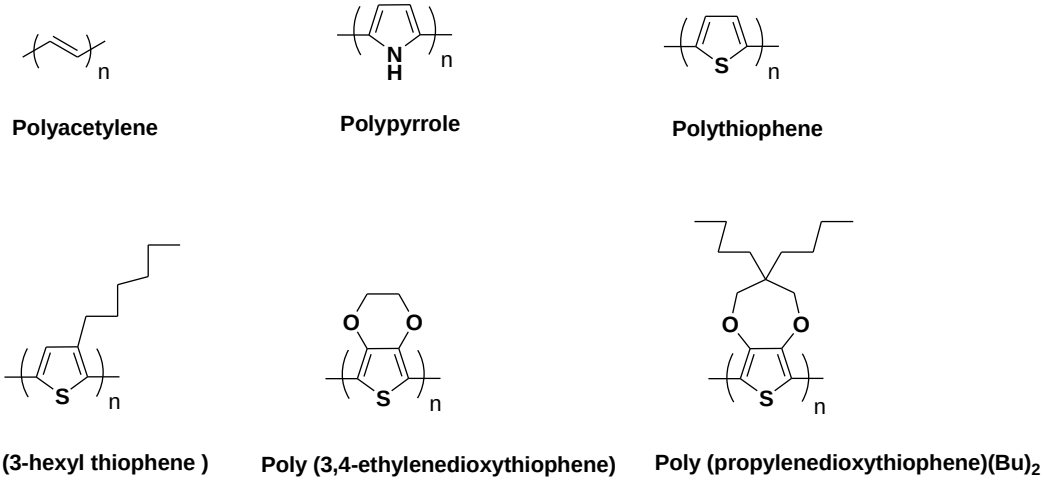

Scheme 1.2. Development of the conjugated polymers from polyacetylene to poly(propylenedioxythiophene).

1.6. Acceptor Materials

Some of the conjugated backbones have electron defficiency in their structures. These materials are used as the electron acceptor groups in DAD approach. The most common acceptors are benzazole derivatives. Benzothiadiazole (**BTD**), benzotriazole (**BTZ**), benzoselenadiazole (**BSe**), benzoxadiazole (**BOx**) and benzimidazoles (**BIm**) are the most commonly used acceptors in the applications of conducting polymers.

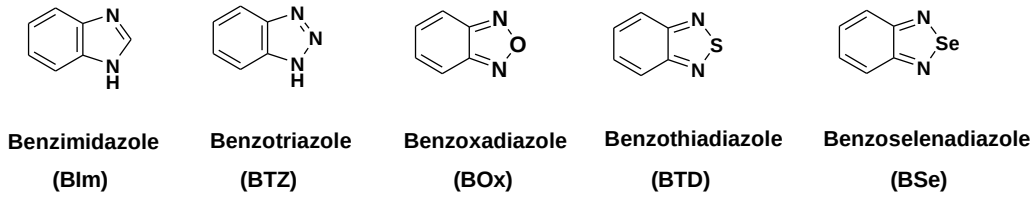

Scheme 1.3. The well-known acceptor groups used in DAD systems.

Studies on DAD type conjugated polymers focused on both donor effect and acceptor effect in the resulting polymer. Benzazole derivatives were widely investigated in terms of acceptor unit effect in the literature [123-126].

Instead of sulfur atom in the heterocyclic structure of acceptor unit, other benzazole derivates bearing different chalcogen atoms (i.e. Se, Si, Ge and Te) were also investigated to elucidate information about heteroatom effect. It is observed that larger heteroatoms (eg; Se as compared to S, Te as compared to Se) increase the conjugation length and decrease the band gap accompanied with a change in the electrochromic properties [127,128].

In 2012, Huang et al. published a review about DAD type CPs for bulk-heterojunction photovoltaic applications [129]. They compared various type of CPs in terms of effect of acceptor units. As seen from Table 1.1, similar DAD type polymers were synthesized by using well-known acceptor groups. The polymers then were constructed as OPV devices and power conversion efficiencies (PCE %) were measured (PCE represents the percentage of sunlight which is converted to the electricity). When the band gap energy levels of these polymers were considered, the wider band gap value belongs to **BTD** based CP. The narrower band gap corresponds to dimethyllated **BIm** based CP and the PCE % of OPV device for **BIm** based CP is quite higher than **BSe** and **BTZ** containing CPs.

Table 1.1. The CPs compared with respect to acceptor unit in ref [129].

CPs	HOMO (eV)	$E_g^{optical}$ (eV)	PCE (%)
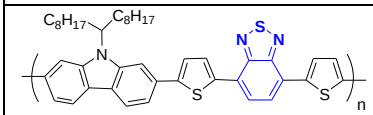 [130]	-5.50	1.88	3.16
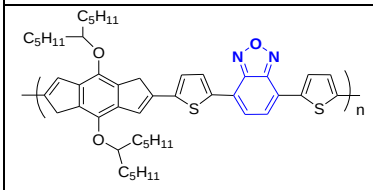 [131]	-5.34	1.68	6.1
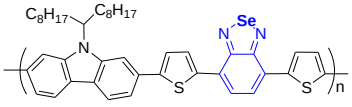 [133]	-5.28	1.73	2.6
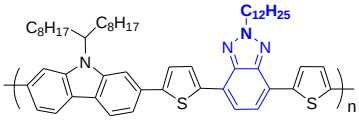 [134]	-5.54	2.18	2.8
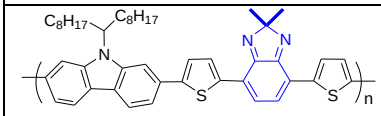 [135]	-5.47	1.64	3.1

When S atom is replaced with Se atom in the acceptor unit, a decrease in the band gap value was noted together with a red shift in the absorption spectra. These changes were explained in terms of size and electronegativity differences between Se and S atoms [132]. If S atom is replaced with N atom, resulting acceptor, **BTZ**, is less electron deficient than **BTD**. That's why the band gap of **BTZ** based CP would have higher band gap value than that of **BTD** analogue. On the other hand, **BTZ** has the advantage of functionalizing with alkyl units to supply better solubility for related CPs. The OPV constructed with CP including **BTZ** acceptor (alkylated with $C_{12}H_{25}$ from the lone pair position of N) exhibited relatively high band gap value (2.18 eV) but lower HOMO level (-5.54 eV) resulting with a moderate power conversion efficiency of 2.75 % [134].

Changing the S atom with the C atom brings another type acceptor, **BIm**, which can be functionalized from its second carbon position to get different optical properties or better solubility. Advantage of this acceptor is its easy functionalization without

disturbing the quinoidal structure and planarity. The CP containing **BIm** (functionalized with dimethyl groups) possesed good solubility in common organic solvents [135]. Besides, corresponding polymer had band gap of 1.64 eV which is smaller than that of **BTD** analogue (1.88 eV).

1.7. Benzimidazoles

Benzimidazoles (**BIm**s) are the most interesting acceptor unit among other well-known analogues due to having availability of functionalizing on its 2-C position. **BIm**s have been widely used in biological and medical applications and pharmaceutical activities such as antimicrobial, antiviral, antidiabetic and anticancer activity [137-141]. Besides, polybenzimidazoles have been reported as having great thermal stability and resistance to high temperatures [136] .

In 1998, Yamamoto's group synthesized the homopolymers of **BIm** with different alkyl chains (H, phenyl and heptyl) on its 2-C (Scheme 1.4-**A**). The study revealed that the polymers are electrochromic and electrochemically active upon n-doping. Due to its photoluminescence and solvatochromism properties, **BIm** was found to be an interesting building block for π-conjugated polymers [142].

Since **BIm** structure includes (C=N) bond, which is electron-withdrawing imine nitrogen like in pyridine and quinoxaline, it was used instead of pyridine and quinoxaline by Yamamato's group (Scheme 1.4-**B**) [143]. **BIm** units (bearing different alkyl chain lengths) were chemically co-polymerized with thiophene and a blue shift both in absorption and emission maxima were noted with increasing alkyl chain length (λ_{max}= 460 nm for pentyl substituent and λ_{max}= 436 nm for octadecyl substituent).

BIm unit can also be functionalized with cyclic or aromatic units on its 2-C position. This gives to this acceptor group very unique property of developing various type of new acceptors upon numerous modifications on it.

In 2010, a series of benzimidazole containing DAD type polymers with EDOT donor unit was introduced to investigate the acceptor unit effect by deriving the **BIm** on 2-C position with EDOT, ferrocene and benzene, separately. Resulting features revealed different electrochromic properties from each other (Scheme 1.4-**C**-**D**-**E**) [144]. The lowest optical band gap was obtained as 1.69 eV for **D** (E_g= 1.75 eV for **C** and 1.77 eV for **E**). Very high optical contrasts and subsecond level switching times were obtained especially for **C** and **D**. Moreover, **D** have found to be multichromic electrochrome upon both n- and p-doping. So, these benzimidazole containing DAD type polymers are reported to be strong candidates as high performance electrochromic materials.

The H atom on the N atom of the imidazole ring may probably make H-bonding with the neighboring oxygen on donor unit (eg: EDOT). This was investigated by Toppare's group [145,146] by coupling benzene ring bearing **BIm** with EDOT to obtain the corresponding monomer (**C**) and the existence of H-bonding was experimentally proved.

In 2012, two different **BIm** including conjugated polymers synthesized. 4'-(*tert*-butyl)spiro[benzo[d]imidazole-2,1'-cyclohexane] was used as acceptor group and coupled with 3-hexylthiophene and EDOT unit on both sides via Stille coupling reaction (Scheme 1.4-**F**-**G**) [147]. Both electrochemically obtained polymer films showed high optical contrast and gave broad absorption peaks. As expected, polymer film of **F** showed lower oxidation potential (0.55 V and 0.82 V) than **G** (0.79 V) because of having strong donor feature of EDOT moiety. **F** and **G** polymer films possesed green and blue color in their neutral states, respectively. Both polymers have two optical absorption band due to donor-acceptor pattern. **F** showed its dual absorption band in the visible region at 430 nm (due to $\pi - \pi^*$ transition) and 837 nm (due to intramolecular charge transfer, ICT). On the other hand, ICT band for **G** was found to be at about 640 nm. This blue shift indicates weaker ICT between donor and acceptor units in **G**. Moreover, **F** showed multichromic property (- : light green, orange, brick-red; n: green; + : light gray, light blue) and 0.9 s switching time of oxidation.

In the same year, another **BIm** and dithieno based conjugated polymer was synthesized by Toppare's group (Scheme 1.4-**H**). This polymer was transparent both in neutral and doped states. 95 % transmittance was measured with 0.3 % optical change upon doping and this was reported as the best result in conjugated systems up to 2012 [148].

Although all polymers mentioned above are good candidates for electrochemical and other device applications, **BIm**s were aimed to be synthesized especially for photovoltaic device applications.

Suh et al. focused on improving the solubility of CPs without disturbing the coplanarity of the backbone. The group widely used alkylated **BIm** as acceptor unit, to synthesize soluble DAD type CPs or small molecules for photovoltaic applications [149].

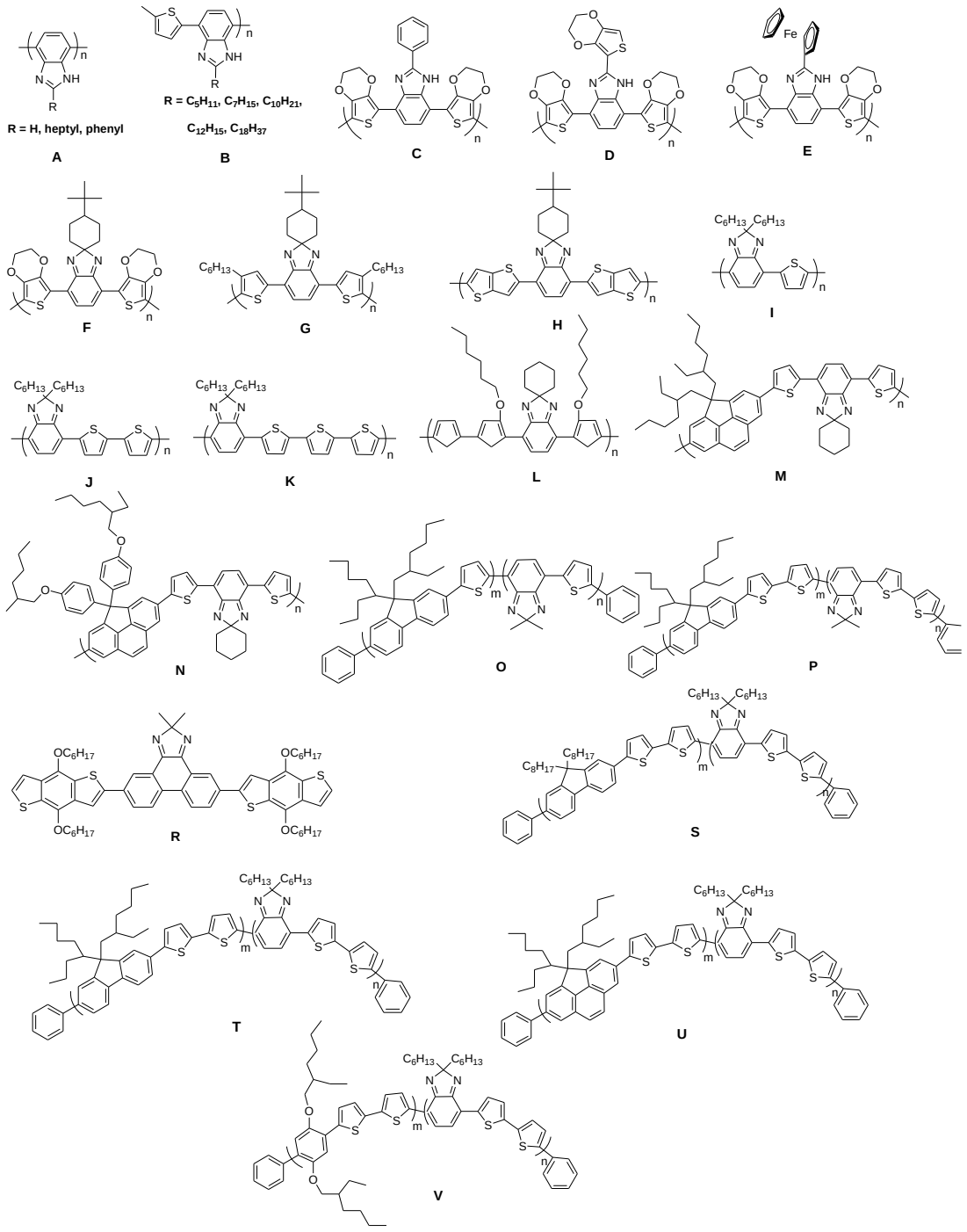

Scheme 1.4. BIm including CPs in the literature.

Suh et al. synthesized a series DAD polymers with dihexylated **BIm** as acceptor unit and thiophenes as donor unit. When thiophene is alkylated in order to achieve solubility (3-hexylthiophenes), the planarity of resulting system is affected and resulted in a blue shift in the optical absorption spectrum (Scheme 1.4-**I**-**J**-**K**). Contribution of alkylated **BIm**s supplies solubility along with keeping the coplanarity. The polymer films showed absorption maxima at 529 nm (E_g: 2.64 eV), 562 nm (E_g: 2.32 eV) and 569 nm (E_g: 2.21 eV) with increased number of the thiophene unit.

Same group synthesized a series **BIm** containing block copolymers in 2010 (Scheme 1.4-**S**-**T**-**U**-**V**) [150]. The acceptor group, **BIm** was alkylated with dihexyl chain and connected to bithiophene. Then, this unit was copolymerized with different groups alternately via Stille coupling reaction. It was reported that **BIm** supplied good solubility at room temperature in organic solvents along with facilitating the absorption at longer wavelengths. Higher red shift was observed in **V** because of stronger ICT between dialkoxy-phenylene unit and **BIm** acceptor.

In another study, a soluble CP by combining alkoxy substituted terthiophene (as donor unit) and cyclohexane bearing **BIm** (as acceptor unit) was synthesized (Scheme 1.4-**L**) [151]. The chemically synthesized polymer was found to be soluble, and showed red shifted absorption peak (at 475 and 755 nm; E_g: 1.32 eV) as compared to **BTD** containing counterparts.

Suh and his co-workers also used di(thien-2-yl)-2H-benzimidazole-2'-spirocyclohexane as acceptor unit in synthesizing two different type DAD polymers via chemical polymerization (Scheme 1.4-**M**-**N**) [152]. One of the resulting polymers (**M**) revealed deeper HOMO levels (0.12 eV deeper) and lower band gaps (0.3 eV lower) compared to the case of the polymer with **BTD** acceptor unit.

They also used dimethyl-2H-benzimidazole as acceptor unit instead of **BTD** in order to increase the solubility while protecting the planarity for solar cell application (Scheme 1.4-**O**-**P**) [153]. They observed an increase in the solubility and a decrease

in the band gap when dimethyl-functionalized **BIm** was used as acceptor unit as compared **BTD**.

Recently, in 2015, Suh et al. reported **BIm** based DAD type small molecule for photovoltaic applications (Scheme 1.4-R) [154]. For comparison, the same molecule was synthesized by using **BTD** unit and the effect of ICT was investigated among these two molecules. **BIm** unit was functionalized with dimetyl to get better solubility. **BIm** containing molecule exhibited two optical absorption band at longer wavelengths and proved the better ICT as well as showed the lower band gap (E_g: 1.64 eV). Power conversion efficiency of **BIm** containing small molecule (0.28 %) was found higher than **BTD** including moiety (0.15 %).

Since P**BIm**'s are bio-compatible and widely used in biological applications, functionalized DAD type benzimidazole based polymers were studied as biosensors. For example, benzene ring bearing **BIm** was coupled with EDOT and resulting DAD type polymer was combined with poly(methylmetacrylate) - clay nanocomposite for glucose biosensor applications [155].

Another example of biosensor is reported about aldehyde functionalized DAD type **BIm** containing polymer with thiophene donor unit. This polymer film was investigated in terms of its optical properties. Color of the polymer film is yellowish orange neutrally and pale green when oxidized. Band gap and HOMO level of the polymer was reported as 1.92 eV and -6.1 eV, respectively [156].

While electro-optical properties of **BIm** containing DAD polymers are still being studied [157-161], there are still missing studies about **BIm** containing CPs since this unit can be functionalized with many possible substituents.

1.8. Aim of This Study

According to the comparative literature summary mentioned in “Acceptor Materials” and “Benzimidazoles” sections, **BIm** has great advantage of having ability of functionalization from its 2-C position, which can positively affect the solubility while keeping the planarity of the related CP [129]. Functionalized **BIm**s can also alter the optical absorption spectrum at lower energies which allows the photovoltaic device to harvest more sunlight and also lower the band gap [149-154]. **BIm**s can change the degree of ICT and exhibit different electrochromic colors in DAD systems by bearing different substituents [144-148].

In this thesis, a series of novel benzimidazole-type acceptor units were designed and synthesized. These acceptors include cyclic alkyl units at their 2-C position (cyclohexane, cycloheptane and cyclooctane rings). The major aim is to understand the effect of the ring size on the acceptor group on the properties of DAD type monomers and their polymers. EDOT and PRODOT(C6) are the selected donor units to be coupled with the novel acceptor groups via Stille coupling reaction.

In synthesizing these DAD type novel monomers it is aimed to investigate not only the effect of ring size on the acceptor unit but also the effect of different donor units on the electrochemical and photophysical properties of the monomers and their corresponding polymers.

The following steps are included for six DAD type monomers in the scope of the study:

i. Synthesis, electro-optical characterization and comparison of monomers.
ii. Obtaining electroactive polymer films via electrochemical polymerization.
iii. Investigating the electrochemical and spectroelectrochemical behaviors of each polymer film.

iv. Comparing all CPs with each other as well as to their well-known moieties in terms of their electro-optical properties in terms of acceptor and donor group effects.

v. Constructing electrochromic device with two of the CPs.

Three different **BIm** based acceptor groups: (4,7-dibromo-2-cyclohexyl-2H-benzo[d]imidazole, 4,7-dibromo-2-cycloheptyl-2H-benzo[d]imidazole, and 4,7-dibromo-2-cyclooctyl-2H-benzo[d]imidazole were designed and used as acceptor groups. 3,4-ethylenedioxythiophene (EDOT) and dihexyl substituted 3,4-propylenedioxythiophene (PRODOT(C6) were selected as the donor groups. For this aim, six DAD type monomers, **E6E** (4-(2,3-dihydrothieno[3,4-b][1,4]dioxin-5-yl)-7-(2,3-dihydrothieno[3,4-b][1,4]dioxin-7-yl)-2-cyclohexyl-2H-benzo[d]imidazole), **E7E** (4-(2,3-dihydrothieno[3,4-b][1,4]dioxin-5-yl)-7-(2,3-dihydrothieno[3,4-b][1,4]dioxin-7-yl)-2-cycloheptyl-2H-benzo[d]imidazole), **E8E** (4-(2,3-dihydrothieno[3,4-b][1,4]dioxin-5-yl)-7-(2,3-dihydrothieno[3,4-b][1,4]dioxin-7-yl)-2-cyclooctyl-2H-benzo[d]imidazole), **P6P** (4-(3,3-dihexyl-3,4-dihydro-2H-thieno[3,4-b][1,4]dioxepin-6-yl)-7-(3,3-dihexyl-3,4-dihydro-2H-thieno[3,4-b][1,4]dioxepin-8-yl)-2 -cyclohexyl-2H-benzo[d]imidazole), **P7P** (4-(3,3-dihexyl-3,4-dihydro-2H-thieno[3,4-b][1,4]dioxepin-6-yl)-7-(3,3-dihexyl-3,4-dihydro-2H-thieno[3,4-b][1,4]dioxepin-8-yl)-2-cycloheptyl-2H-benzo[d]imidazole), **P8P** (4-(3,3-dihexyl-3,4-dihydro-2H-thieno[3,4-b][1,4]dioxepin-6-yl)-7-(3,3-dihexyl-3,4-dihydro-2H-thieno[3,4-b][1,4]dioxepin-8-yl)-2-cyclooctyl-2H-benzo[d]imidazole) and their corresponding polymers **P(E6E)** **(**poly**(**4-(2,3-dihydrothieno[3,4-b][1,4]dioxin-5-yl)-7-(2,3-dihydrothieno[3,4-b][1,4]dioxin-7-yl)-2-cyclohexyl-2H-benzo[d]imidazole)), **P(E7E)** (poly(4-(2,3-dihydrothieno[3,4-b][1,4]dioxin-5-yl)-7-(2,3-dihydrothieno[3,4-b][1,4]dioxin-7-yl)-2-cycloheptyl-2H-benzo[d]imidazole)), **P(E8E)** (poly(4-(2,3-dihydrothieno[3,4-b][1,4]dioxin-5-yl)-7-(2,3-dihydrothieno[3,4-b][1,4]dioxin-7-yl)-2-cyclooctyl-2H-benzo[d]imidazole)), **P(P6P)** (poly(4-(3,3-dihexyl-3,4-dihydro-2H-thieno[3,4-b][1,4]dioxepin-6-yl)-7-(3,3-dihexyl-3,4-dihydro-2H-thieno[3,4-b][1,4]dioxepin-8-yl)-2-cyclohexyl-2H-benzo[d]imidazole)), **P(P7P)** (poly(4-(3,3-dihexyl-3,4-dihydro-2H-thieno[3,4-b][1,4]dioxepin-6-yl)-7-(3,3-dihexyl-3,4-dihydro-2H-thieno[3,4-b][1,4]dioxepin-8-

yl)-2-cycloheptyl-2H-benzo[d]imidazole)) and **P(P8P)** (poly(4-(3,3-dihexyl-3,4-dihydro-2H-thieno[3,4-b][1,4]dioxepin-6-yl)-7-(3,3-dihexyl-3,4-dihydro-2H-thieno[3,4-b][1,4]dioxepin-8-yl)-2-cyclooctyl-2H-benzo[d]imidazole)) were synthesized, characterized and their properties were comparatively evaluated.

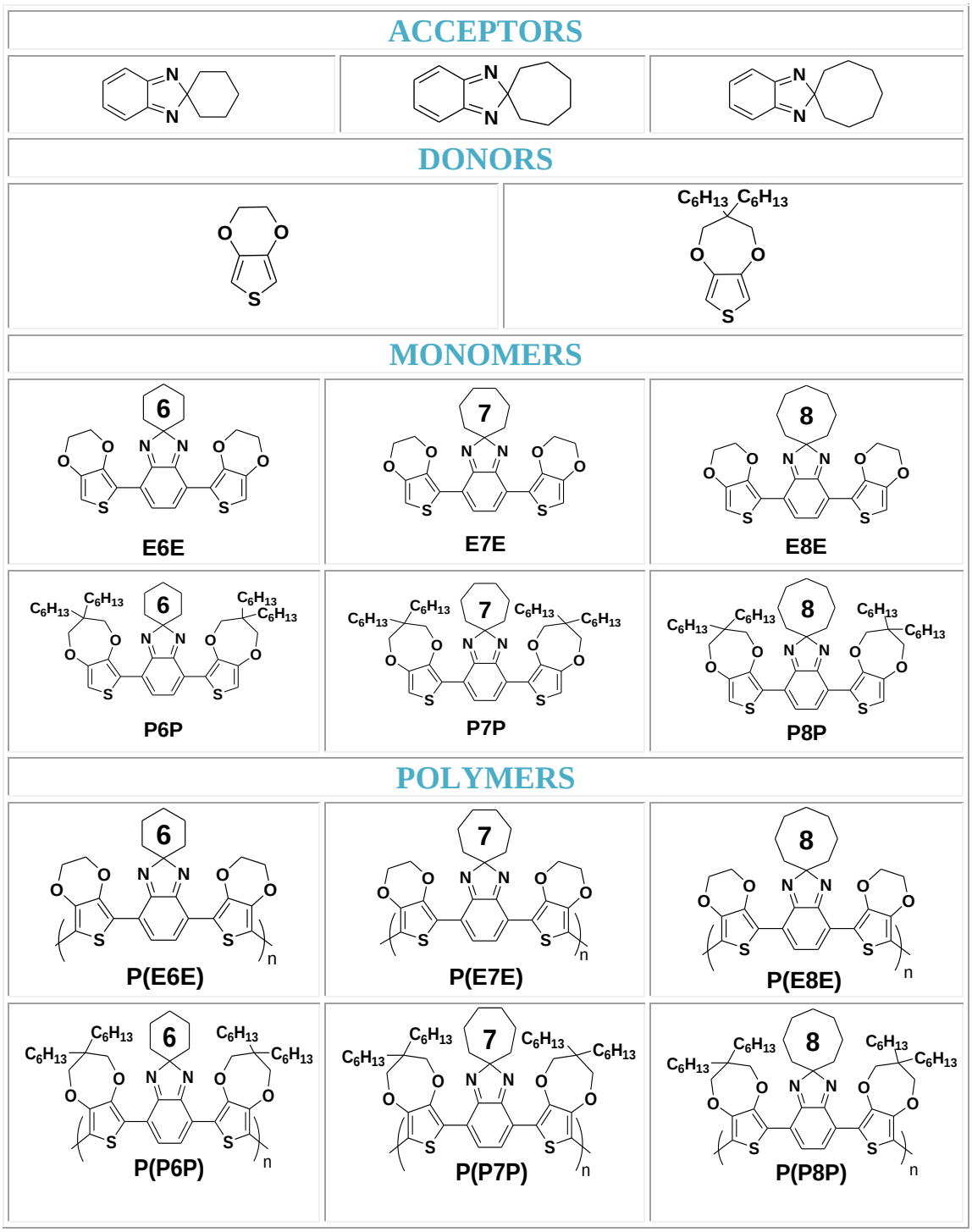

Scheme 1.5. Monomers, polymers, acceptor and donor groups that are aimed to be studied in this thesis.

CHAPTER 2

EXPERIMENTAL

2.1. Materials

All chemicals were purchased from Sigma Aldrich Chemicals and used as received except tetrahydrofuran (THF), ethanol and toluene. THF was dried over sodium and benzophenone, ethanol was distilled over iodine and magnesium, toluene was dried over calcium hydride (CaH_2) prior to use.

Electrolyte solutions were prepared by dissolving lithium perchlorate ($LiClO_4$) or tetrabutylammonium tetrafluoroborate ($N(Bu)_4BF_4$) in acetonitrile (ACN). Gel electrolyte for electrochromic device was prepared by mixing $TBABF_4$ - PMMA - PC - ACN in the following ratio 3 : 7 : 20 : 70 (w/w), respectively.

2.2. Methods and Equipment

The molecular structures of the synthesized compounds and final monomers were characterized with Bruker-Instrument, (DPX-400) model Nuclear Magnetic Resonance Spectrometer (NMR) in deuterochloroform ($CDCl_3$). Chemical shifts (δ) were given relative to tetramethylsilane (TMS) as the internal standard. Chemical shifts were reported in ppm with respect to 7.27 ppm of $CDCl_3$ as the reference signals for ^1H NMR (see Appendix A). Agilent (6224) model HRMS instrument was used for the molecular weight determination of monomers (see Appendix B). Electrochemical studies were performed in three electrode system by using Pt disk electrode, Pt plate and Ag/AgCl electrodes as working (WE), counter (CE) and reference (RE) electrodes, respectively. The cyclic voltammograms were recorded

with Gamry Reference 600 model potentiostat - galvanostat. The cyclic voltammetry measurements were calibrated with 10 mM solution of ferrocene in DCM. Spectroelectrochemistry studies were carried out with Specord S600 model UV-VIS spectrometer where it is combined with Gamry Reference 600 model potentiostat - galvanostat. Indium tin oxide (ITO) coated glass, Pt wire and Ag wire were used as WE, CE, and pseudo RE, respectively in spectroelectrochemical studies. The monomer included and monomer free electrolyte solution that was used for polymerization and polymer characterization purged with Argon (Ar) especially before n-doping measurements. Emission wavelengths were determined with Thermo Lumina fluorescence spectrometer. All measurements were performed at room temperature and ambient conditions. Thin layer chromatography (TLC) technique was used for monitoring the reactions. TLC plates (60 F 254, Merck) were used to see the reaction spots under UV light having 254 and 366 nm wavelengths. Merck Silica Gel (35-60 mesh) was used for purification of the target compounds by column chromatography.

2.3. Synthesis of Monomers

The synthesis part includes three steps: Synthesis of the acceptor units (**6**, **7**, **8**); synthesis of stannylated donor units (**9**, **10**) and the synthesis of final DAD monomers (**E6E**, **E7E**, **E8E**, **P6P**, **P7P**, **P8P**). Six different monomers were synthesized via Stille Coupling Reaction and characterized via ^{1}H-NMR and HRMS instrumental techniques. Several reaction steps were achieved for the preparation of donor and acceptor groups up to last step of Stille Coupling reaction.

2.3.1. Synthesis of Acceptor Groups

For the synthesis of acceptor groups, the skeleton unit called 3,6-dibromobenzene-1,2-diamine (**2**) was synthesized first. Then, the acceptor groups were obtained via

the reaction of diamine with cyclohexanone, cycloheptanone and cyclooctanone, separately (Scheme 2.1).

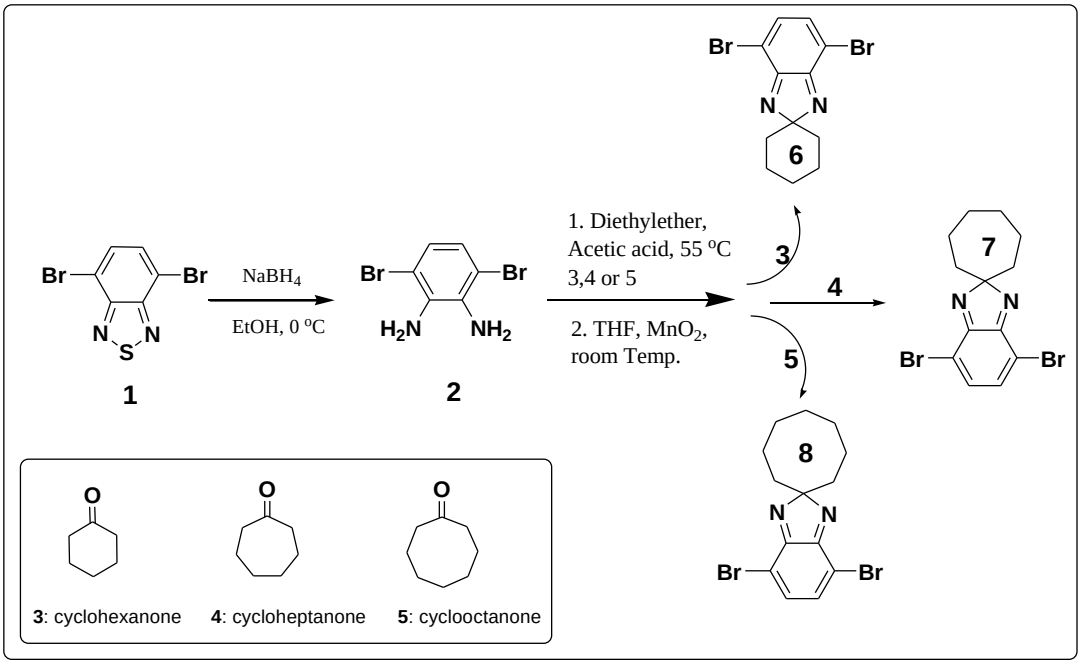

Scheme 2.1. General reaction scheme for the synthesis of acceptor units.

2.3.1.1. Synthesis of 3,6-dibromobenzene-1,2-diamine (2) [162]

1 g of 4,7-dibromobenzo[c][1,2,5]thiadiazole (**1**) was dissolved in 50 mL of diethyl ether and 400 mL ethyl alcohol (EtOH) at 0 °C. 5 g of $NaBH_4$ was added portionwise at the same temperature. After addition is completed, reaction mixture was allowed to stir overnight. EtOH was evaporated and the extraction with ether and brine was performed. After drying over $MgSO_4$, 1.04 g brown solid was obtained. Column chromatography was used for purification (4:1 Petroleum ether: diethyl ether) and 330 mg diamine was obtained as white solid (37 %).

^{1}H NMR (400 MHz, $CDCl_3$) δ (ppm): 6.83 (s, 2H); 3.77 (s, 4H); ^{13}C NMR (100 MHz, $CDCl_3$) δ (ppm): 133.7; 123.3; 109.7.

2.3.1.2. Synthesis of Acceptors: 4,7-dibromo-2-cyclohexyl-2H-benzo[d]imidazole (6), 4,7-dibromo-2-cycloheptyl-2H-benzo[d]imidazole (7) and 4,7-dibromo-2-cyclooctyl-2H-benzo[d]imidazole (8)

General procedure for the synthesis of acceptor unit is in following [163]: 1 eq of 3,6-dibromobenzene-1,2-diamine (**2**) and 3.7 eq of cyclohexanone (**3**) or cycloheptanone (**4**) or cyclooctanone (**5**) were dissolved in diethyl ether under Ar atmosphere with continuous stirring. After addition of 0.1 eq acetic acid, reaction mixture was refluxed at 50 °C and followed by TLC during 10 days. After reaction was stopped and solvent was removed under reduced pressure, crude product was diluted with ethyl acetate and washed with saturated aqueous brine. The collected organic phase was dried over $MgSO_4$ and purified with column chromatograpy (20:1 Hexane: Ethyl acetate). The yellowish oil was collected for the 2nd step. The yellowish oil was stirred under Ar atmosphere with 3 eq of 85 % activated MnO_2 in fresh THF overnight. Reaction mixture was filtered, washed with THF and solvent was evaporated. Lastly the product was purified with column chromatography (15:1 Hexane: Ethyl acetate). Final product (**6**, **7** or **8**) was collected as yellow needles (see Figure 2.1).

4,7-dibromo-2-cyclohexyl-2H-benzo[d]imidazole (6): Yield: 83 %
^{1}H NMR (400 MHz, $CDCl_3$) δ (ppm): 7.19 (s, 2H); 2.01-1.95 (m, 6H); 1.76 (s, br, 2H); 1.72 (s, br, 2H); ^{13}C NMR (100 MHz, $CDCl_3$) δ (ppm): 156.9; 135.8; 118.8; 107.4; 32.6; 25.5; 24.5.

4,7-dibromo-2-cycloheptyl-2H-benzo[d]imidazole (7): Yield: 63 %
^{1}H NMR (400 MHz, $CDCl_3$) δ (ppm): 7.17 (s, 2H); 1.82-1.76 (m, 12 H); ^{13}C NMR (100 MHz, $CDCl_3$) δ (ppm): 164.9; 135.8; 100; 79.9; 33.8; 25.2; 23.4.

4,7-dibromo-2-cyclooctyl-2H-benzo[d]imidazole (8): Yield: 14 %

^{1}H NMR (400 MHz, $CDCl_3$) δ (ppm): 7.17 (s, 2H); 1.78-1.71 (m, 14H); ^{13}C NMR (100 MHz, $CDCl_3$) δ (ppm): 156.8; 135.7; 110.8; 77.2; 41.9; 27.2; 22.7.

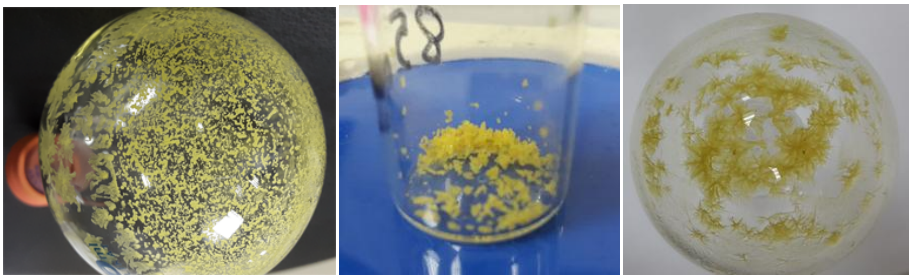

Figure 2.1. Views of the acceptor units. From left to right; **6**, **7** and **8**.

2.3.2. Synthesis of Donor Groups

In the aim of coupling the donor groups with the acceptor group via Stille coupling reaction, tributyltin substituted EDOT and PRODOT(C6) were prepared by lithiation with n-butyl lithium (n-BuLi) solution followed with treatment with tributyltin chloride ($Sn(Bu)_3Cl$). EDOT was used as received. PRODOT(C6) was synthesized via several steps.

2.3.2.1. Tributyl(2,3-dihydrothieno[3,4-*b*][1,4]dioxin-7-yl)stannane (9) [164]

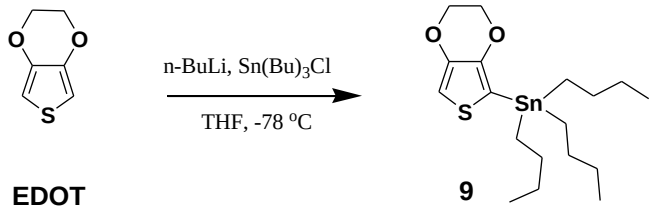

EDOT **9**

Scheme 2.2. Synthesis route of compound **9**

A 0.77 g (5.42 mmol, 1 eq) sample of EDOT in 70 mL of freshly dried THF was cooled to -78 °C under Ar atmosphere. 2.3 mL (5.69 mmol, 1.05 eq) of 2.5 M n-BuLi was added to the solution dropwise. When the addition is finished, solution was taken out to room temperature for 1 hour. Then the reaction solution was cooled again to -78 °C for one hour, and then 1.46 mL (1 eq) of tributylstannyl chloride were slowly added to the solution. The solution was stirred at -78 °C for additional 2 h. Then the solution was warmed to room temperature very slowly and stirred overnight. 3-4 drops of 2 M aqueous solution of H_2SO_4 was added to the solution to deactivate the excess n-BuLi. After evaporation of the solvent, the residue was extracted with dichloromethane and saturated aqueous brine. Lastly the organic phase was dried over $MgSO_4$. The solvent was removed and tributyl(2,3-dihydrothieno[3,4-*b*][1,4]dioxin-7-yl)stannane (**9**) was obtained as viscous yellow liquid (1.6 g, 68%). The compound **9** was used for the coupling reactions without further purifications.

^{1}H NMR (400 MHz, $CDCl_3$) δ (ppm): 6.32 (s, 1H); 4.20 (s, 4H); 1.6-1.5 (m, 6H); 1.37-1.28 (m, 6H); 1.15-1.07 (m, 6H); 0.92-0.82 (m, 9H); ^{13}C NMR (100 MHz, $CDCl_3$) δ (ppm): 147.7; 108.9; 105.8; 64.7; 28.9; 27.1; 13.7; 10.5.

2.3.2.2. Synthesis of 3,3-dihexyl-3,4-dihydro-*2H*-thieno[3,4-b])dioxepine (PRODOT(C6)) [165]

Couple of reaction steps were followed during the synthesis of PRODOT(C6) (Scheme 2.3).

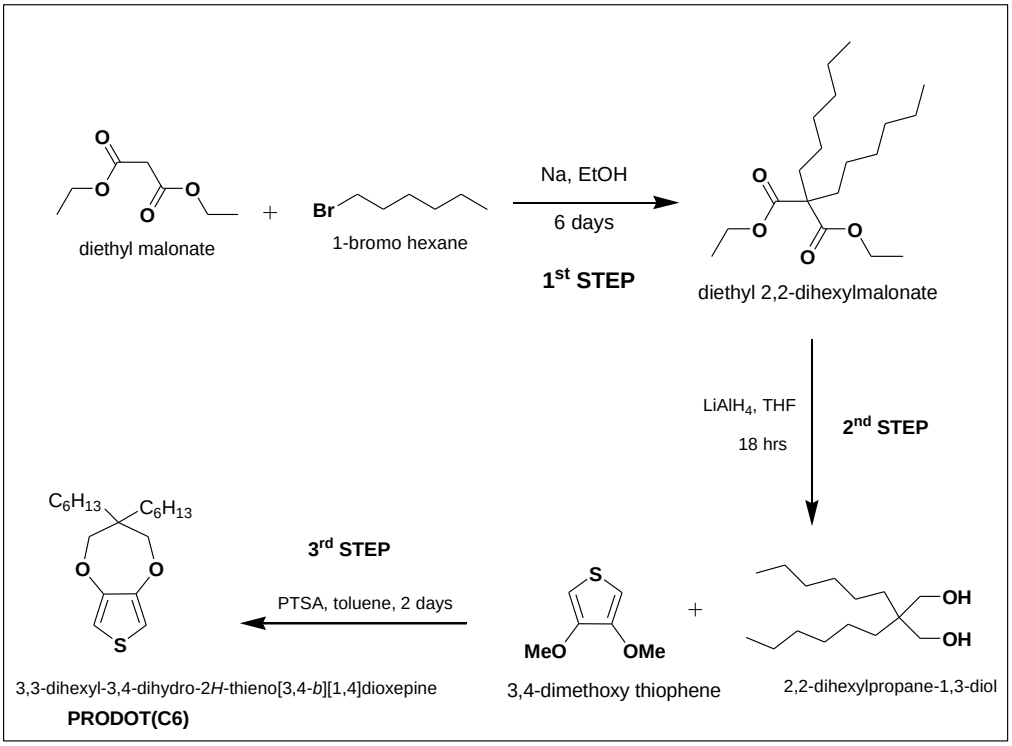

Scheme 2.3. Synthesis route of PRODOT(C6)

Synthesis of 2,2-dialkymalonate (Step 1): 6.90 g (0.3 moles, 3.25 eq) of Na metal was dissolved in 250 mL of freshly distilled ethyl alcohol.15 g (93 mmol, 1 eq) of diethyl malonate was added and the reaction mixture was started to heat. When reflux began, 56 g (340 mmol, 3.65 eq) of 1-bromohexane was added dropwise. The reaction was continued for 4 days. After evaporation of ethyl alcohol, the crude product was dissolved in diethyl ether and washed with cold water. The collected

organic phase was dried over $MgSO_4$. 22 g of 2,2-dihexylmalonate was obtained as yellow oil (72 %).

Synthesis of 2,2-dihexylpropane-1,3-diol (Step 2): 200 mL of freshly dried THF was added onto 5.40 g of $LiAlH_4$ dropwise while stirring under Ar atmosphere. After addition is completed, the temperaturewas raised to reflux temperature. Then 22 g of 2,2-dihexylmalonate was added to this system drop by drop after diluting with 50 mL THF. The reaction was cooled after 18 hours. 2 M of H_2SO_4 was added dropwise in order to deactivate excess $LiAlH_4$. Then THF was removed and the product was washed with ether and saturated aqueous brine. The organic phase was dried over $MgSO_4$. After evaporation of solvent, 14 g of 2,2-dihexylpropane-1,3-diol was obtained as yellow oil (86 %).

Synthesis of 3,3-dihexyl-3,4-dihydro-*2H*-thieno[3,4-b])dioxepine, PRODOT(C6)) (Step3):

5 Å moleculer sieve was dried on a bunsen burner for 3 hours for using as drying agent in a soxhlet apparatus during the reflux. 2g (13.8 mmol, 1 eq) of 3,4-dimethoxythiophene, 6.76 g (27.6 mmol, 2 eq) of 2,2-dihexylpropane-1,3-diol and 0.27 g (1.38 mmol, 0.1 eq) para-toluene sulfonic acid (PTSA) were mixed in 120 mL of freshly distilled toluene under Ar atmosphere. Soxhlet apparatus was placed on the reaction flask. The reflux unit was placed on the soxhlet. The reaction mixture was refluxed at 120 °C by following with TLC. After 2 days, reaction was stopped and concentrated reaction product was diluted with dichloromethane (DCM) to wash with saturated aqueous brine. The collected organic phase was dried over $MgSO_4$. After solvent evaporation, further purification was done by column chromatography (4:1 Hexane : DCM) and 4.36 g viscous yellow product was obtained (97 %).

^{1}H NMR (400 MHz, $CDCl_3$) δ (ppm): 6.41 (s, 2H); 3.84 (s, 4H); 1.39-1.28 (m, 12H); 1.28 (s, br 8H); 0.89 (s, br 6H); ^{13}C NMR (100 MHz, $CDCl_3$) δ (ppm): 149.7; 104.6; 77.5; 31.9; 31.7; 30.15; 22.7; 22.6; 14.07.

2.3.2.3. Synthesis of Tributyl(3,3-dihexyl-3,4-dihydro-2H-thieno[3,4-*b*][1,4] dioxepin-8-yl)stannane (10) [164]

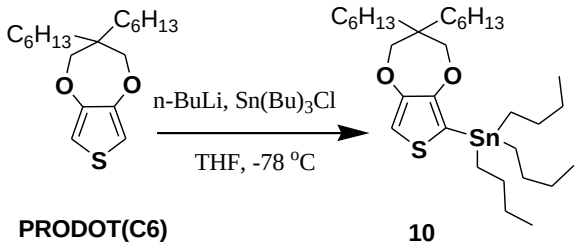

Scheme 2.4. Reaction scheme for stannylation of PRODOT (C6)

A 3.8 g (11.73 mmol, 1 eq) solution of PRODOT(C6) in 200 mL of freshly distilled THF was cooled to -78 °C under Ar atmosphere. 5.0 mL (12.32 mmol, 1.05 eq) of 2.5 M n-butyllithium was added to the solution dropwise. When the addition is finished, solution was taken out to room temperature for 1 hours. Then after the reaction solution was cooled again for 1 h at -78 °C, 3.2 mL (1 eq) of tributylstannyl chloride were slowly added to the solution. The solution was stirred at -78 °C for additional 2 h. Then the solution was warmed to room temperature very slowly and stirred overnight. 3-4 drops of 2 M aqueous solution of H_2SO_4 was added to the solution to deactivate the excess n-BuLi. After evaporation of the solvent, the residue was extracted with dichloromethane and saturated aqueous brine. Lastly the organic phase was dried over $MgSO_4$. The solvent was removed and tributyl(3,3-dihexyl-3,4-dihydro-2H-thieno[3,4-*b*][1,4]dioxepin-8-yl)stannane (**10**) was obtained as very viscous dark yellow liquid (7.4 g, 99 %). The compound **10** was used for the coupling reactions without further purifications.

^{1}H NMR (400 MHz, $CDCl_3$) δ (ppm): 6.42 (s, 1H); 3.84 (s, 4H); 1.36-1.28 (m, 18H); 1.28 (s, br, 16H); 1.0-0.86 (m, 15H); ^{13}C NMR (100 MHz, $CDCl_3$) δ (ppm): 149.7; 128.2; 104.6; 77.5; 43.7; 31.8; 31.7; 30.14; 28.2; 27.1; 25.6; 22.7; 16.3; 15.6; 13.7.

2.3.3. DAD Type Monomer Synthesis via Stille Coupling Reaction

The Stille reaction is a widely used method in organic synthesis for the C-C bond formation and the building of sp^2-sp^2 bond containing molecules [166]. It is also known as "Migita-Kosugi-Stille coupling", since it is introduced first by Migita and developed by Stille [167,168]. Coupling of organostannanes with organohalides can be achieved by Stille reaction in the presence of palladium-catalyst.

All monomers (**E6E**, **E7E**, **E8E**, **P6P**, **P7P**, **P8P**) were synthesized via Stille coupling reaction. Color of the progress was the same for all monomers. In the beginning, all solutions were in yellow color. After 30 minutes, the color was started to turn red. After two hours, the reaction color was fixed itself to red. The purifying steps were also similar. The fluorescence red compounds were collected from column chromatography.

General procedure of monomer synthesis is in following: 1 eq of acceptor compound, 2.1 eq of donor compound and 2 % eq of Pd(II) were dissolved in freshly distilled toluene under Ar atmosphere. Reaction was followed by TLC during two days. The solvent was evaporated, the crude product was dissolved in DCM and washed with aqueous brine. After drying the organic part over $MgSO_4$, the product was purified with column chromatography (3:1 Hexane : DCM).

E6E: Purple like solid film. Yield: 47%
^{1}H NMR (400 MHz, $CDCl_3$) δ (ppm): 7.83 (s, 2H); 6.47 (s, 2H); 4.35-4.25 (dt, 8H); 2.04-2.0 (t, 10H); HRMS: 467.1052 g / mol; 8.96 ppm.

E7E: Purple like solid film.Yield: 22%
^{1}H NMR (400 MHz, $CDCl_3$) δ (ppm): 7.80 (s, 2H); 6.48 (s, 2H); 4.35-4.25 (dt, 8H); 1.56 (t, br, 8H); 1.77 (t, 4H); HRMS: 481.1189 g / mol; 12.69 ppm.

E8E: Purple like solid film.Yield: 37%

^{1}H NMR (400 MHz, $CDCl_3$) δ (ppm): 7.81 (s, 2H); 6.48 (s, 2H); 4.36-4.25 (dt, 8H); 1.72 (t, 4H); 1.25 (t, br 10H); HRMS: 495.1358 g / mol; 9.85 ppm

P6P: Red solid film.Yield: 80 %

^{1}H NMR (400 MHz, $CDCl_3$) δ (ppm): 7.86 (s, 2H); 6.55 (s, 2H); 4.01 (s, 4H); 3.9 (s, 4H); 1.45-1.42 (m, br 10H); 1.31-1.22 (m, 40H); 0.9 (t, 12H); HRMS: 831.5137 g / mol; 3.15 ppm.

P7P: Red solid film. Yield: 24 %

^{1}H NMR (400 MHz, $CDCl_3$) δ (ppm): 7.74 (s, 2H); 6.47 (s, 2H); 3.94 (s, 4H); 3.82 (s, 4H); 1.23 (m, 40 H); 1.36 (m, 8H); 1.67 (t, 4H); 1.83 (t, 12H); HRMS: 845.5255 g / mol; 7.6 ppm

P8P: Red solid film.Yield: 16 %

^{1}H NMR (400 MHz, $CDCl_3$) δ (ppm): 7.73 (s, 2H); 6.47 (s, 2H); 3.93 (s, 4H); 3.83 (s, 4H); 1.37 (m, 8H); 1.29 (m, 4H); 1.23 (m, 42H); 0.83 (q, 12 H).

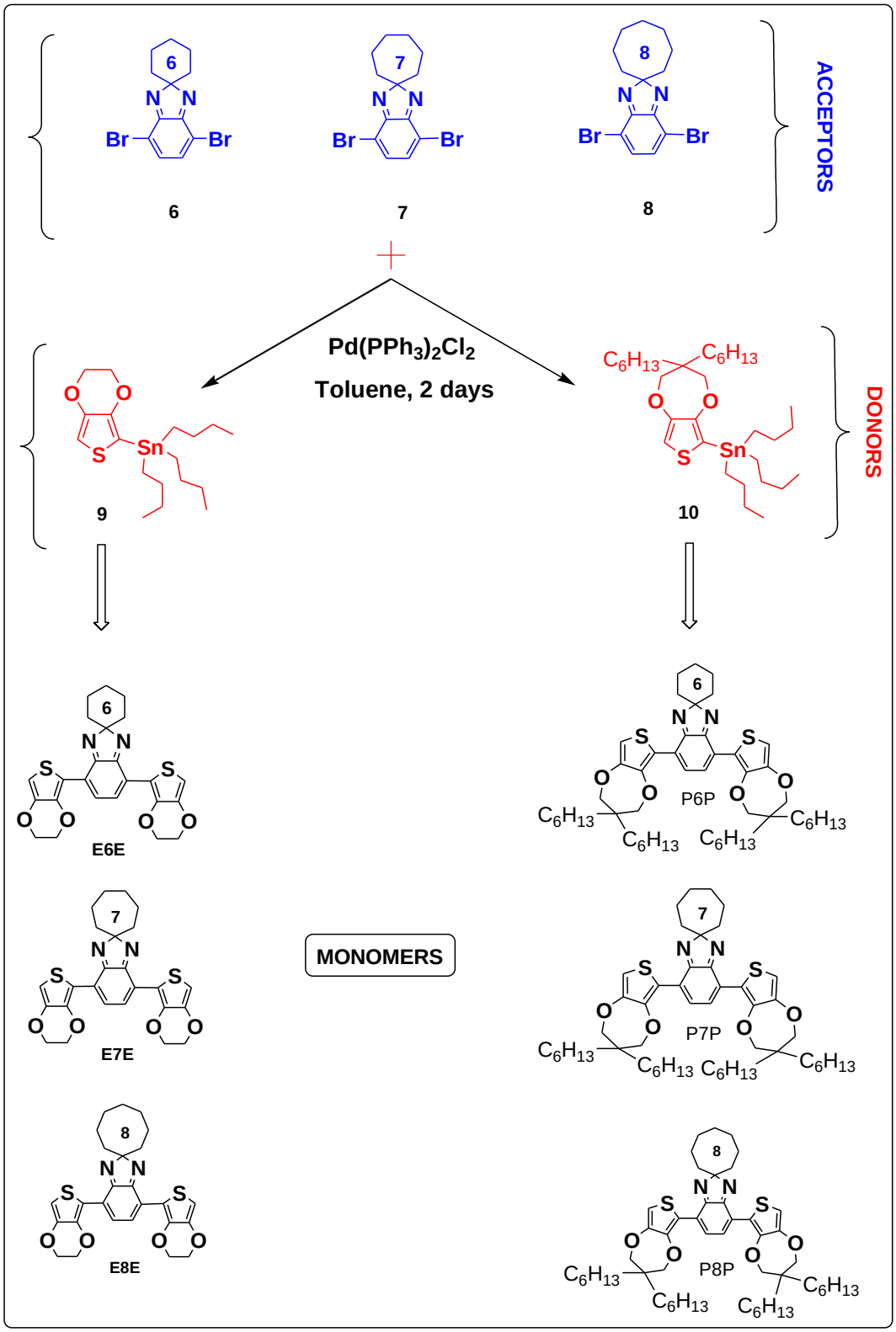

Scheme 2.5. Synthesis route of monomers (**E6E**, **E7E**, **E8E**, **P6P**, **P7P**, **P8P**).

2.4. Synthesis of Polymers via Electrochemical Polymerization of Monomers

The polymer films firstly were obtained by cyclic voltammetry with a certain number of repetitive scans in order to see the deposition of the polymer films. Further studies (determination the redox potentials, stability, scan-rate dependence etc.) were performed with the films which were deposited by constant potential coulometry.

The polymers were deposited on different substrates for different purposes. For electrochemical studies, monomers were electropolymerized on Pt disc WE (0.0314 cm^2 surface area). One compartment three electrode system consisting of a Pt disc WE, Ag/AgCl RE and Pt plate CE was used during electrochemical studies. 0.1 M $LiClO_4$ in ACN-DCM (90:10 v/v) electrolyte solution was used for the electropolymerization of monomers.

For optical studies, indium tin oxide (ITO) coated glass substrate was used as WE. The pseudo-reference electrode was Ag wire and the CE was Pt wire. Electropolymerizations were performed by constant potential electrolysis in UV-cuvette in the electrolyte solution of 0.1 M $LiClO_4$ in ACN-DCM (90:10 v/v).

2.4.1. Cyclic Voltammetry

Cyclic voltammetry (CV) is the mostly used electroanalytical technique for electrochemical reactions. It gives useful information about the redox behavior, such as oxidation-reduction potential values of the substrates [169]. In this method, three electrode system (WE, CE and RE) in the electrochemical cell is connected to the potentiostat (Figure 2.2). Commonly used WEs are Pt disc, glassy carbon disc and ITO coated glass electrodes. The RE may be an Ag wire or Ag/AgCl saturated calomel electrode. The CE is generally a Pt wire or a Pt plate. In CV, WE potential is varied at a specified rate linearly and current flow between WE and CE was monitored as a function of WE potential.

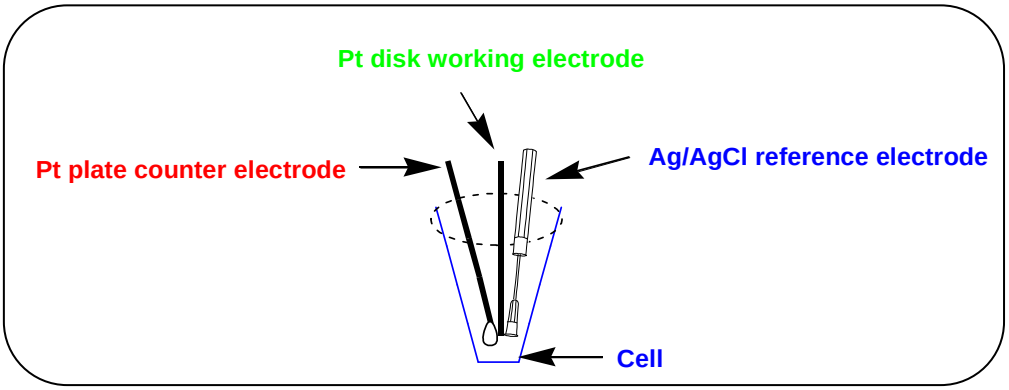

Figure 2.2. General set up for potentiostatic studies.

The peak current is expressed by Randles & Sevcik equation [170]:

$$i_p = (2.69 \times 10^5) n^{3/2} A D^{1/2} C v^{1/2}$$

Where, η is the number of electrons transferred in redox process, A is the area of the electrode, C is the concentration, D is the diffusion coefficient and ν is the voltage scan rate. As it can be seen from the equation, the peak current is directly proportional to the square root of scan rate and the concentration of analyte.

2.4.2. Constant Potential Coulometry

Constant potential coulometry is one of the electroanalytical methods like cyclic voltammetry. In this technique, the monomer is totally oxidized (or reduced) at the WE. The polymer film deposition is achieved by applying a constant potential to the cell, the resulting film will be in its oxidized state. The film thickness can be monitored and controlled by controlling the amount of charge (in coulombs) passing through the electrochemical cell [171].

2.5. Characterization of Polymers

In order to report a CP as a "good electrochrome", certain parameters (redox behavior, electrochemical stability, band gap, HOMO and LUMO values, optical absorption and emission regions, optical stability, electrochromic contrast, switching time, colors in different redox states and coloration efficiency) must be determined and reported. In this thesis, all parameters written above were monitored, calculated and reported for six synthesized polymer films.

2.5.1. Electrochemical Properties of CPs

Electroanalytical techniques can be utilized to elucidate information about oxidation and reduction potentials of the polymers which can be used to evaluate the band gap energy. Furthermore, by recording the repetitive CVs in monomer free electrolytic solution, information about the electrochemical stability of polymer films can be obtained.

In the case of CPs since the polymer is localized on the WE surface, Randels-Sevcik equation does not work due to lack of diffusion. The peak current is expressed by the following equation based on the theory of immobilized redox centers [172]:

$$i_p = \frac{n^2 F^2 \Gamma \upsilon}{4RT}$$

where Γ is the amount of analyte on the electrode surface. According to this equation, the current intensity is directly proportional to the scan rate.

In this thesis, the cyclic voltammograms of the polymer films were recorded at different scan rates and the "current vs scan rate" and "current vs square root of scan rate" graphs were plotted in order to prove if the polymer is well adhered to the electrode surface. Moreover, "amount of charge vs scan rate" graphs were also

plotted to show if the polymer films can do their charge-discharge process even at high scan rates.

Retaining the electroactivity after large number of redox cycles is an important parameter for an electrochromic polymer especially for device applications. The electrochemical stability of the polymer films were tested by square wave potential method by applying potential steps. In this method, two specific potential values (V_1 and V_2) are applied to the WE for specified time intervals. One of the potential value oxidizes the polymer and the other potential keeps the polymer in its neutral form.

2.5.2. Spectroelectrochemistry

Spectroelectrochemistry is the combination of the electrochemical and spectroscopic techniques. Remarkable information about the polymer films can be obtained by operating these methods together. Optical studies can be performed while the redox process is in progress. For example, the optical absorption spectra of the polymer films can be recorded during the p-type or n-type doping process in order to provide support for the polaron / bipolaron formation.

For optical studies, ITO-coated glass substrate was used as WE. The pseudo reference electrode was Ag wire and the CE was Pt wire (Figure 2.3).

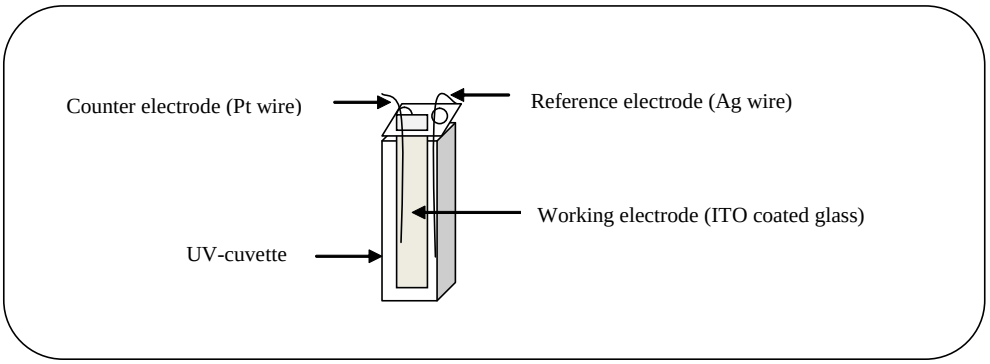

Figure 2.3. General set up for potentiostatic methods in optical studies.

UV-VIS spectrometry was used to determine the maximum absorption wavelengths of the polymers. The optical band gap ($E_g^{optical}$) was determined for each of the polymer by using the onset of longer wavelength absorption spectrum.

The emission spectrum gives an information about the solid state emission of the polymer which is a remarkable property for many of applications such as organic light emitting diodes (OLEDs). The emission spectra of the polymer films were studied in their solid states with the fluorescence spectrometry and emitted colors were determined.

2.5.3. Optical Contrast and Optical Stability

When the CPs are doped, their optical properties, in other words, their light transmittances change depending on the applied potential value. The difference in their transmittance values between fully oxidized (% $T_{bleached}$) and reduced (% $T_{colored}$) states (ΔT %) were studied at the maximum absorption wavelengths. The kinetic program of the UV-VIS spectrometry was performed while the square wave potential method was applied in the same time. The percent transmittance values between fully oxidized and reduced states were calculated and reported. How fast the polymer film achieves the redox process was determined and optical stability of the

films were reported by applying the square wave potential with the residence times of 10, 5, 3, and 2 seconds.

Percent transmittance and the color change (upon redox process) must be stable upon switching many times, which is called optical stability. Redox switching stabilities of the polymers were monitored for 50 cycle redox switchings with a residence time of 5 seconds.

The time required for doping (t_{ox}) and dedoping (t_{red}) is preferred to be in subsecond level for display applications while it is not necessary to be very fast for smart windows. The switching times of the polymers were also determined by monitoring the percent transmittance results. The optical contrast results were given at 95 % of the full contrast since the human eye can perceive in this range.

2.5.4. Colorimetry

An electrochromic polymer changes its color in its oxidized (or may be in reduced or intermediate) states. Each human eye may detect the colors relatively different because of different light sources or back ground colors or may be because of the observer. There exist some scales for standardization of the color values with the numbers. The most widely accepted scale is "The Commission Internationale de I'Eclairge" (CIE). This commitee developed a three dimensional lab color space (called CIELAB) for expressing the color specifically in 1976. According to this system, brightness, hue and saturation are expressed by L*a*b* values respectively and the exact color is indicated on the CIELAB color space (see CIELAB space in Figure 2.4).

Color measurements of the polymer films in the scope of this thesis were performed by spectrophotometer and neutral, oxidized and reduced state colors of the polymers were indicated in terms of L*a*b* values.

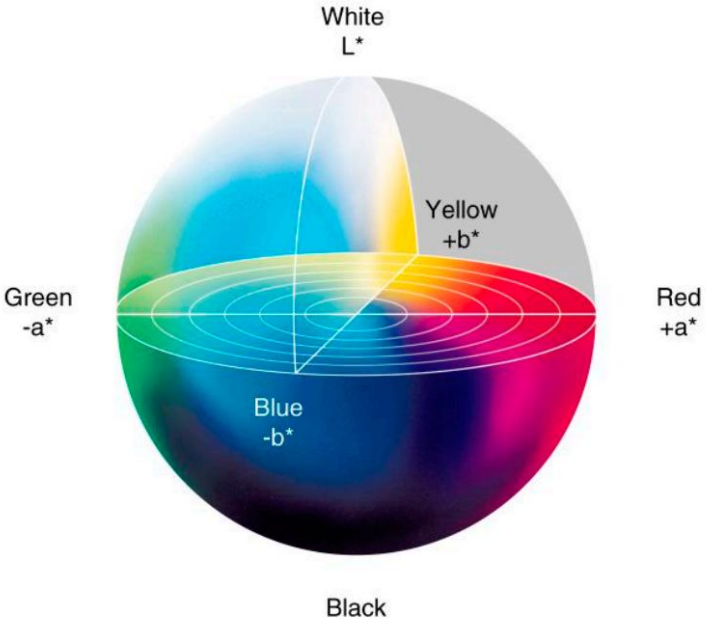

Figure 2.4. CIELAB color space (Adapted from [173])

2.5.5. Coloration Efficiency

Coloration efficiency (CE) is another important parameter which shows the relation between optical absorbance change (at a specific wavelength) and charge / discharge density required for a full switch [174].

CE (ɳ) is calculated with the following equation [175]:

$$\eta = \frac{\Delta OD}{Q_d}$$

Where $\Delta OD = \log \frac{(T_{bleached})}{(T_{colored})}$ and Q_d is the charge density ($C.cm^{-2}$) . The unit of CE is $cm^2.C^{-1}$. CE is commonly measured and reported at 95 % of the full optical contrast.

2.6. Applications of CPs: Electrochromic Device

An electrochromic device (ECD) is a device having an ability of changing its optical contrast at different applied potentials. ECDs are used in the application fields of smart windows, car rear views, display applications or emittance surfaces [176-179].

Type of the conjugated polymers used in device applications determines the color of ECD. The color change in oxidized state is commonly transmissive in conjugated polymers. Hence, the well-known type of organic ECD is absorptive-transmissive type ECDs. Moreover, conjugated polymers can have two different colored state in their neutral and oxidized states, or more than two in between [180]. These electrochromes are suitable candidates for reflective type ECDs.

The basic set up for an ECD consists of two electrochromic polymer films sandwiched between a conducting substrate with gel electrolyte in the middle (Figure 2.5). Gel electrolyte supports the ionic balance as well as encapsulates the device. The coloration switch of the ECD is adjusted by the selecting an anodically coloring and a cathodically coloring polymer films.

In this study, transmissive type ECDs were constructed with P(**E6E**) and PEDOT and P(**P6P**) and PEDOT polymer films. PEDOT was chosen as cathodically coloring polymer (Dark blue in neutral state and transmissive sky blue in oxidized state). Before making a succesful ECD, charge balance must be adjusted for electrochemically depositing polymers in order to prevent remaining extra charge on ECD on redox process. For this aim, PEDOT film on ITO-glass was deposited with different charge densities (10; 20; 29; 30.5 and 43.5 mC. cm^{-2}). Then charge density vs redox charge graph was drawn as reference for P(**E6E**) and P(**P6P**) separately (Figure 2.6). Then, our polymer films were electrochemically deposited on ITO with suitable charge density.

After balancing the charges, PEDOT was left in oxidized form and P(**E6E**) (or P(**P6P**)) was left in its reduced form. After drying of the films for an hour, the

polymer films were sandwiched on their conducting sites with leaving thin layer gel electrode between them. The ECD was left to dry for two days and then it was run by connecting the WE to P(**E6E**) (or P(**P6P**)) and the CE (short cutted by the reference electrode) to PEDOT.

Gel electrolyte was prepared by mixing $TBABF_4$ - PMMA - PC - ACN with the ratio of 3 : 7 : 20 : 70 (w/w) respectively [181]. PMMA was dissolved in ACN while heating and stirring at 70 ^{o} C. Then $TBABF_4$ (dissolved in PC) was slowly added to solution and ACN in resulting mixture was allowed to evaporate overnight. Gel electrolyte was obtained as very viscous colorless product.

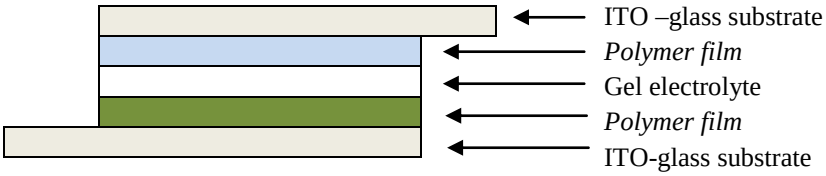

Figure 2.5. Schematic view of an electrochromic device.

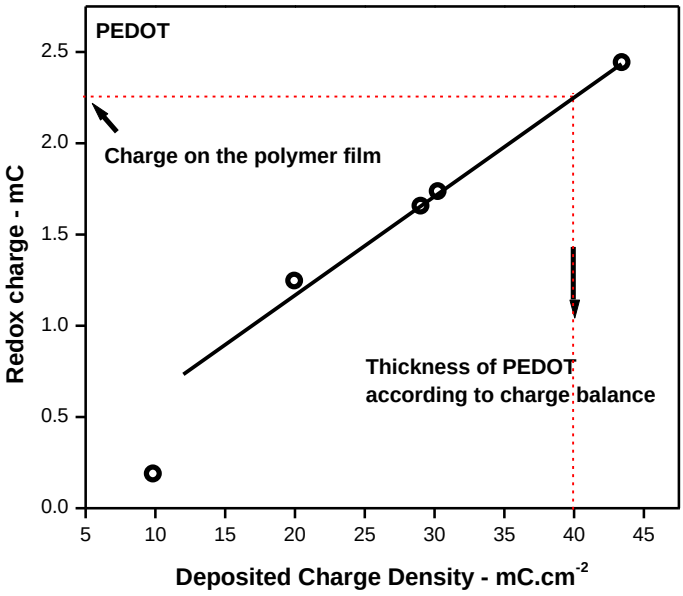

Figure 2.6. Redox charge vs deposited charge density graph of PEDOT films deposited by constant potential electrolysis with 1.5 V.

CHAPTER 3

RESULTS AND DISCUSSION

3.1. Benzimidazole Based DAD Type Monomers and Their Polymers Including EDOT Donor Units

3.1.1. Electrochemical Behaviour of E6E, E7E and E8E

Prior to electrochemical polymerization, electrochemical behaviour of the monomers were investigated not only to find the suitable polymerization potential but also to understand the effect of different ring size of the acceptor units on the electrochemical behaviour of the monomers. The cyclic voltammograms of **E6E, E7E** and **E8E** monomers were recorded in ACN - DCM solvent mixture (90 : 10 v / v) containing 0.1 M $LiClO_4$ as supporting electrolyte and the results are depicted in Figure 3.1. As seen from the figure**,** the monomers exhibit an irreversible oxidation peak at about 0.80 V vs Ag/AgCl (0.50 V vs Fc/Fc^+) during the first anodic scan. Although all three monomer behaviours seem similar, **E8E** (0.73 V vs Ag/AgCl, 0.43 V vs Fc/Fc^+) has the lowest and **E7E** (0.80 V vs Ag/AgCl, 0.50 V vs Fc/Fc^+) has the highest oxidation potential indicating that the monomers which includes even number ring on their acceptor groups can be oxidized relatively easier. On the other hand, no reduction peak was observed during the cathodic scan for all three monomers in $LiClO_4$ electrolyte medium.

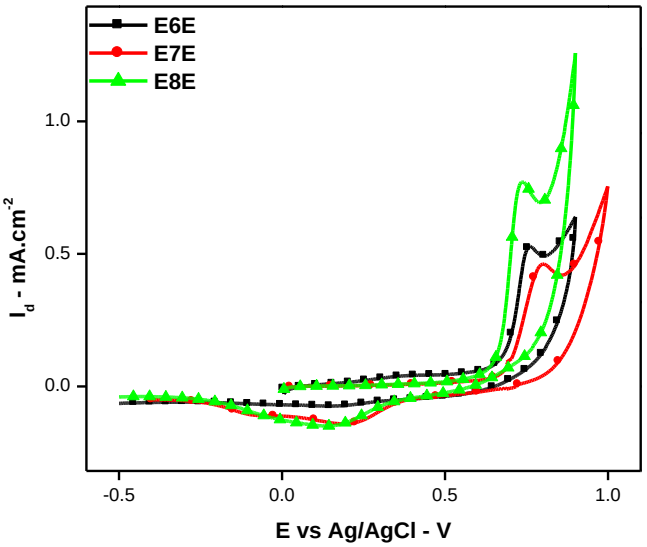

Figure 3.1. The cyclic voltammograms of **E6E**, **E7E**, **E8E** monomers in 0.1 M $LiClO_4$ in ACN - DCM (90:10 v/v) between -0.5 V and 0.90 V for **E6E** and **E8E** and between -0.5 V and 1.00 V for **E7E** vs Ag/AgCl at a scan rate of 100 mV/s.

3.1.2. Optical Characterization of E6E, E7E and E8E

The optical properties of the monomers were determined by recording their electronic absorption spectrum in DCM and the spectra were given in Figure 3.2. All three monomers exhibited two optical absorption bands due to their donor-acceptor pattern. One of the reasons for the existence of second (low lying) absorption band in DAD type molecules might be charge transfer between donor and acceptor units together with $\pi \rightarrow \pi^*$ transition [182]. As seen from Figure 3.2, the maximum absorption wavelengths for **E6E**, **E7E** and **E8E** are at 314 / 539 nm, 312 / 532 nm and 312 / 530 nm, respectively. A close inspection of these values indicates that the ring size on the acceptor unit has no significant effect on absorption maxima except a slight blue shift in the low lying band with increasing ring size. On the other hand, intensity of the absorption peak at longer wavelength gives an important clue for ICT efficiency between donor and acceptor units. In order to clarify this, the electronic

absorption spectra of the monomers were normalized in terms of the shorter wavelength optical absorption bands. The better charge transfer feature between the donor - acceptor units occurs in **E6E** and it decreases with increasing ring size. The optical band gap values of corresponding monomers were calculated by using the onset of the longer wavelengths in the optical absorption spectra. The band gap values of the monomers are found as 1.99 eV for **E6E** and 2.03 eV for **E7E** and **E8E**. Table 3.1 summarizes the obtained electrochemical-optical properties of the monomers.

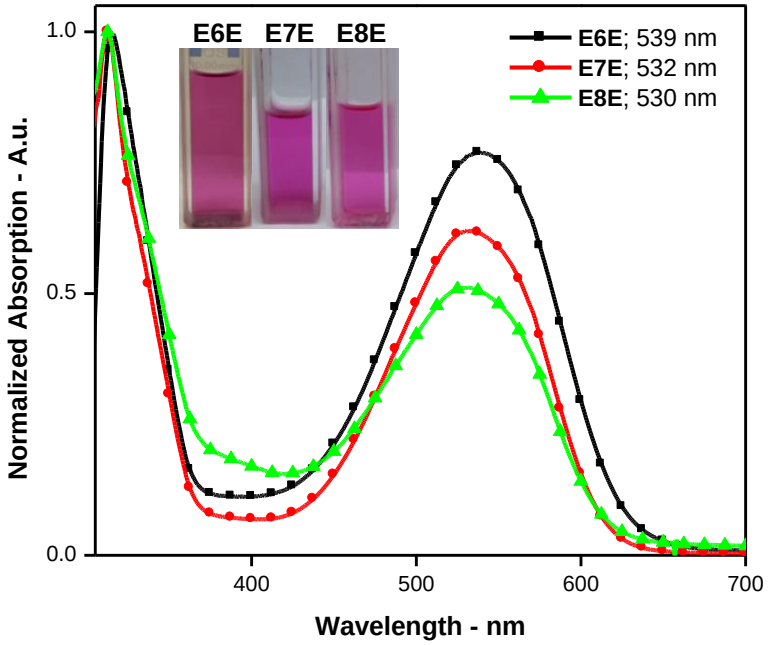

Figure 3.2. Normalized optical absorption spectra of **E6E**, **E7E** and **E8E** monomers in DCM. Inset: Colors of the monomers under day light.

The fluorescence spectra of the monomers were also recorded in DCM and the results are presented in Figure 3.3. The fluorescence spectra of all the monomers exhibited strong luminescence maxima in the wavelength region 640–650 nm corresponding to red color, upon their excitation at 525 nm. Emission maxima for the three monomers are very close (650 nm, 648 nm and 645 nm for **E6E**, **E7E** and **E8E**, respectively) exhibiting a small blue shift as the ring size increases from **6** to **8**. The fluorescence results are compatible with the UV results indicates the bathochromic shift and the stronger ICT with decreasing the ring size.

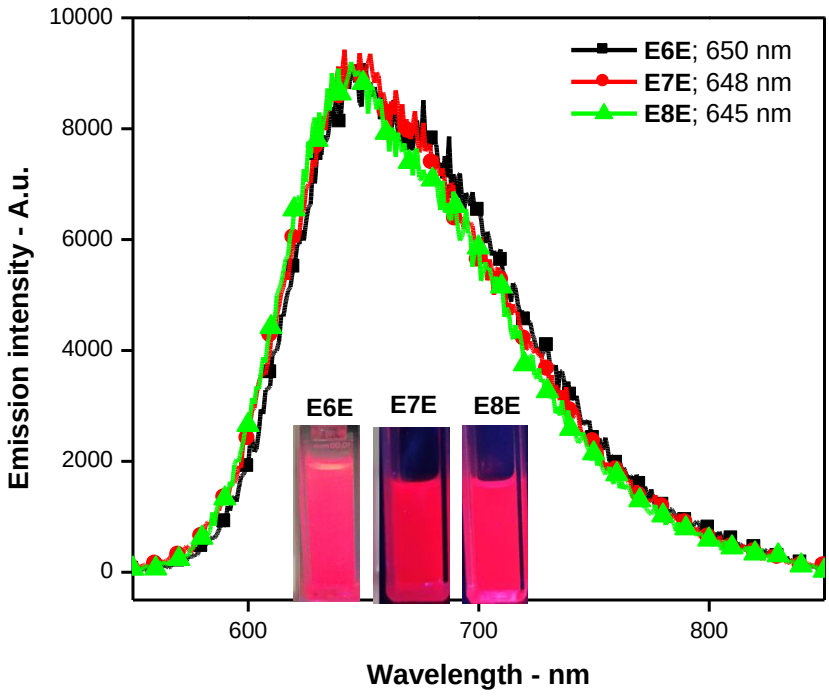

Figure 3.3. Emission spectra of **E6E**, **E7E** and **E8E** in DCM. Inset: Colors of the monomers under 366 nm UV-light.

Photoluminescence (PL) solvatochromism is a useful method for examining the electronic properties of excited states by systematically changing the dielectric properties (polarity) of the surrounding environment (solvent). If the excited-state dipole of a chromophore is larger than that of the ground state, increasing the polarity of the solvent will stabilize the excited state more than the ground state, producing a red shifted emission [183]. In order to clarify the existence of intramolecular charge transfer between D and A units, solvatochromic experiments were performed. The optical absorption and emission spectra of monomers were monitored in three different solvents with different dielectric constants: DCM (9.1), THF (7.5) and toluene (2.4) and the results are shown in Figure 3.4. Although λ_{max} values for the three monomers investigated did not show a straight trend with increasing solvent polarity, a slight red shift was observed in the emission maxima with increasing solvent polarity. In the case of **E6E**, λ_{max} appears at 542 nm in toluene (the least polar solvent) and this value shifts to 548 nm in THF with increasing solvent polarity. However, λ_{max} undergoes almost 9 nm blue shift, in DCM, with further increase in solvent polarity. The same relation was also observed for **E7E** (λ_{max}= 532 nm in DCM, 537 nm in THF and 536 nm in toluene) and **E8E** (λ_{max}= 530 nm in DCM, 537 nm in THF and 536 nm in toluene). However, when the emission spectra of the monomers recorded in different solvents were examined (see Figure 3.4) a slight red shift in the emisson maxima was observed for all three monomers with increasing solvent polarity. In the case of **E6E**, emission spectra shifts from 636 nm (toluene) to 648 nm (THF) and to 650 nm (DCM). Similar trend was also observed in the case of **E7E** ($\lambda_{emission}$= 643 nm, 645nm and 648 nm in toluene, THF and DCM, respectively) and **E8E** ($\lambda_{emission}$= 641 nm, 644 nm and 645 nm in toluene, THF and DCM, respectively). This red shift in the emission wavelength proves that the low-energy band present in the absorption spectrum is originating most probably from intramolecular charge transfer [184]. Furthermore, since the observed red shift with increasing the polarity of solvents is highest in **E6E** and lowest in **E8E**, it can be concluded that the extent of intramolecular charge transfer decreases with increasing ring size on benzimidazole unit for the monomers, **E6E**, **E7E** and **E8E**.

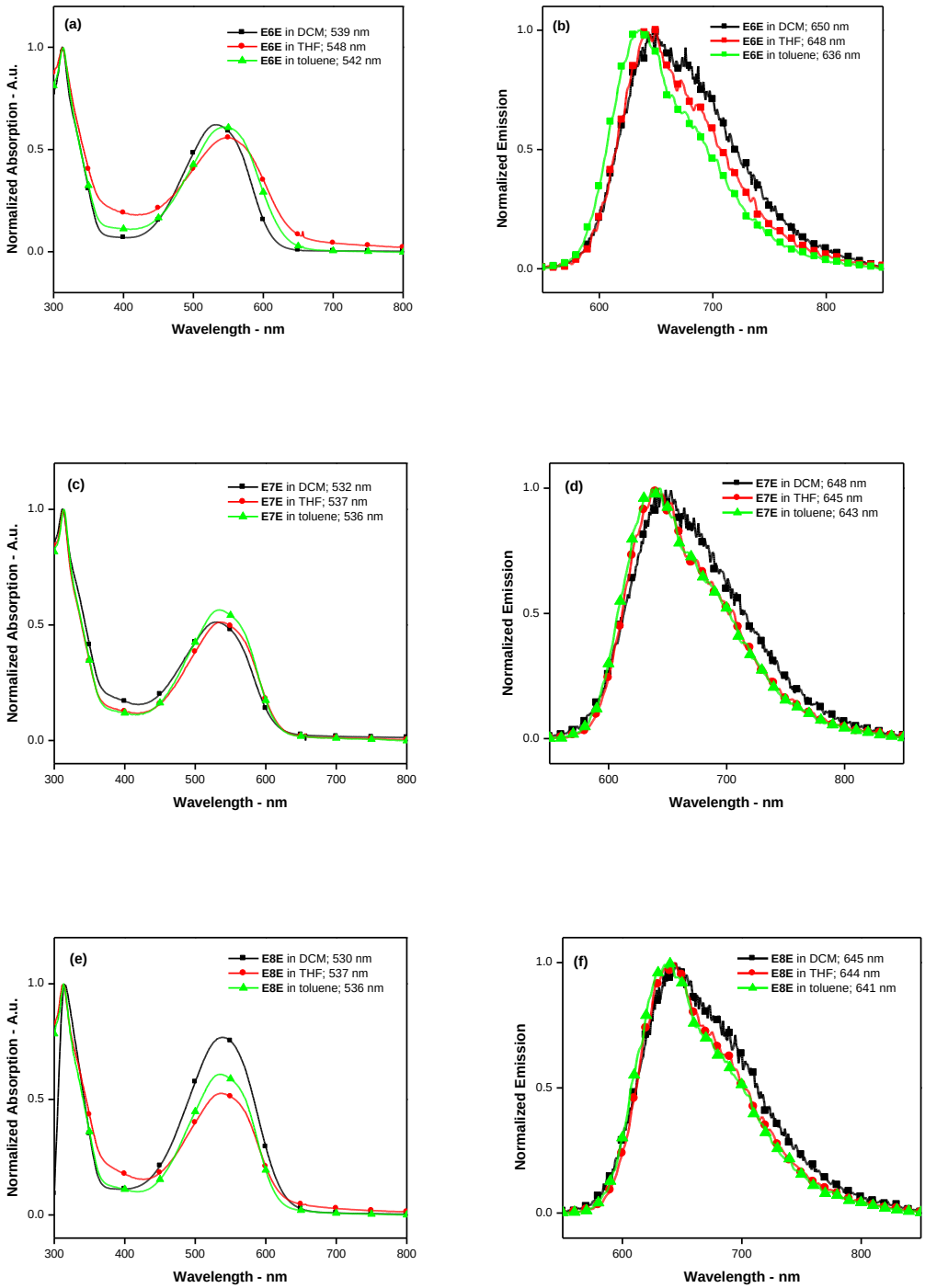

Figure 3.4. The normalized absorption and emission spectra of **E6E** (**a, b**); **E7E** (**c, d**) and **E8E** (**e, f**) in different solvents of DCM, THF and toluene.

Table 3.1. Electrochemical and spectroelectrochemical properties of **E6E**, **E7E**, **E8E**.

Monomers	λ_{max} (abs) nm	λ_{max} (ems) nm	E_{ox} (V)	$E_{ox(onset)}$ (V)	HOMO (eV)	LUMO (eV)	$E_g^{(UV)}$ (eV)
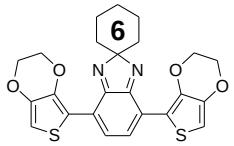 E6E	314 539	650	0.46 *	0.38 *	-5.18 **	-3.19 **	1.99
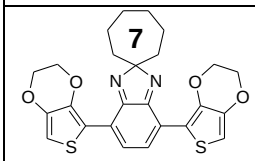 E7E	312 532	645	0.50 *	0.39 *	-5.19 **	-3.16 **	2.03
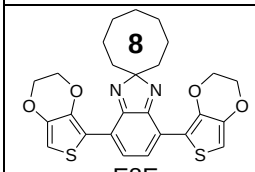 E8E	312 530	648	0.43 *	0.35 *	-5.15 **	-3.12 **	2.03

* with respect to $E_{ox(onset)}$ of Fc/Fc^+ (0.30 V)
** $E_g = -[E_{ox(onset)} + 4.80]$ and HOMO = [LUMO - E_g] [185]

3.1.3. Polymerization of E6E, E7E and E8E and Their Characterizations

3.1.3.1. Electrochemical Polymerization of E6E, E7E and E8E

The electrochemical polymerizations of **E6E**, **E7E** and **E8E** were achieved in electrolyte solutions consisting of 0.1 M $LiClO_4$ dissolved in ACN - DCM mixture (90:10 v/v) via repetitive cycling. The solvent mixture was used because of poor solubility of monomers in ACN. Polymer films, P(**E6E**), P(**E7E**) and P(**E8E**), were deposited on the Pt-WE surface via potential cycling from -0.5 V to 0.85 V (for **E6E** and **E8E**); -0.4 V to 1.0 V (for **E7E**). During potential scanning, new oxidation and reduction peaks appeared in all three polymerization. Appearance of the new redox peak is the fingerprint of the polymer formation. Also, the current intensities were

increased in every successive scan which indicated the increase in polymer film thickness on the electrode surface. Figure 3.5 (a-b-c) shows the cyclic voltammograms recorded during repetitive cycling.

Although $LiClO_4$ was used as supporting electrolyte, instead of more commonly used $TBABF_4$, during electrochemical polymerizations the latter was used during investigating the electrochemical behaviours of the polymer films. The reason for using $LiClO_4$ during polymerizations of the monomers is because of better polymerization efficiency. BF_4^- anions caused the right shifted oxidation potentials for the monomers and also resulted in less current increase during the electropolymerization. Higher current densities were obtained when $LiClO_4$ was used as the electrolytic medium. In case of investigating electrochemical behaviour of polymers we have used $TBABF_4$ since $N(Bu)_4^+$ cations are better than Li^+ during the n-doping process. The n-doping property was obtained for the polymers when $TBABF_4$ was used instead of $LiClO_4$.

After 15 succesive scans, the polymer film coated electrode was washed with and left in ACN to remove any unreacted monomer and oligomeric species. The redox behaviour of the polymer films were investigated by recording their cyclic voltammograms in monomer free electrolyte solution, consisting of 0.1 M $TBABF_4$ in ACN, and the results are given in Figure 3.5-d.

Further electrochemical studies (i.e. oxidation-reduction potentials, polymer film stability, n-doping, scan-rate dependence etc.) were performed on the polymer films obtained via constant potential electrolysis at applied potential of 0.90 V in the supporting electrolyte solution of 0.1 M $LiClO_4$ - ACN/ DCM mixture (90:10 v/v) vs Ag/AgCl.

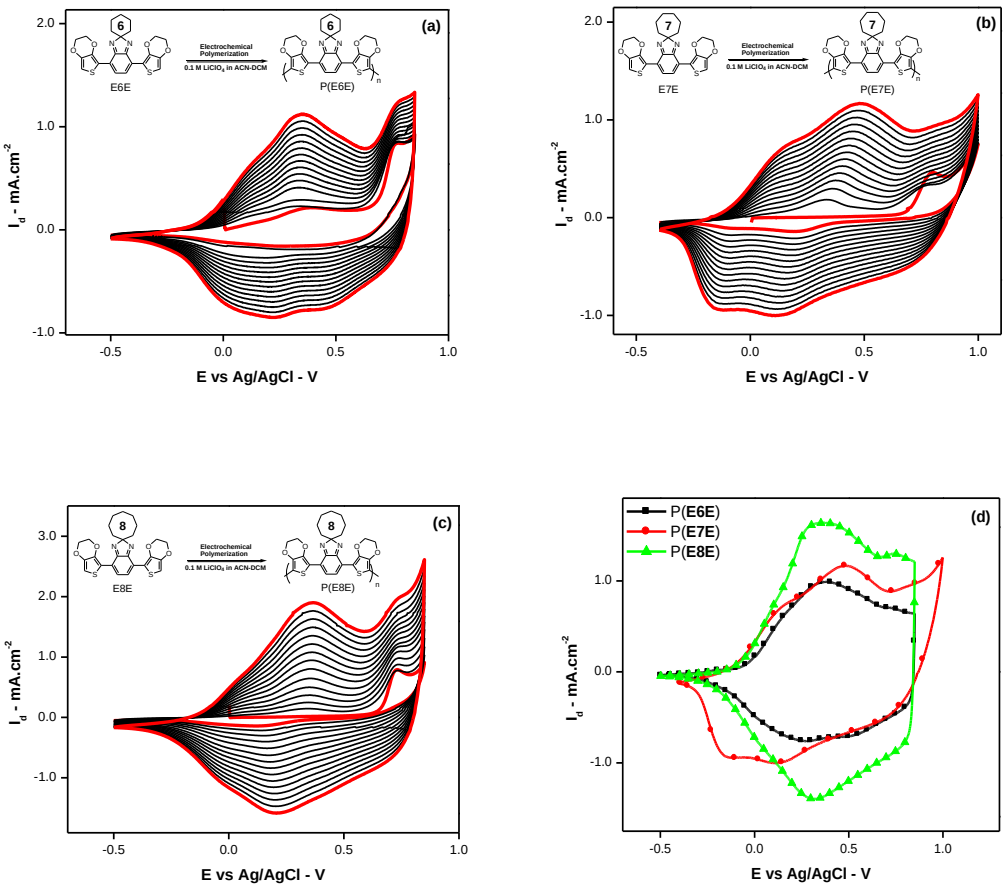

Figure 3.5. Electropolymerization of **E6E** between -0.5 V and 0.85 V **(a)**, **E7E** between -0.4 V and 1.0 V **(b)**, **E8E** between -0.5 V and 0.85 V **(c),** with 15 cycles in 0.1 M $LiClO_4$ solution of ACN-DCM at a scan rate of 100 $mV.s^{-1}$ on Pt WE. The cyclic voltammograms of the resulting polymers **(d),** versus Ag/AgCl in monomer free electrolyte solution of 0.1 M $TBABF_4$-ACN at a scan rate of 100 $mV.s^{-1}$.

When the total Faradaic charge reached to 80 mC.cm^{-2} electrolysis was stopped and polymer coated WE was transfered into monomer free electrolyte solution to monitor their redox behaviour. When P(**E6E**), P(**E7E**), and P(**E8E**) were scanned anodically in monomer-free electrolyte solution, they exhibited well-defined reversible redox couples due to p-doping (E_p^{ox} = +0.28 V and +0.61 V (-0.02 V and +0.31 V vs Fc/Fc$^+$) for P**(E6E)**; E_p^{ox} = +0.25 V and +0.61 V (-0.05 V and + 0.31 V vs Fc/Fc$^+$) for P**(E7E)** and E_p^{ox} = +0.32 V together with two shoulders at about -0.11 V and 0.73 V (main peak at +0.02 V and the shoulders at -0.19 V and at 0.43 V vs Fc/Fc$^+$) for P**(E8E)** (see Figure 3.6-a). Oxidation onset potentials of the P(**E6E**) and P(**E8E**) measured as equal and 30 mV lower than that of P(**E7E**). P(**E7E**) exhibited highest oxidation onset among the others as in the case its monomers.

Unlike the monomers, polymer films exhibited well-defined reversible n-doping process. This might be due to using two different supporting electrolytes in investigating electrochemical behaviour of monomers and their corresponding polymer films. The results followed during n-dopings are depicted in Figure 3.6-b. ($E_n^{red-onset}$ = -1.01 V (-1.31 vs Fc/Fc$^+$) for P**(E6E)**; $E_n^{red-onset}$ = -1.00 V (-1.30 vs Fc/Fc$^+$) for P**(E7E)** and $E_n^{red-onset}$ = -1.05 V (-1.35 vs Fc/Fc$^+$) for P**(E8E)**). It can be concluded that removing an electron from the cycloheptane ring bearing monomer (and also its polymer) is harder than that of the even number ring bearing monomers. On the other hand, inserting an electron is easier in P(**E7E**) than P(**E6E**) and P(**E8E**). Based on the results, it can be said that, **E6E**, **E8E**, P(**E6E**) and P(**E8E**) are more electron rich than **E7E** and P(**E7E**).

The oxidation-reduction onset potentials, optical band gap values, HOMO-LUMO levels and the colors of the polymer films were given in Table 3.2. Furthermore, the oxidation and reduction onset values were utilized to elucidate electrochemical band gap value of the polymer films (E_g^{CV}) and tabulated in Table 3.3.

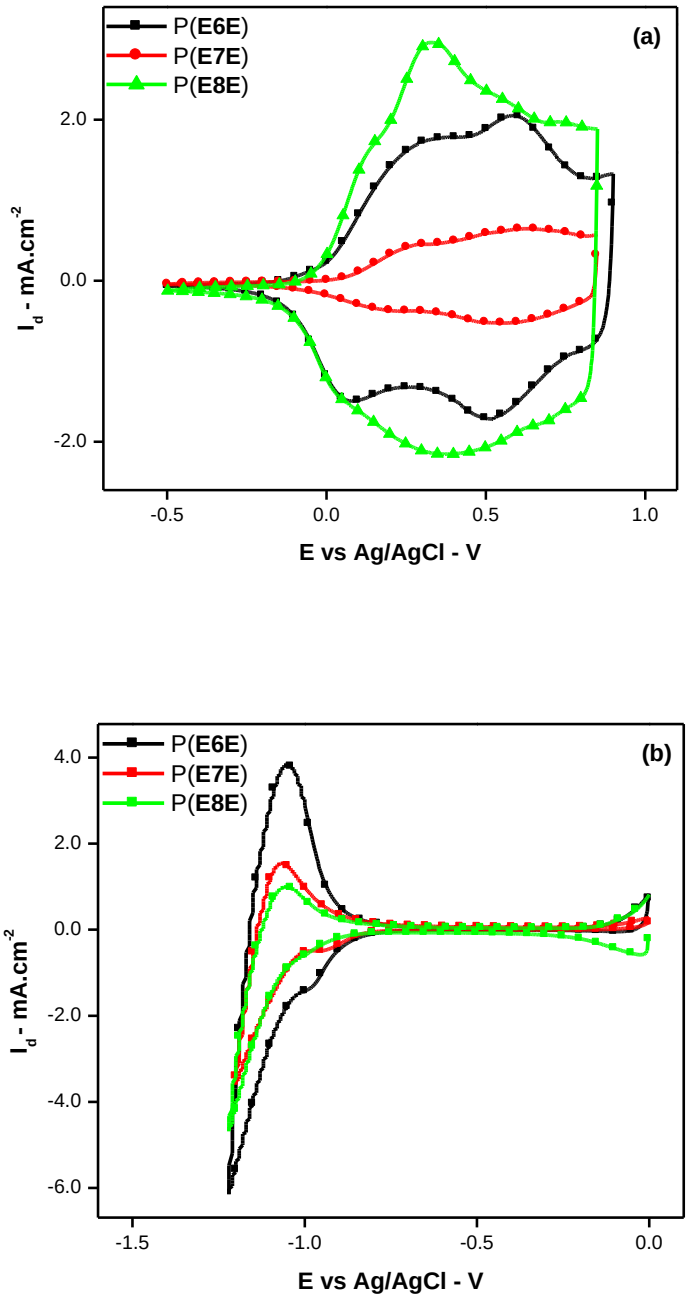

Figure 3.6. (a) Cyclic voltammograms of the polymers (P(**E6E**), P(**E7E**), P(**E8E**)) obtained by constant potential electrolysis with the charge of 80 mC.cm^{-2} on Pt working electrode between -0.5 V and 0.9 V in 0.1 M $TBABF_4$-ACN monomer free electrolyte solution vs Ag/AgCl. **(b)** Cyclic voltammograms of the polymers (P(**E6E**), P(**E7E**), P(**E8E**)) during n-doping process between 0.0 V and -1.25 V in 0.1 M $TBABF_4$-ACN monomer free solution vs Ag/AgCl reference electrode.

The scan rate dependence of the polymers was also investigated in order to see if the polymer films well adhered to the electrode surface. Scan rate is increased with the increments of 20 up to 200 $mV.s^{-1}$ starting with 20 $mV.s^{-1}$. Scan rate dependence experiments showed that both anodic and cathodic peak currents increase linearly with increasing scan rate, indicating a well-adhered polymer film on the WE surface and a non-diffusional redox process, which was shown in Figures 3.7. Moreover, charge vs scan rate graphs show that if the polymer films can achieve charging-discharging process effectively. The anodic and cathodic charges vs scan rate graphs of the polymer films showed that the charging-discharging process of the polymer film is effectively achieved even at higher scan rates.

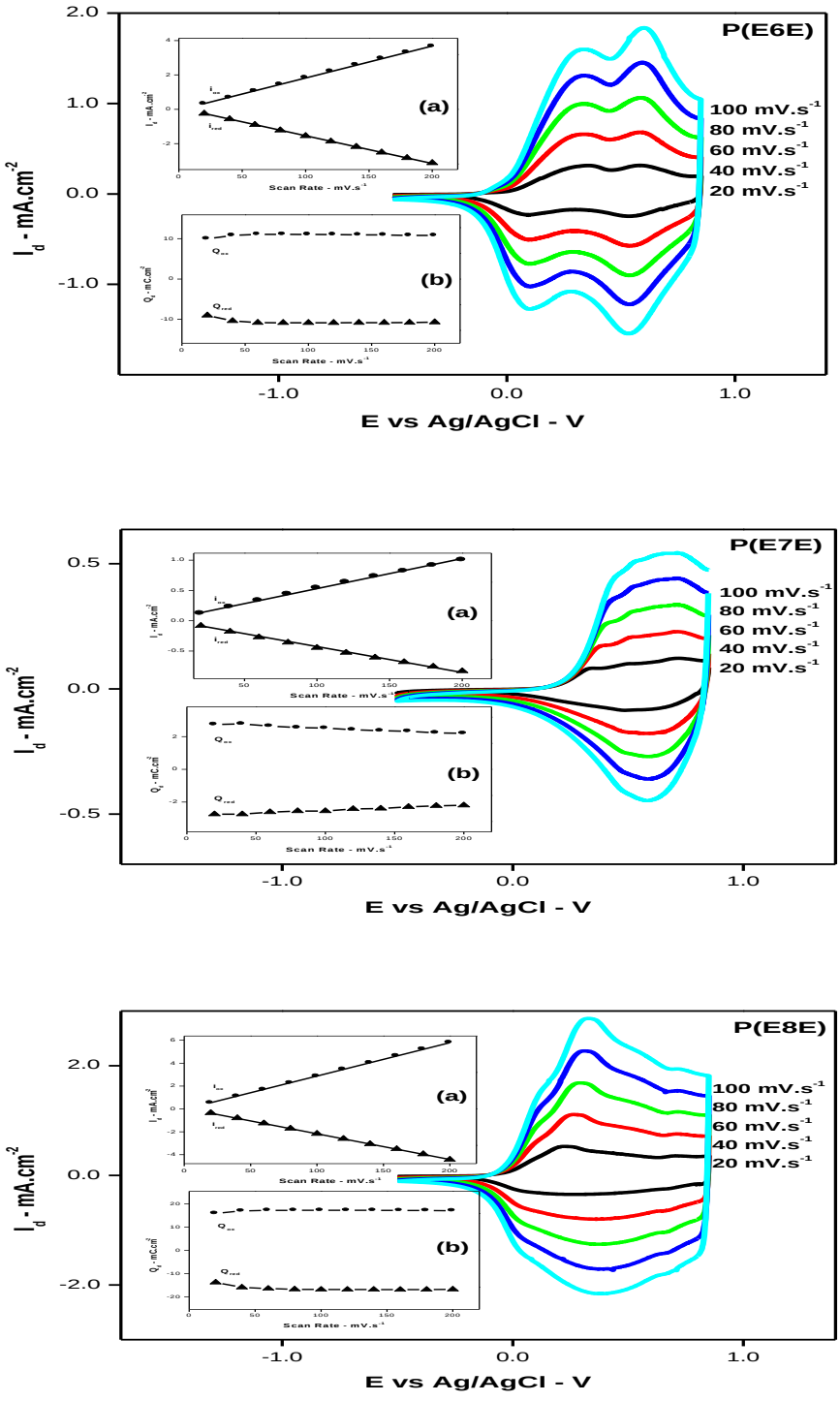

Figure 3.7. Scan rate dependence of P(**E6E**), P(**E7E**) and P(**E8E**) on Pt disc electrode in 0.1 M $TBABF_4$-ACN at a scan rate of 20 - 40 - 60 - 80 - 100 $mV.s^{-1}$ between -0.5 V and 0.90 V. Inset: The current vs scan rate **(a)** and the charge density vs scan rate **(b)** plots of the polymer films with increasing scan rates.

The electrochemical stability can be defined as the ability of retaining electrochemical properties upon repetitive doping-dedoping process. This is an important parameter for conjugated polymers for being a good candidate in electronic device applications. Electrochemical stability of the polymer films obtained by constant potential electrolysis (+ 0.90 V vs Ag/AgCl, 80 $mC.cm^{-2}$) on Pt disc WE were studied with square wave potential method under ambient conditions by applying the potentials of -0.2 V and 0.6 V of 3 s for each. Cyclic voltammograms were recorded after 100, 350, 600 and 1000 switchings. After 1000 cycle is complete, the first cyclic voltammogram of the polymers were compared to their last cycles in terms of amount of charge lost. If there is no lost in current intensity or charge, the cycle number was further increased.

According to the voltammograms, P(**E6E**) showed 9.6 % charge lost in anodic region after 1000 switcing. In the cathodic part, the charge lost value was determined as 9.4 %. P(**E7E**) exhibited different trend in stability survey. There was a right shift in cyclic voltammogram after 1000 cycles. The oxidation onset potential value of P(**E7E**) was right shifted by 0.15 V after 1000 cycles. Moreover, P(**E7E**) lost its charge by 29 % and 27 % in anodic and the cathodic part, respectively. P(**E8E**) showed the best stability profile. Even after 5000 switching, there was only 5 % charge lost both in anodic and cathodic region (Figure 3.8).

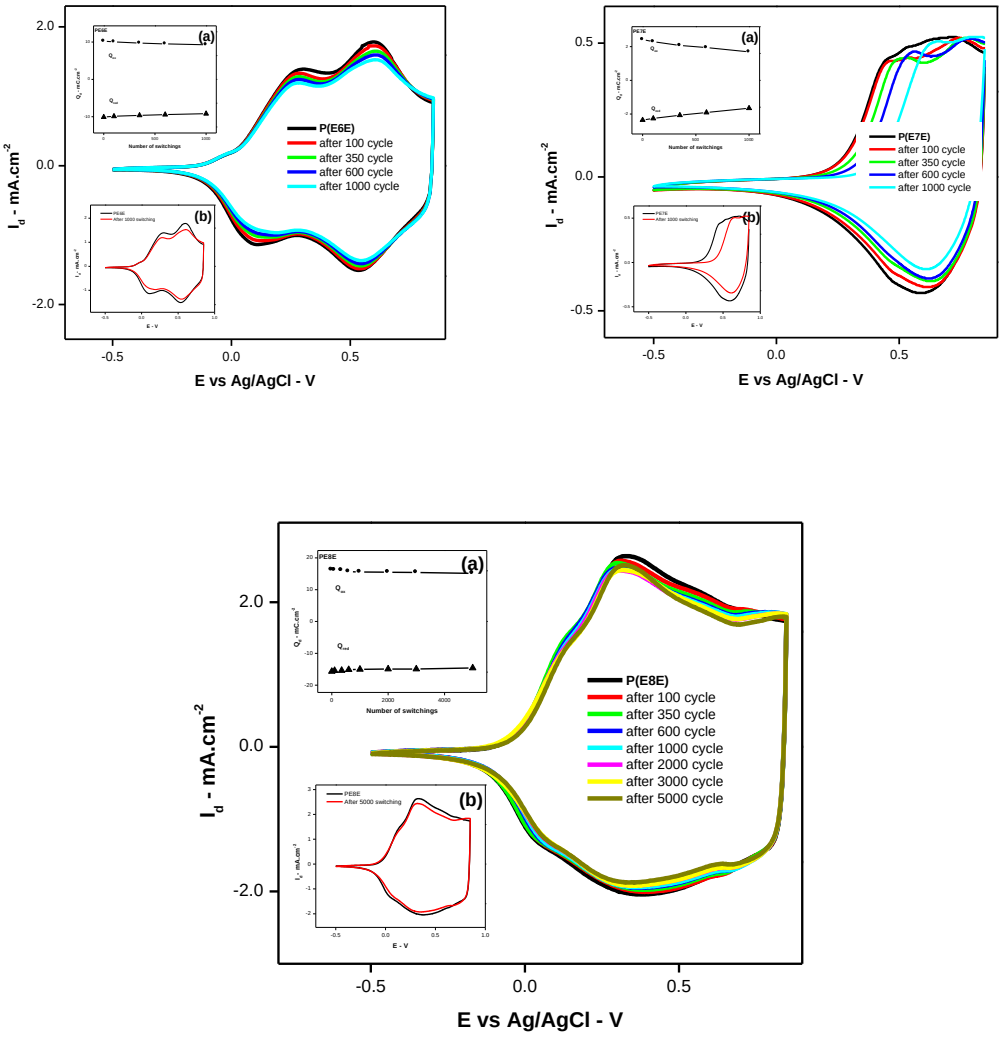

Figure 3.8. Cyclic Voltammograms of P(**E6E**), P(**E7E**) and P(**E8E**) films after many of switchings. Insets: **(a)** Anodic and cathodic charge density vs number of switching graphs of P(**E6E**) film in 0.1 M $TBABF_4$ - ACN achieved by square wave potential (-0.2 V for 3 s and 0.6 V; 3 s for each) under ambient conditions. **(b)** The first and the last cyclic voltammograms of polymer films in 0.1 M $TBABF_4$ - ACN.

Table 3.2. Electrochemical and spectroelectrochemical properties of P(**E6E**), P(**E7E**) and P(**E8E**).

Polymers	λ_{max} (abs) nm	E_{ox} (onset) (V)	E_{red} (onset) (V)	HOMO (eV)	LUMO (eV)	Eg^{UV} (eV)	Red.	Neut.	Ox.
P(E6E)	433 835	-0.32 *	-1.31 *	-4.48	-3.31	1.17			
P(E7E)	430 820	-0.25 *	-1.30 *	-4.55	-3.36	1.19			
P(E8E)	431 828	-0.32 *	-1.35 *	-4.48	-3.30	1.18			

* with respect to $E_{ox(onset)}$ of Fc/Fc^+: 0.30 V.

3.1.3.2. Optical Characterization of P(E6E), P(E7E) and P(E8E)

In order to elucidate the electrochromic features, polymer films were deposited on ITO WE via constant potential electrolysis in ACN-DCM solvent mixture (90:10 v/v) containing 0.1 M $LiClO_4$ as supporting electrolyte. After completion of electrolysis, polymer coated ITO electrode was first washed with and left in ACN to remove any unreacted monomer and then transferred into UV cuvette containing monomer free electrolyte solution (0.1 M $TBABF_4$ in ACN) to monitor the transitions between the neutral (dedoped), oxidized (p-doped) and reduced (n-doped) states under a voltage pulse. P(**E6E**), P(**E7E**) and P(**E8E**) exhibited two absorption maxima, in their neutral form, due to their DAD characteristics. Absorption maxima of the polymer films appeared at 433 / 835 nm, 430 / 820 nm and 431 / 828 nm for P(**E6E**), P(**E7E**) and P(**E8E**), respectively. The latter band can be attributed to the ICT between the donor and the acceptor unit while the former band can be assigned to the $\pi \rightarrow \pi^*$ transition [107].

The evolution of the spectra upon electrochemical doping shows a simultaneous decrease of the absorbance at 433 / 835 nm for P(**E6E**), 430 / 820 nm for P(**E7E**) and 431 / 828 nm for P(**E8E**), which is accompanied by the formation of a new absorption band beyond 800 nm in the potential range from −0.5 V to +1.0 V indicating the formation of charge carriers. The polymer films also exhibits a color change from green (neutral) to gray (oxidized). All spectra recorded during potential cycling between −0.5 V and +1.0 V passes through the isosbestic points at about 965 nm for P(**E6E**), 950 nm for P(**E7E**) and 956 nm for P(**E8E**), indicating that polymer films were being interconverted between their neutral and oxidized states (see Figure 3.9 a, b and c). The n-doping behaviour of the polymer films were also confirmed by recording the changes in the electronic absorption spectra during cathodic scan from 0.0 to -1.7 V vs Ag wire. During reduction the intensity of dual band present in the neutral form of polymer films decreases in intensity (insets of Figure 3.9) which is accompanied by a color change from green to brick red indicating that polymer films exhibit electrochromic behaviour. However, no new band formation was observed due to instrumental limitation during the cathodic scan. Electrochromic response of polymer films observed during p and n-doping were also reported in terms of L*, a*, b* values in Table 3.3.

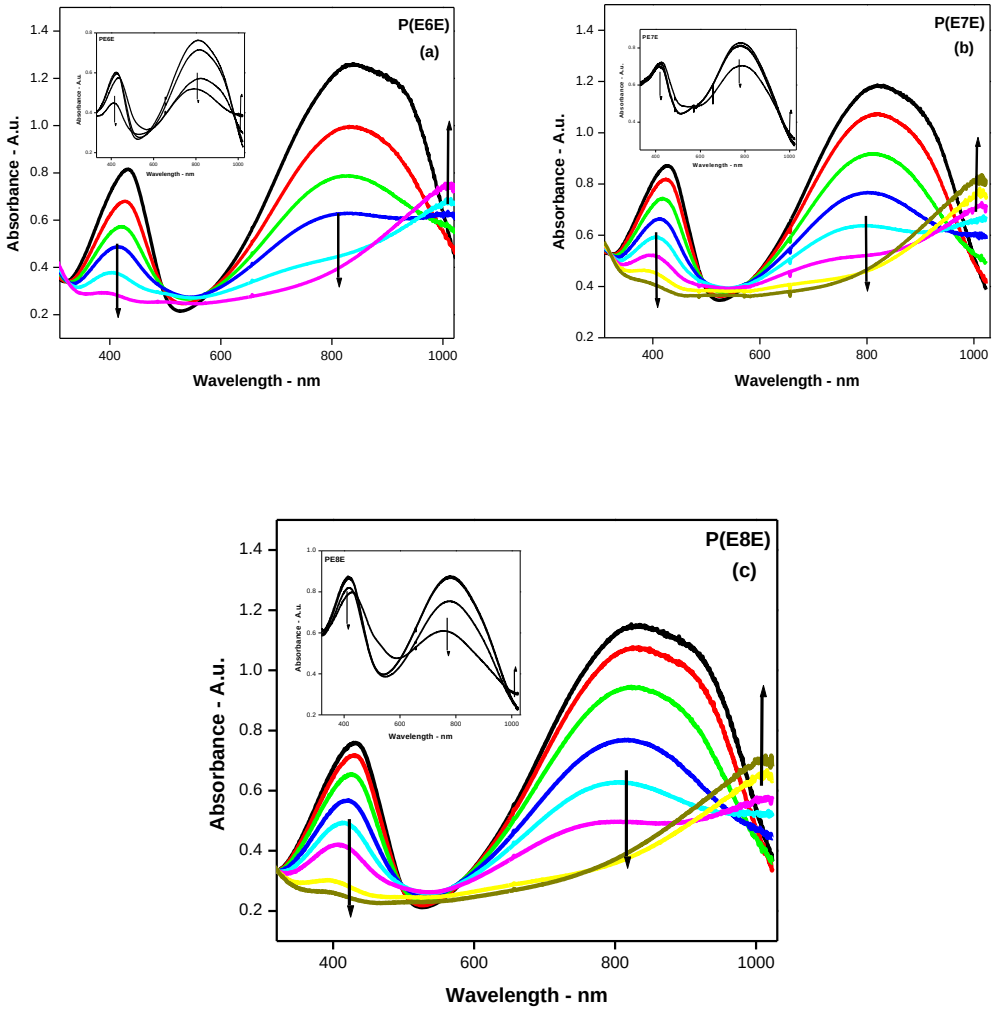

Figure 3.9. UV-VIS spectra of the polymer films ((**a**) P(**E6E**) of 30 mC.cm^{-2}, (**b**) P(**E7E**) of 35 mC.cm^{-2}, (**c**) P(**E8E**) of 20 mC.cm^{-2}) during oxidation from -0.5 V to 1.0 V via cyclic voltammetry with the scan rate of 20 mV.s^{-1}. Inset: reduction from 0.0 V to -1.7 V with the scan rate of 100 mV.s^{-1}.

The optical band gaps (E_g) of P(**E6E**), P(**E7E**), and P(**E8E**) were calculated from the onset of the low energy end of the π-π^* transitions to be 1.17 eV, 1.19 eV, and 1.18 eV, respectively, which were in well agreement with the band gaps calculated from cyclic voltammogram data (see Table 3.2). An inspection of E_g values obtained from two different methods indicates that P(**E6E**) has the smallest band gap value indicating stronger intramolecular charge transfer between D and A units in accordance with the fluorescence measurements. Oxidation potentials are reported vs. Fc/Fc^+ to calculate HOMO and LUMO levels of the polymers. The energy level of Fc/Fc^+ was taken as 4.80 eV below vacuum [185]. The oxidation onset potential of Fc/Fc^+ was measured as 0.30 V vs Ag/AgCl. HOMO and LUMO energy levels were obtained from the onset of the oxidation and reduction potentials of polymers and the results are given in Table 3.3.

3.1.3.3. Switching Behaviour of P(E6E), P(E7E) and P(E8E)

Switching study provides informations about switching time, optical contrast and coloration efficiencies which are important parameters for the application of conjugated polymers in electrochromic devices. Therefore, such properties of polymer films on ITO were also investigated under square wave input of predetermined potential ranges with the residence times of 10, 5, 3, and 2 s by monitoring the transmittance and the kinetic responses of the films at given wavelengths and the results are listed in Table 3.3. The switching times of the polymers were found as in subsecond levels (at 95 % of the full contrast and at their longer wavelengths) and the fastest switching behaviour was observed in P(**E8E**) (0.5 s). Furthermore, the CE values of the polymer films were calculated as 304 C/cm^2, 266 C/cm^2 and 316 C/cm^2 for P(**E6E**), P(**E7E**) and P(**E8E**), respectively, indicating that P(**E7E**) has the lowest CE.

Percent transmittance values are 40 %, 42.5% and 41% for P(**E6E**), P(**E7E**) and P(**E8E**), respectively in 10 s residence times with the potentials -0.5 V and 1.1 V which were measured at shorter absorption wavelengths. At longer wavelengths of

polymer films, the percent transmittance values were measured as 29 %, 36 % and 32.5 % for P(**E6E**), P(**E7E**) and P(**E8E**), respectively (Figure 3.10-11-12). As seen from the Figures 3.10-11-12, the transmittance of the polymers at their longer wavelengths exhibited a sudden increase during oxidation following by a decrease in the progressing seconds. This phenomenon is observed due to the overlapping of the polaron bands with the absorption maxima of the polymer films upon further oxidation.

In order to test the optical stability, the polymers were fully oxidized (by applying 1.1 V) and fully neutralized (by applying -0.5 V) with 5 s time intervals. The lost in percent transmittance after 50 switches for P(**E6E**), P(**E7E**) and P(**E8E**) were measured as 3 %, 24 % and 6 %, respectively, at their shorter wavelengths. P(**E6E**) and P(**E8E**) did not loose their percent transmittance at longer absorption maxima after 50 switching. However, 12 % loss was observed for P(**E7E**) at its longer absorption wavelength upon 50 repetitive redox process. The switching times of the polymers were given at Table 3.3.

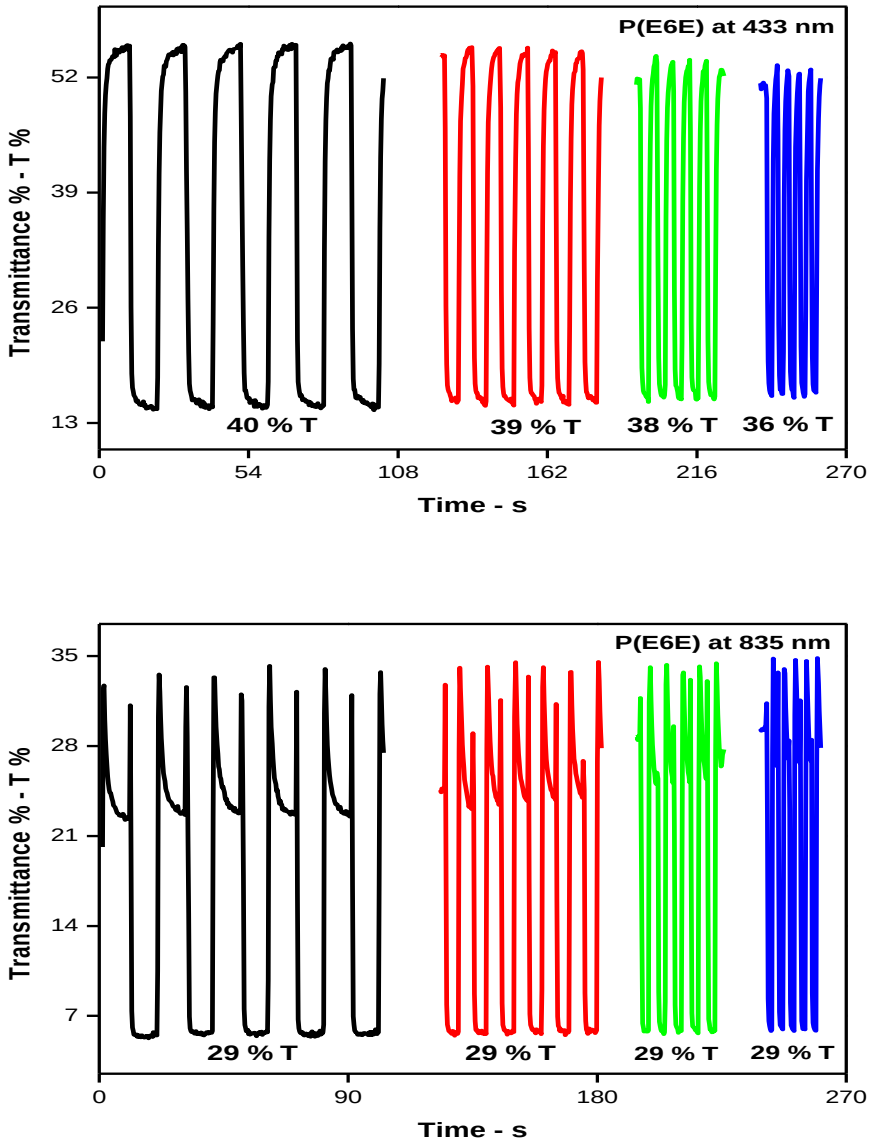

Figure 3.10. Transmittance change of P(**E6E**) film (25 mC.cm^{-2}) at 433 nm and 835 nm, in its fully oxidized (1.1 V) and reduced (-0.5 V) states in different switching times (10 s, 5 s, 3 s and 2 s).

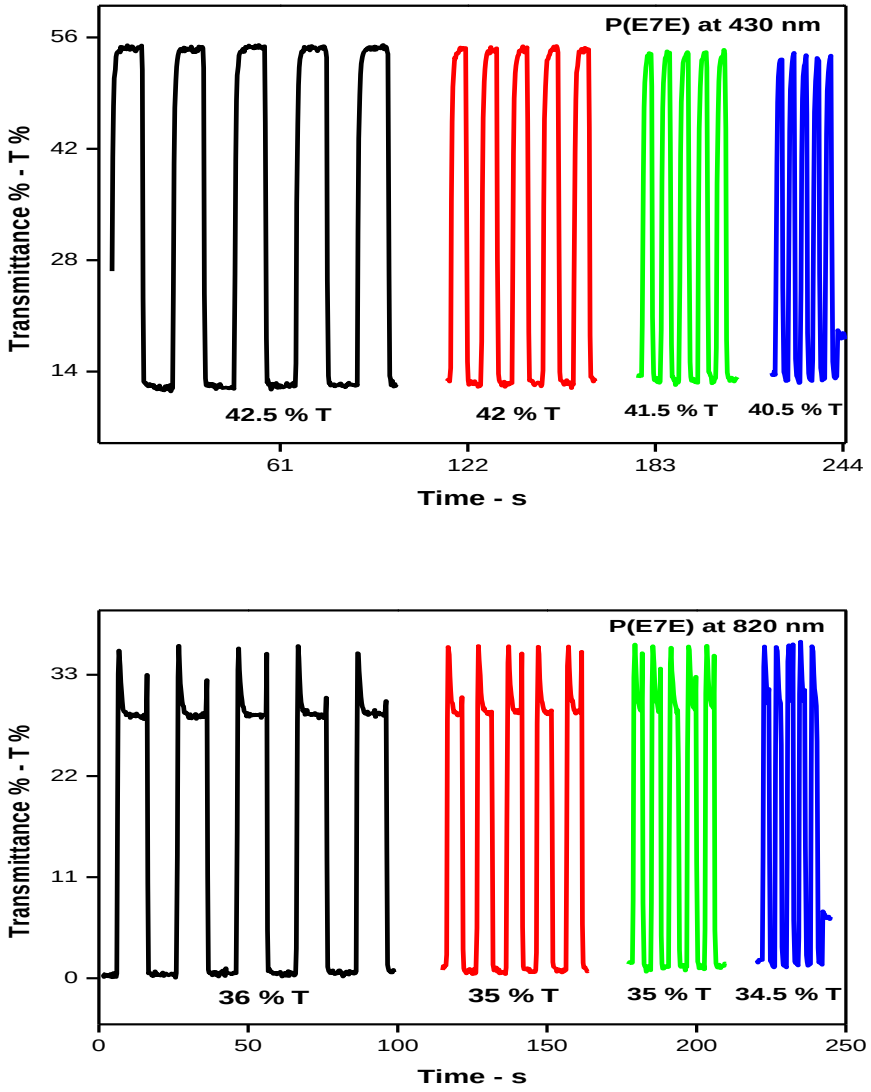

Figure 3.11. Transmittance change of P(**E7E**) film (25 mC.cm^{-2}) at 430 nm and 820 nm, in its fully oxidized (1.1 V) and reduced (-0.5 V) states in different switching times (10 s, 5 s, 3 s and 2 s).

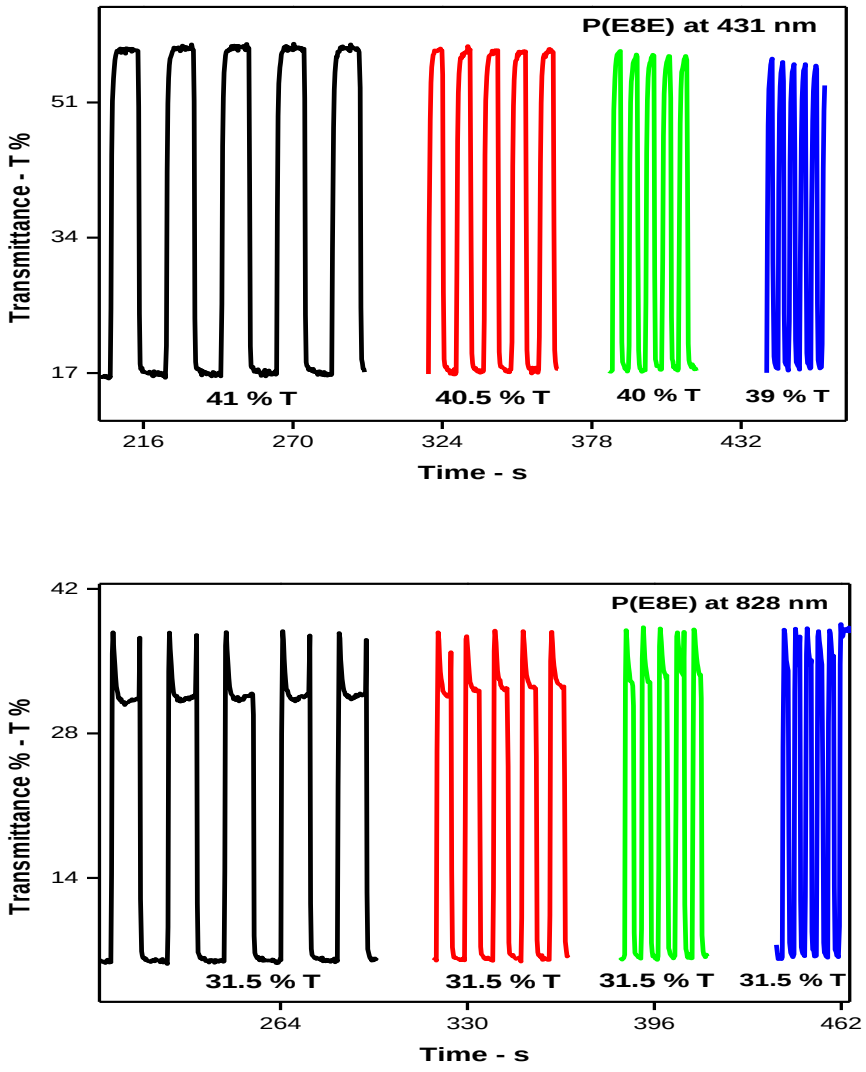

Figure 3.12. Transmittance change of P(**E8E**) film (20 mC.cm^{-2}) at 431 nm and 828 nm, in its fully oxidized (1.1 V) and reduced (-0.5 V) states in different switching times (10 s, 5 s, 3 s and 2 s).

Table 3.3. Electrochemical and optical properties of P(**E6E**), P(**E7E**), P(**E8E**)

		P(E6E)		P(E7E)		P(E8E)	
$E_{ox(onset)}$ (vs Fc/Fc^+)		-0.32		-0.25		-0.32	
$E_{red(onset)}$ (vs Fc/Fc^+)		-1.31		-1.30		-1.35	
E_g (from CV) (V)		0.99		1.05		1.03	
E_g (optical) (eV)		1.17		1.19		1.18	
HOMO (eV)		-4.48		-4.55		-4.48	
LUMO (eV)		-3.31		-3.46		-3.30	
λ_{max} (nm)		λ_{max1}	λ_{max2}	λ_{max1}	λ_{max2}	λ_{max1}	λ_{max2}
		433	835	**430**	820	**431**	828
t_{ox} (s) ** (95 % of full contrast)		1.7	0.6	1.2	0.6	1.7	0.6
t_{red} (s) ** (95 % of full contrast)		1.6	0.8	0.7	0.8	0.7	0.5
T % **		40	29	42.5	36	41	31.5
CE at 100 % of full contrast	Ox **	140	334	132	258	127	310
	Red **	164	156	198	253	154	233
CE at 95 % of full contrast	Ox **	162	304	164	266	135	316
	Red **	160	166	182	215	191	247
Colors at different redox states	Oxidized *	L: 79 a*: - 2 b*: 1.7		L: 72 a*: - 0.7 b*: 0.6		L: 81 a*: - 2 b*: 0.5	
	Neutral *	L: 76 a*: - 19 b*: 27		L: 68 a*: - 18 b*: 25		L: 77 a*: - 24 b*: 34	
	Reduced *	L: 65 a*: 7 b*: 26		L: 60 a*: 6 b*: 25		L: 61 a*: 5 b*: 20	
	Charge passed during polymerization	*30 $mC.cm^{-2}$ **25 $mC.cm^{-2}$		*35 $mC.cm^{-2}$ **25 $mC.cm^{-2}$		*20 $mC.cm^{-2}$ **20 $mC.cm^{-2}$	

* and ** indicates the amount of deposited charge on the polymer films given in the last row.

3.2. Benzimidazole Based DAD Type Monomers and Their Polymers Including PRODOT(C6) Donor Units

3.2.1. Electrochemical Behaviour of P6P, P7P, P8P

In order to investigate the ring size effect on the electrochemical behaviour of monomers, their cyclic voltammograms were recorded in ACN-DCM solvent mixture (90:10 v/v) containing 0.1 M $LiClO_4$ as supporting electrolyte and the results are depicted in Figure 3.13. As it is seen from the figure, the monomers, **P6P, P7P** and **P8P** exhibited an irreversible oxidation peak at around + 0.9 V vs Ag/AgCl during the first anodic scan. However, no reduction peak was observed during the cathodic scan for all three monomers in $LiClO_4$ electrolyte. Although **P7P** has the highest oxidation potential (0.88 V vs Ag/AgCl, 0.56 V vs Fc/Fc^+) among the three monomers, the difference in their oxidation potentials is not greater than 60 mV. This small difference is not unexpected, since the three monomers have the same donor units. Monomer oxidation potentials followed the same trend with EDOT containing monomers such that, the even number ring containing monomers (**P6P** and **P8P)** can be oxidized relatively easier than the odd number ring containing monomer (**P7P**).

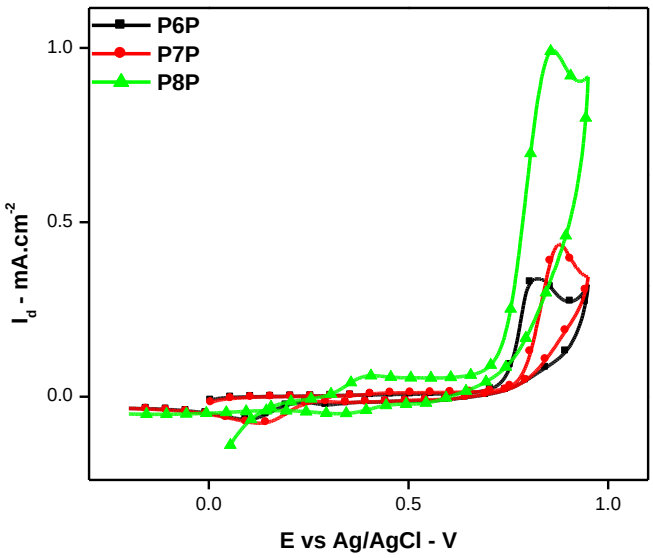

Figure 3.13. The cyclic voltammograms of **P6P**, **P7P**, **P8P** in 0.1 M $LiClO_4$ in ACN - DCM (90:10 v/v) between -0.2 V and 0.95 V vs Ag/AgCl at a scan rate of 100 mV/s.

3.2.2. Optical and Photophysical Properties of P6P, P7P and P8P

The optical properties of the monomers were determined by recording their electronic absorption spectrum in DCM and the results are shown in Figure 3.14. Similar to the first DAD type monomers (i.e. monomers with EDOT donor units), all three monomers exhibited two optical absorption bands, one at about 310 nm in the UV region and the other in the visible region at about 520 nm, due to their donor-acceptor pattern. The negligible variations in the absorption wavelengths for **P6P**, **P7P** and **P8P** (see Table 3.4) clearly show that the ring size on the acceptor unit has no significant effect on absorption maxima. A comparison of these values with that of EDOT containing monomers (**E6E, E7E, E8E)** indicates a blue shift in the low lying absorption bands of **P6P, P7P, P8P**. This observation reveals the existence of stronger intramolecular charge transfer in **E6E, E7E, E8E** as compared to **P6P, P7P, P8P**. It is well known that the intramolecular charge transfer also depends on the

planarity of the DAD type monomer. Presence of the hexyl substituents on the PRODOT donor unit might lower the planarity causing a decrease in the extend of intramolecular charge transfer [186]. On the other hand, when the absorption peaks were normalized in terms of the higher energy peaks, **P8P** showed the more intense low lying absorption peak among three monomers which indicates the **P8P** has stronger ICT between its donor-acceptor units. **P6P** and **P7P** exhibited the same peak intensity which are lower than that of **P8P**.

The optical band gap values of corresponding monomers were calculated by using the onset of the longer wavelengths in the optical absorption spectra. The band gap values of the monomers were found as 2.04 eV for **P7P** and 2.05 eV for **P6P** and **P8P**. These values are slightly higher that that of their EDOT containing analogous. Table 3.4 summarizes the collected data related to electrochemical and optical properties of the monomers.

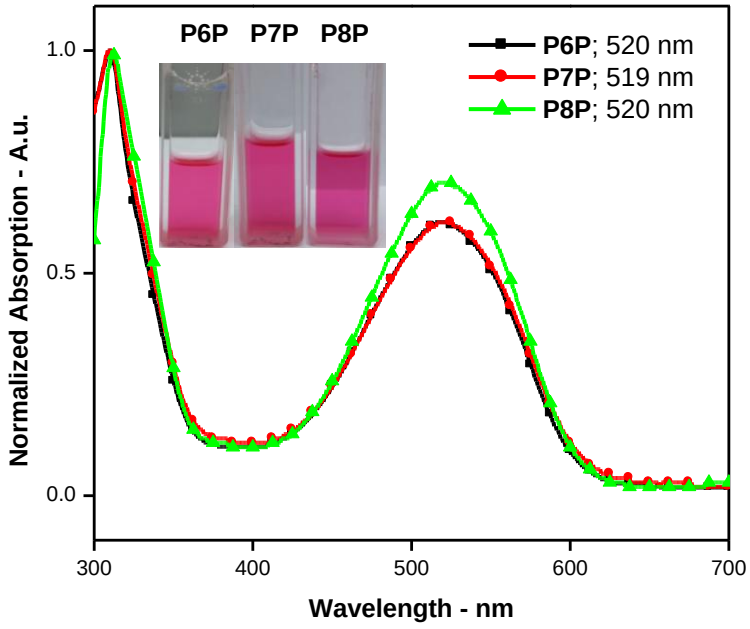

Figure 3.14. Optical absorption spectra of **P6P**, **P7P** and **P8P** monomers in DCM. Inset: Colors of the monomers under day light.

The fluorescence spectra of the monomers were recorded in DCM and the results are given in Figure 3.15. As seen from the figure, emission maxima for the three monomers are very close (643 nm, 645 nm and 645 nm for **P6P**, **P7P** and **P8P**, respectively) indicating no significant effect of the ring size on the acceptor unit. Solvatochromic experiments were also performed to clarify the existence of intramolecular charge transfer between D and A units. As in the case of first group of DAD type monomers, same three solvents with different dielectric constants were used in recording the electronic absorption and emission spectra and the resulting spectra are shown in Figure 3.16.

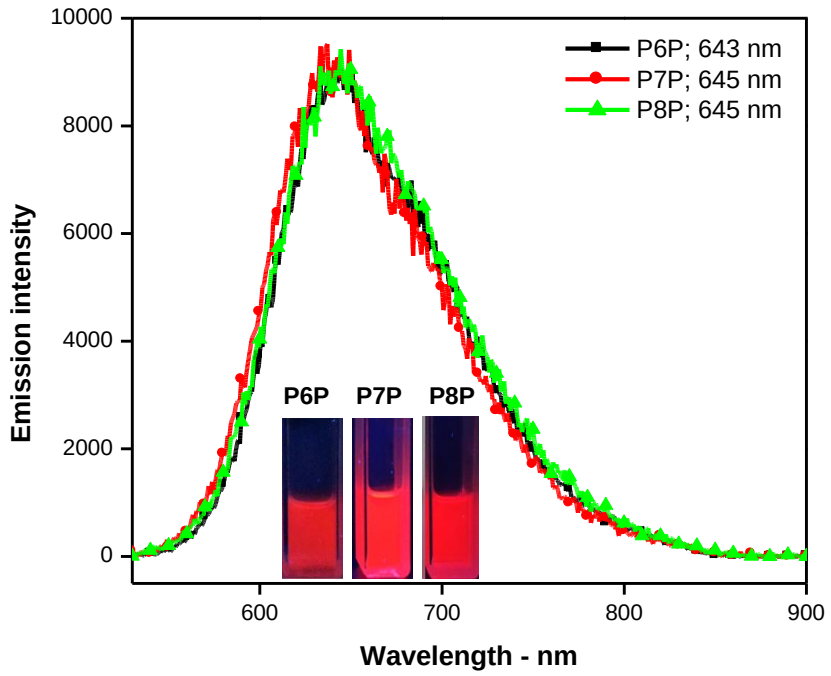

Figure 3.15. Emission spectra of **P6P**, **P7P** and **P8P** in DCM. Inset: Colors of the monomers under 366 nm UV-light.

The λ_{max} values for the three monomers showed a slight red shift with decreasing solvent polarity. For example, λ_{max} appears at 520 nm in DCM (the most polar solvent) and this value shifts to 525 nm in THF and 526 nm in toluene (the least polar solvent). The same trend was observed for **P8P** (λ_{max}= 520 nm in DCM, 524 nm in THF and 526 nm in toluene). While there was no change in the optical absorption band of **P7P** in THF and toluene, there was a blue shift in in DCM (λ_{max}= 519 nm in DCM, 526 nm both in THF and toluene). On the other hand, a significant red shift was observed in the emission maxima of the monomers with increasing solvent polarity. In the case of **P6P**, λ_{max} appears at 627 nm in toluene and this value shifts to 631 nm in THF and 643 nm in DCM. In the case of **P7P** and **P8P** the same trend was also observed (**P7P**; $\lambda_{emission}$= 625 nm, 636 nm and 645 nm in toluene, THF and DCM, respectively and **P8P**; $\lambda_{emission}$= 629 nm, 635 nm and 645 nm in toluene, THF and DCM, respectively). This red shift in the emission spectrum provides a further support for the low-energy band present in the absorption spectrum being ICT band.

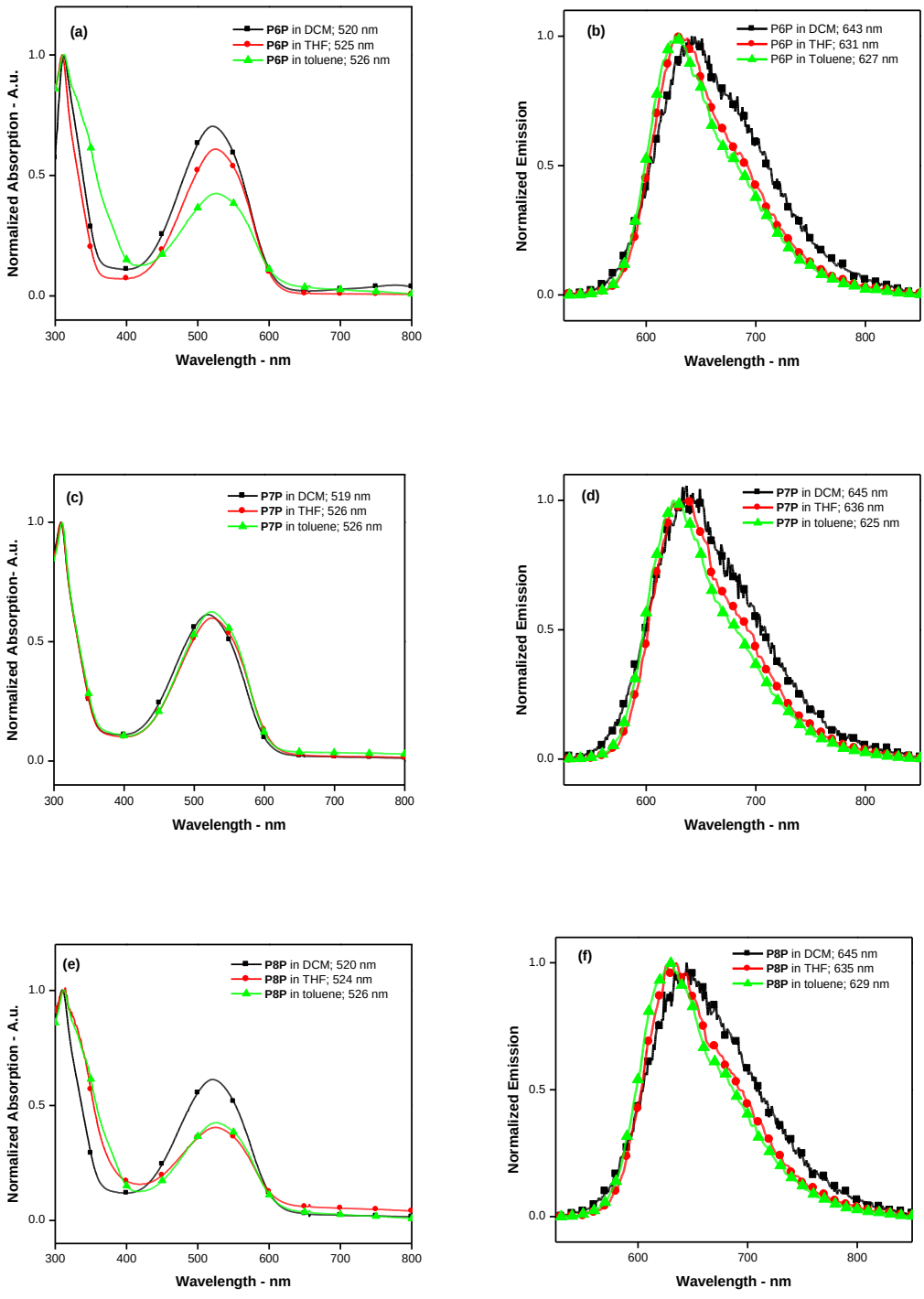

Figure 3.16. The normalized absorption and emission spectra of **P6P** (**a, b**); **P7P** (**c, d**) and **P8P** (**e, f**) in different solvents of DCM, THF and toluene.

Table 3.4. Electrochemical and spectroelectrochemical properties of **P6P**, **P7P**,**P8P**.

Monomers	λ_{max} (abs) nm	λ_{max} (ems) nm	E_{ox} (V)	$E_{ox(onset)}$ (V)	HOMO (eV)	LUMO (eV)	E_g^{UV} (eV)
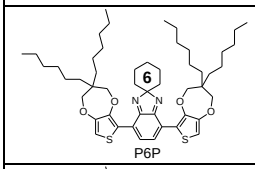 P6P	310 520	643	0.50 *	0.43 *	-5.23 **	-3.18 **	2.05
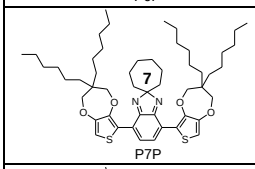 P7P	310 519	645	0.56 *	0.46 *	-5.26 **	-3.22 **	2.04
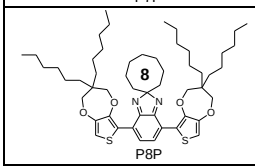 P8P	311 520	645	0.54 *	0.41 *	-5.21 **	-3.16 **	2.05

* with respect to $E_{ox(onset)}$ of Fc/Fc^+ (0.32 V) ;
** $E_g = -[E_{ox(onset)} + 4.80]$ and HOMO = [LUMO - E_g] [185]

3.2.3. Polymerization of P6P, P7P and P8P and Their Characterizations

3.2.3.1. Electrochemical polymerization of P6P, P7P and P8P

The electrochemical polymerization of **P6P**, **P7P** and **P8P** were achieved in electrolyte solution consisting of 0.1 M $LiClO_4$ dissolved in ACN/DCM mixture (90:10 v/v) via potential cycling. Polymer films, **P**(**P6P**), **P**(**P7P**) and **P**(**P8P**), were deposited on the Pt-WE surface via potential cycling from -0.2 V to 0.95 V (for **P6P** and **P7P**); -0.2 V to 1.0 V (for **P8P**). During the second scan new reversible redox couples appeared around +0.3 and + 0.5 V vs Ag/AgCl and after each successive scan, the peak currents were intensified, indicating the formation of an electroactive polymer film on the working electrode with increasing polymer film thickness. After electrodeposition (15 succesive scans), the polymer film coated on the electrodes were washed with and left in ACN to remove any unreacted monomer and

oligomeric species. The redox behaviours of polymer films were investigated by recording their cyclic voltammograms in monomer free electrolyte solution, consisting of 0.1 M $TBABF_4$ in ACN (Figure 3.17 (a-d)).

Further electrochemical studies (i.e. oxidation-reduction potentials, polymer film stability, n-doping, scan-rate dependence etc.) were performed on the polymer films obtained via constant potential electrolysis at applied potential 0.90 V vs Ag/AgCl in the same electrolyte solution. When the total Faradaic charge reached to 80 $mC.cm^{-2}$ electrolysis was stopped and polymer coated WE was transfered in to monomer free electrolyte solution to monitor their redox behaviour. When P(**P6P**), P(**P7P**), and P(**P8P**) were scanned anodically in monomer-free electrolyte solution, they exhibited well-defined reversible redox couples due to p-doping (E_p^{ox} = +0.45 V and 0.78 V (+0.13 V and +0.46 V vs Fc/Fc^+) for P**(P6P)**; E_p^{ox} = +0.59 V and +0.74 V (+0.27 V and +0.42 V vs Fc/Fc^+) for P**(P7P)** and E_p^{ox} = +0.57 V and +0.76 V (+0.25 V and +0.44 V vs Fc/Fc^+) for P**(E8E)**), (see Figure 3.18 (a)).

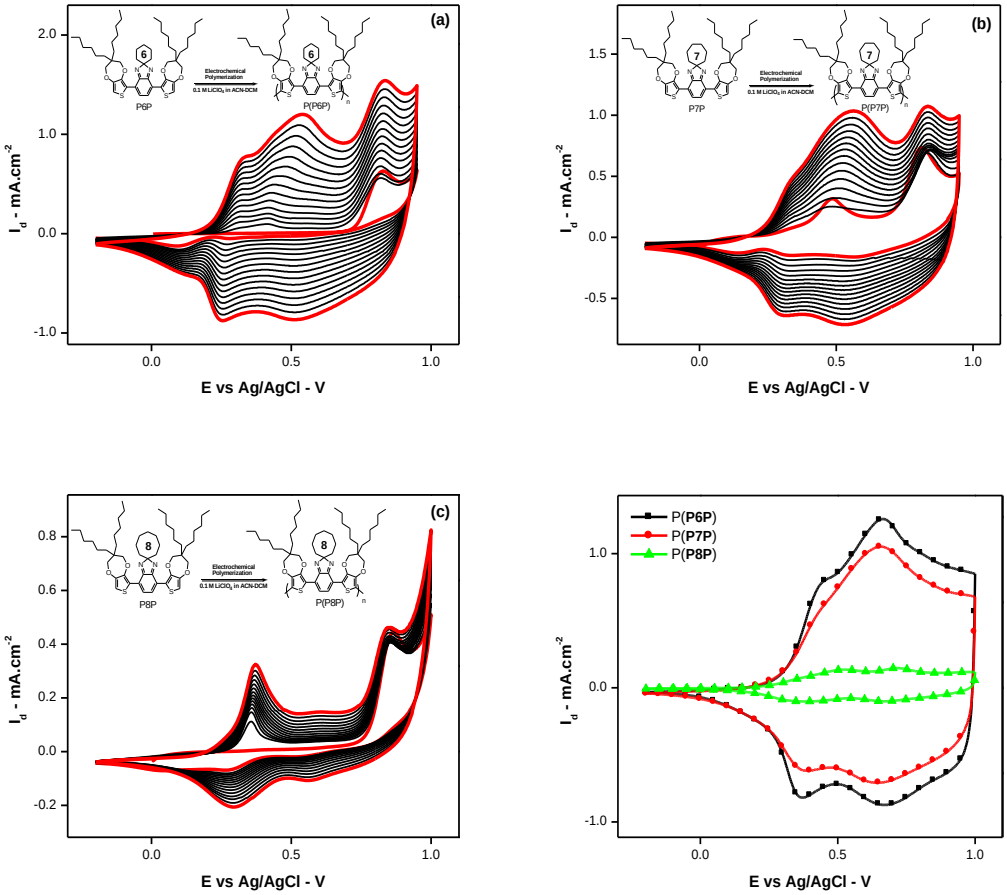

Figure 3.17. Electropolymerization of **P6P** between -0.2 V and 0.95 V **(a)**, **P7P** between -0.2 V and 0.95 V **(b)**, **P8P** between -0.2 V and 1.00 V **(c)** with 15 cycles in 0.1 M $LiClO_4$ solution of ACN - DCM (90:10 v/v) at a scan rate of 100 $mV.s^{-1}$ on Pt WE. The cyclic voltammograms of the resulting polymers (P(**P6P**), P(**P7P**) and P(**P8P**)) **(d)** vs Ag/AgCl in monomer free electrolyte solution of 0.1 M $TBABF_4$-ACN at a scan rate of 100 $mV.s^{-1}$.

The redox behaviour of the polymer films were also examined during n-doping and the results are depicted in Figure 3.18 (b). As seen from the figure, polymer films exhibited well-defined reversible n-doping process. ($E_n^{red-onset}$ = -0.91 V (-1.23 V vs Fc/Fc^+) for P**(P6P)**; $E_n^{red-onset}$ = -0.90 V (-1.22 V vs Fc/Fc^+) for P**(P7P)** and $E_n^{red-onset}$ = -0.88 V (-1.20 V vs Fc/Fc^+) for P**(P8P)**). The oxidation-reduction onset potentials, HOMO-LUMO levels, optical band gap values and the colors of the polymer films were given in Table 3.5. Furthermore, the oxidation and reduction onset values were utilized to elucidate electrochemical band gap value of the polymer films (E_g^{CV}) and the results are tabulated in Table 3.6.

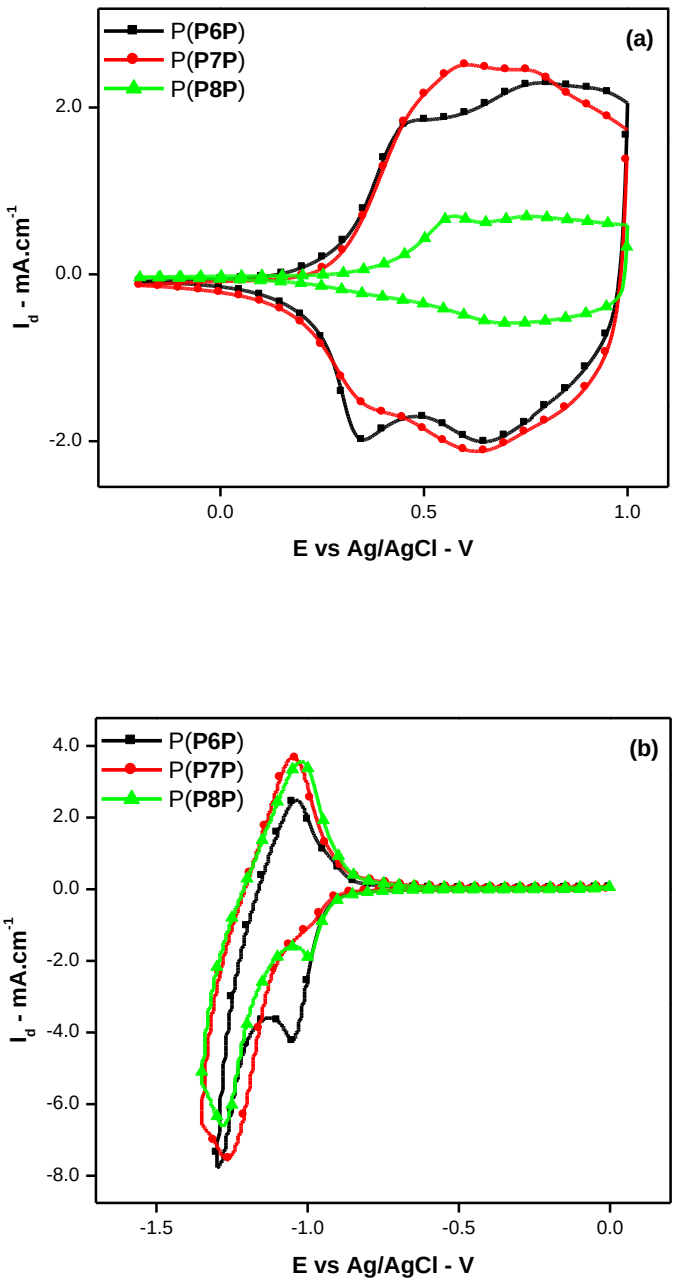

Figure 3.18. (a) Cyclic voltammograms of the polymers (P(**P6P**), P(**P7P**), P(**P8P**)) obtained by constant potential electrolysis with the charge of 80 mC.cm^{-2} on Pt working electrode between -0.2 V and 1.0 V in 0.1 M $TBABF_4$ - ACN monomer free electrolyte solution vs Ag/AgCl. **(b)** Cyclic voltammograms of the polymers (P(**P6P**), P(**P7P**), P(**P8P**)) during n-doping process between 0.0 V and -1.35 V in 0.1 M $TBABF_4$ - ACN monomer free electrolyte solution vs Ag/AgCl.

Scan rate dependence experiments showed that both anodic and cathodic peak currents increase linearly with increasing scan rate, indicating a well-adhered polymer film on the WE surface and a non-diffusional redox process, which was shown in Figure 3.19. Moreover, the anodic and cathodic charges vs scan rate graphs of the polymer films showed that the charging-discharging process of the polymer film is effectively achieved even at higher scan rates (See inset of Figure 3.19).

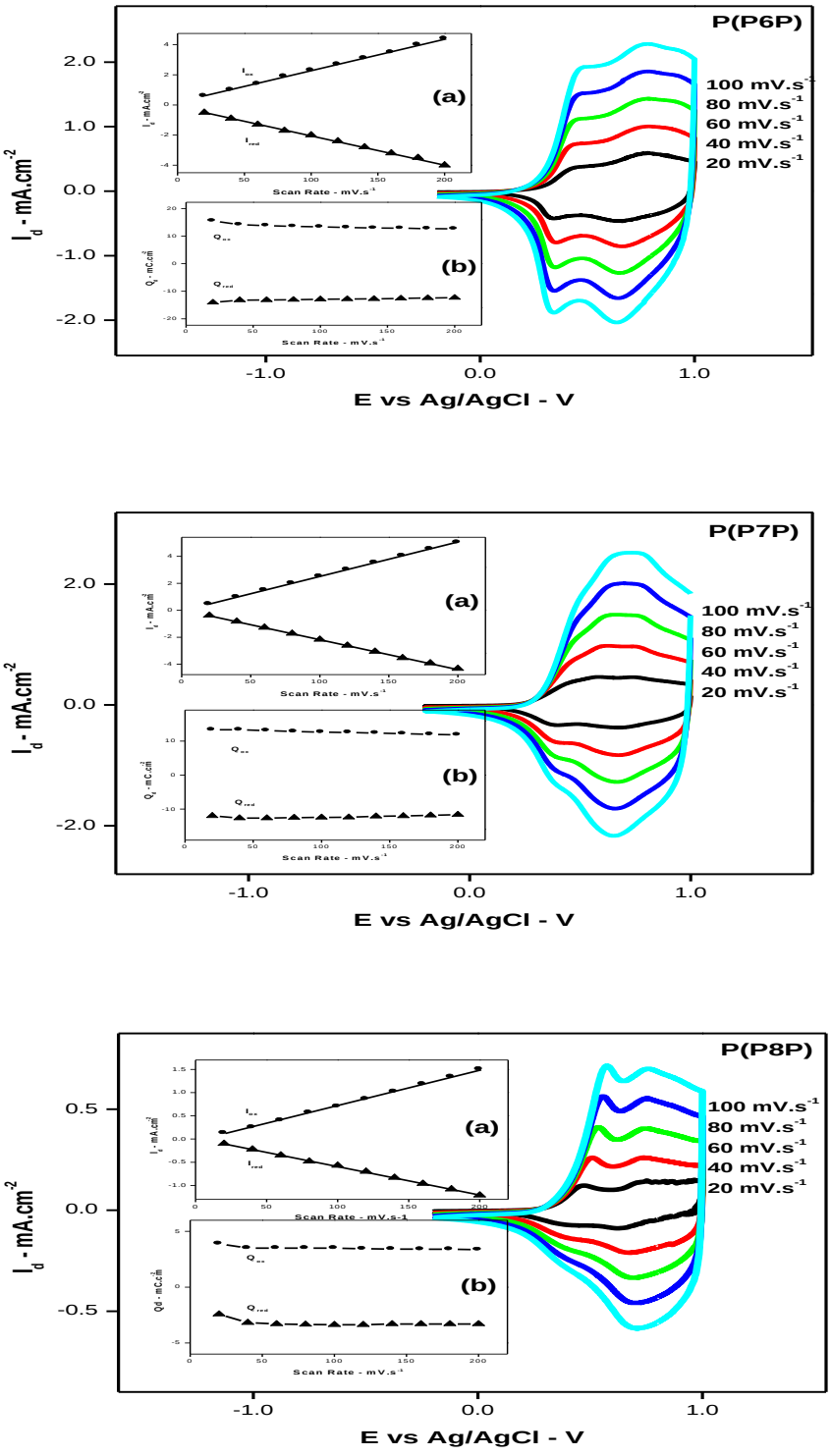

Figure 3.19. Scan rate dependence of P(**P6P**), P(**P7P**) and P(**P8P**) on Pt disc electrode in 0.1 M $TBABF_4$-ACN at a scan rate of 20 - 40 - 60 - 80 - 100 $mV.s^{-1}$

between -0.2 V and 1.0 V. Insets**:** The current vs scan rate **(a)** and the charge density vs scan rate **(b)** plots of the polymer films with increasing scan rates.

Due to its importance for electrochromic device applications, electrochemical stability of the polymer films obtained by constant potential electrolysis (+ 0.95 V vs Ag/AgCl, 80 $mC.cm^{-2}$) on Pt disc WE were also investigated under square wave input of -0.1 V and 0.6 V in 3 s intervals. Cyclic voltammograms were recorded after 100, 350, 600, 1000 and 2000 switchings. After 2000 cycle is complete, the first cyclic voltammogram of the polymers were compared to their last cycles in terms of amount of charge lost.

According to the voltammograms, P(**P6P**) showed 3.7 % of charge lost in anodic region and 15 % in its reversible cathodic reagion after 2000 switcings. Also the oxidation onset was 22.5 % right shifted (from 0.31 V to 0.40 V) (Figure 3.20). P(**P7P**) exhibited 14.8 % right shift in oxidation onset (from 0.46 V to 0.54 V) and the polymer film lost its charge by 6.3 % and 5.5 % in anodic and the cathodic part respectively after 2000 switchings. P(**P8P**) showed 10.6 % of the right shifted oxidation onset potential (from 0.42 V to 0.47 V). After 2000 cycle switchings, there was 20.5 % charge lost in anodic region. The charge lost in reversible cathodic region was only 2 %.

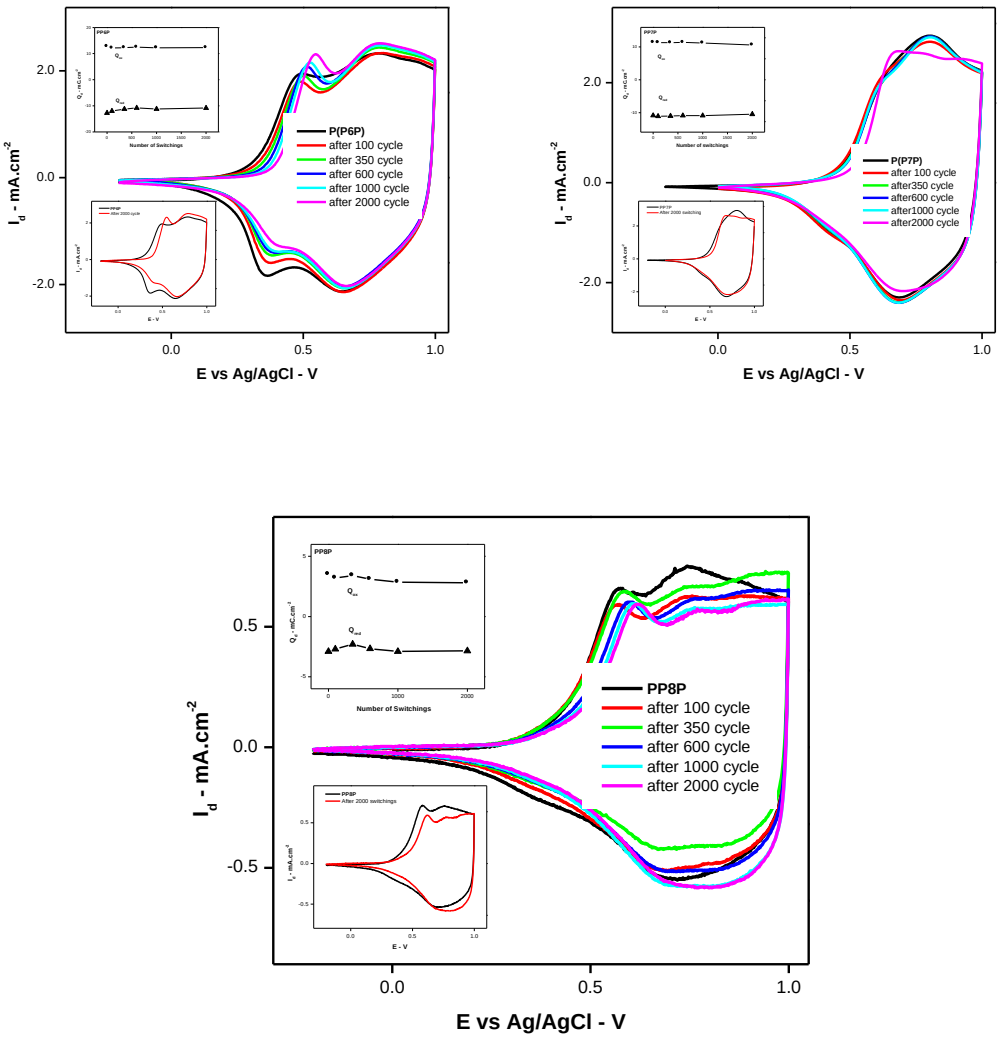

Figure 3.20. Cyclic voltammograms of P(**P6P**), P(**P7P**) and P(**P8P**) films after many of switchings. Insets: **(a)** Anodic and cathodic charge density vs number of switching graphs of the polymer films in 0.1 M $TBABF_4$ - ACN achieved by square wave potential (-0.1 V for 3 s and 0.6 V; 3 s for each) under ambient conditions **(b)**. The first and the last (after 2000 of switchings) cyclic voltammograms of the polymers in 0.1 M $TBABF_4$ - ACN.

Table 3.5. Electrochemical and spectroelectrochemical properties of P(**P6P**), P(**P7P**) and P(**P8P**)

Polymers	λ_{max} (abs) nm	E_{ox} (onset) (V)	E_{red} (onset) (V)	HOMO (eV)	LUMO (eV)	E_g^{UV} (eV)	Red.	Neut	Ox.
P(P6P)	410 768	-0.04 *	-1.23 *	-4.76	-3.47	1.29			
P(P7P)	410 766	-0.04 *	-1.22 *	-4.76	-3.45	1.31			
P(P8P)	410 769	0.04 *	-1.20 *	-4.84	-3.53	1.31			

* with respect to $E_{ox(onset)}$ of Fc/Fc^+: 0.32 V.

3.2.3.2. Optical Characterization of P(P6P), P(P7P) and P(P8P)

The electro-optical properties of the polymer films deposited on ITO electrode via constant potential electrolysis were investigated by monitoring the changes in the electronic absorption spectra under a voltage pulse in a monomer free electrolyte solution. The results are depicted in Figure 3.22. P(**P6P**), P(**P7P**) and P(**P8P**) exhibited two absorption maxima, appeared as 410 / 768 nm, 410 / 766 nm and 410 / 769 nm for P(**P6P**), P(**P7P**) and P(**P8P**), respectively. The latter band can be attributed to the ICT between donor and the acceptor unit while the former band can be assigned to the $\pi - \pi^*$ transition [107].

These optical bands lose intensity during oxidation of the polymer films which is accompanied by the appearance of new intensifying band beyond 850 nm due to formation of charge carriers. All spectra recorded during potential cycling between −0.2 V and 1.0 V passes through the isosbestic points at about 905 nm for P(**P6P**), 910 nm for P(**P7P**) and 915 nm for P(**P8P**), indicating that polymer films were

being interconverted between their neutral and oxidized states (see Figure 3.21 a, b and c). The polymer films also exhibit color change from green (neutral) to gray (oxidized) during potential cycling from -0.2 V to 1.0 V. The n-doping behaviour of the polymer films were also confirmed by recording the changes in the electronic absorption spectra during cathodic scan from 0.0 to -1.5 V vs Ag wire. During reduction the intensity of dual band present in the neutral form of polymer films decreases in intensity (see insets of Figure 3.21) which is accompanied by a color change from green to brick-red, indicating that polymer films exhibit electrochromic behaviour. Electrochromic response of polymer films observed during p- and n-doping were also reported in terms of L*, a*, b* values in Table 3.6.

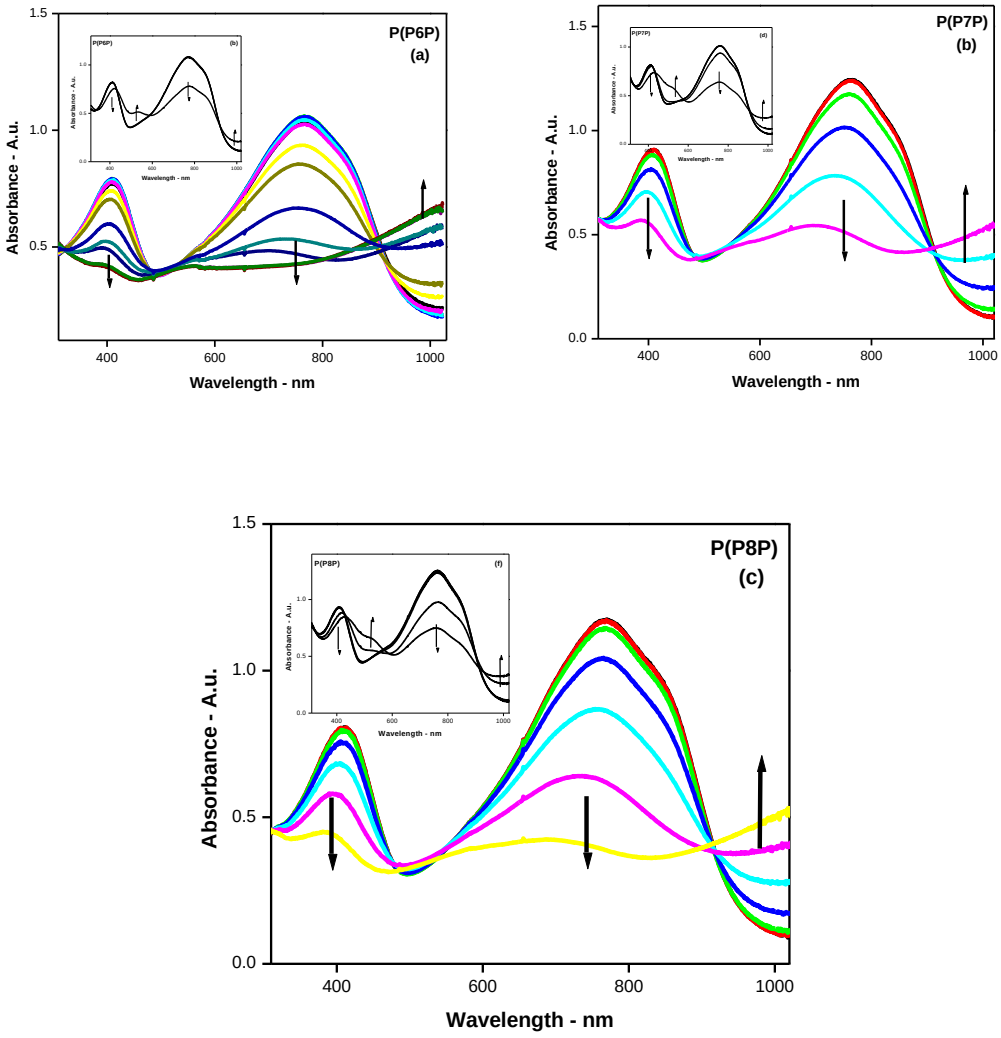

Figure 3.21. UV-VIS spectra of the polymer films **(a)** (P(**P6P**), **(b)** P(**P7P**) and **(c)** P(**P8P**) of 20 mC.cm^{-2} during oxidation from -0.2 V to 1.0 V via cyclic voltammetry with the scan rate of 20 mV.s^{-1}. Insets: UV-VIS spectra of the polymer films (P(**P6P**), P(**P7P**) and P(**P8P**) of 20 mC.cm^{-2} during n-doping from 0.0 V to -1.5 V with the scan rate of 100 mV.s^{-1}.

The optical band gaps (E_g) of P(**P6P**), P(**P7P**) and P(**P8P**) were also calculated from the onset of the low energy end of the π-π* transitions and were found to be 1.29 eV, 1.31 eV and 1.31 eV, respectively. These values are slightly higher (about 0.10 eV) than those obtained from electrochemical data (see Table 3.6). An inspection of E_g values obtained from two different methods indicates that P(**P6P**) has the smallest band gap value. Furthermore, comparison of E_g values of polymers with different donor units indicates that polymers obtained from EDOT containing monomers have smaller band gap values as compared to PRODOT containing analogous. Oxidation potentials are reported vs Fc/Fc^+ to calculate HOMO and LUMO levels of the polymers. The energy level of Fc/Fc^+ was taken as 4.80 eV below vacuum [185]. The oxidation onset potential of Fc/Fc^+ was measured as 0.32 V vs Ag/AgCl. HOMO and LUMO energy levels were obtained from the onset of the oxidation and reduction potentials of polymers, and the results are given in Table 3.6.

3.2.3.3. Switching Study of P(P6P), P(P7P), P(P8P)

Switching times and optical contrast of the polymer films on ITO were also investigated under square wave input of -0.2 and +1.1 V in 10, 5, 3 and 2 s intervals by monitoring the visible transmittance and the kinetic responses of the film, and the results are shown in Figures 3.22, 3.23 and 3.24 and listed in Table 3.7. Inspection of these figures reveals that P(**P6P**), P(**P7P**) and P(**P8P**) polymer films on ITO WE show a reversible response within the range of applied potential pulses.

Percent transmittance values are 31.4 %, 30 % and 38 % P(**P6P**), P(**P7P**) and P(**P8P**) respectively in 10 s residence times with the potentials -0.2 V and +1.1 V which were measured at shorter absorption wavelengths. At longer wavelengths of polymer films, the percent transmittance values were measured as 31 %, 32 % and 41 % for P(**P6P**), P(**P7P**) and P(**P8P**), respectively (Figure 3.22-23-24). As seen from the Figures 3.22-23-24, the transmittance of the polymers at their longer wavelengths exhibited a sudden increase during oxidation following by a decrease in the progressing seconds. This phenomena is observed due to the overlapping of the

polaron bands with the absorption maxima of the polymer films upon further oxidation.

The coloration efficiencies of the polymers were calculated, (see Table 3.6) and P(**P8P**) was found to have the highest value (572 C/cm^2) at its longer wavelength. The lowest coloration efficiency was calculated for P(**E6E**) (279 C/ cm^2).

In order to test the optical stability, the polymers were fully oxidized (by applying 1.1 V) and fully reduced (by applying -0.2 V) with 5 s time intervals. The lost in percent transmittance after 50 switch for P(**P6P**), P(**P7P**) and P(**P8P**) were measured as 4.3 %, 14 % and 7 %, respectively at their shorter wavelengths. Although, P(**P6P**) did not loose its percent transmittance at longer absorption maxima after 50 switching, P(**P7P)** and P(**P8P**) exhibit 6 % and 26 % loss in percent transmittance, respectively. The switching times of the polymers are given at Table 3.6.

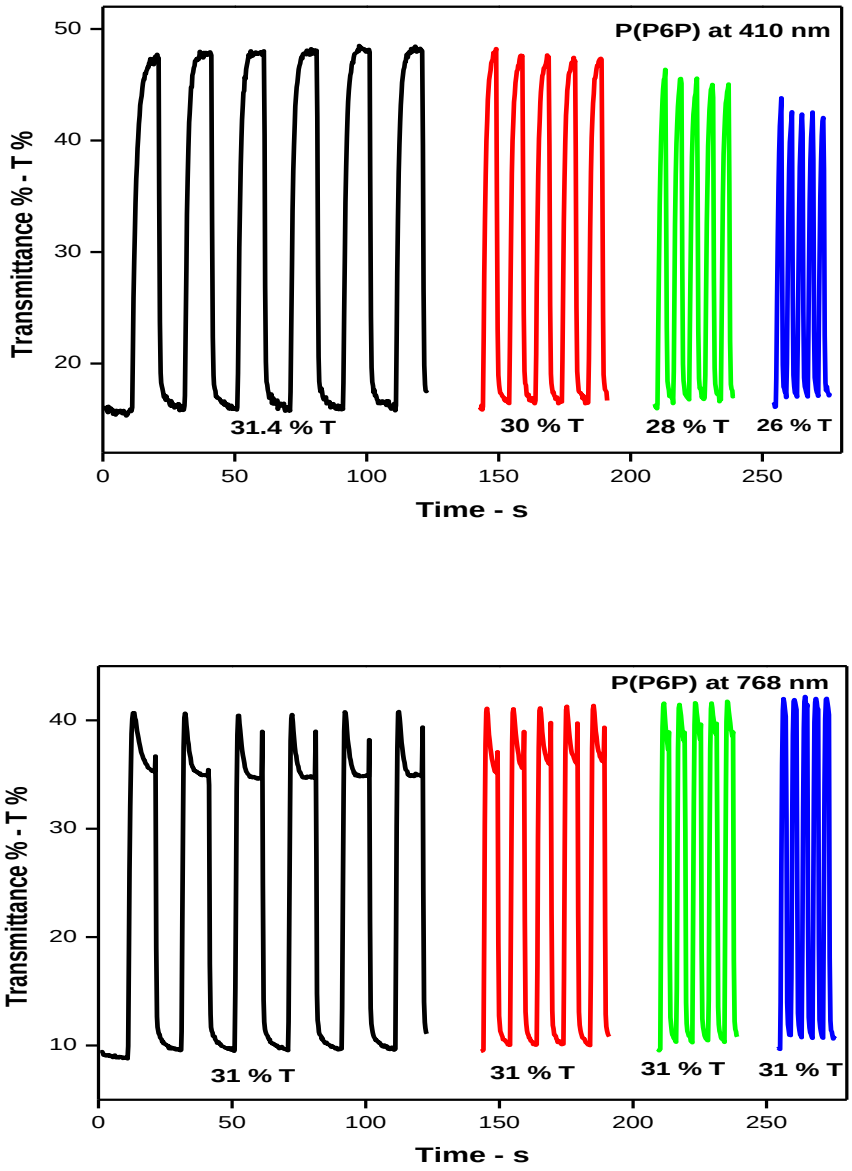

Figure 3.22. Transmittance change of P(**P6P**) film (20 mC.cm^{-2}) at 410 nm and 766 nm, in its fully oxidized (1.1 V) and reduced (-0.2 V) states in different switching times (10 s, 5 s, 3 s and 2 s).

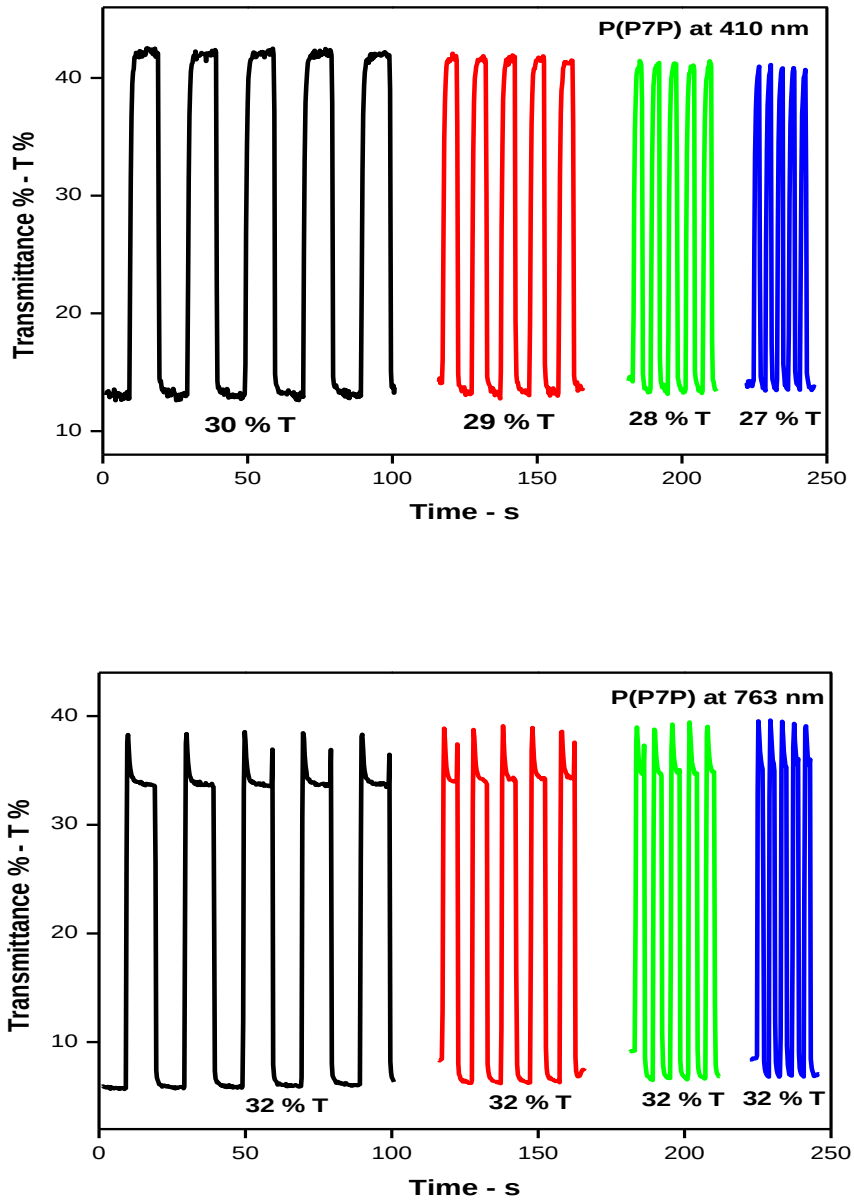

Figure 3.23. Transmittance change of P(**P7P**) film (20 mC.cm^{-2}) at 410 nm and 763 nm, in its fully oxidized (1.1 V) and reduced (-0.2 V) states in different switching times (10 s, 5 s, 3 s and 2 s).

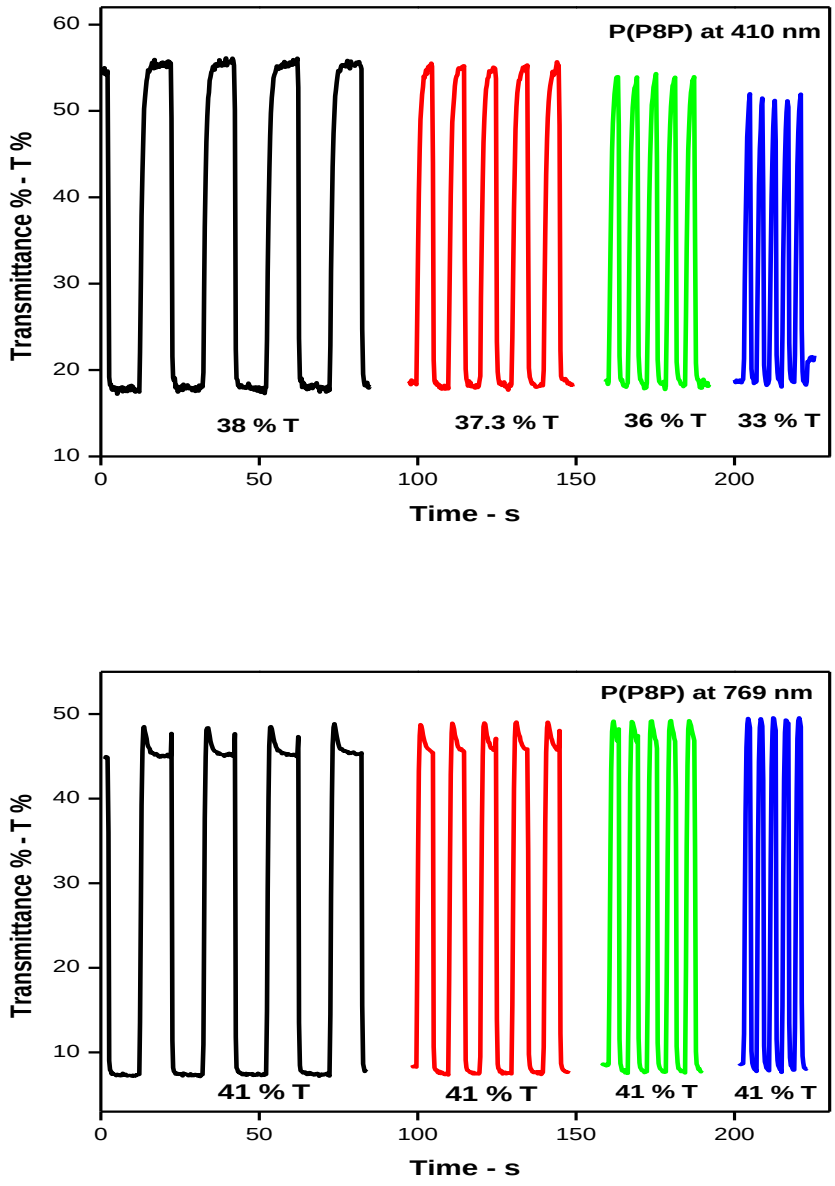

Figure 3.24. Transmittance change of P(**P8P**) film (25 mC.cm^{-2}) at 410 nm and 769 nm, in its fully oxidized (1.1 V) and reduced (-0.2 V) states in different switching times (10 s, 5 s, 3 s and 2 s).

Table 3.6. Electrochemical and optical properties of P(**P6P**), P(**P7P**), P(**P8P**)

		P(P6P)		P(P7P)		P(P8P)	
$E_{ox(onset)}$ (vs Fc/Fc^+)		-0.04		-0.04		0.04	
$E_{red(onset)}$ (vs Fc/Fc^+)		-1.23		-1.22		-1.20	
E_g from CV (V)		1.19		1.18		1.24	
$E_g$optical (eV)		1.29		1.31		1.31	
HOMO (eV)		-4.76		-4.76		-4.84	
LUMO (eV)		-3.47		-3.45		-3.53	
λ_{max} (nm)		λ_{max1}	λ_{max2}	λ_{max1}	λ_{max2}	λ_{max1}	λ_{max2}
		410	768	**410**	766	**410**	769
t_{ox} (s) ** (95 % of full contrast)		3	1	1.2	0.5	3	1.1
t_{red} (s) ** (95 % of full contrast)		1.2	1.4	0.6	0.6	1.6	0.5
T % **		31.4	31	30	32	38	41
CE at 100 % of full contrast	Ox **	146	189	213	382	206	331
	Red **	166	214	295	369	223	358
CE at 95 % of full contrast	Ox **	149	279	251	401	247	572
	Red **	161	203	286	332	245	394
Colors at different redox states	Oxidized *	L: 67 a*: - 3.5 b*: 2.2		L: 67 a*: - 5.7 b*: -2.6		L: 72 a*: - 4.2 b*: -3.6	
	Neutral *	L: 65 a*: - 21 b*: 15		L: 64 a*: - 25 b*: 11		L: 68 a*: - 25 b*: 11	
	Reduced *	L: 61 a*: 5.4 b*: 18		L: 57 a*: 3.4 b*: 17		L: 62 a*: 4 b*: 17	
	Charge passed during polymerization	*20 $mC.cm^{-2}$ **20 $mC.cm^{-2}$		*20 $mC.cm^{-2}$ **20 $mC.cm^{-2}$		*20 $mC.cm^{-2}$ **25 $mC.cm^{-2}$	

* and ** indicates the amount of deposited charge on the polymer films given in the last row.

3.3. Electrochromic Device Applications of P(**E6E**) and P(**P6P**)

Among the six polymer films, P(**E6E**) and P(**P6P**) were selected as anodically coloring polymers for constructing transmissive type ECDs with PEDOT, which is mostly used as cathodically coloring polymer.

First of all, charge balance of the polymers was adjusted as explained before (see Section 2.6. Anodically coloring polymers were electrochemically deposited on ITOs with the charge densities of 25 $mC.cm^{-2}$ for P(**E6E**) and 22.4 $mC.cm^{-2}$ for P(**P6P**). The redox charges of the P(**E6E**) and P(**P6P**) were measured as 2.25 mC and 2.3 mC which both suited with the PEDOT film of 40 $mC.cm^{-2}$ according to reference graph (Figure 2.8). Then the ECDs were constructed as explained in experimental part (Section 2.6).

ECDs were tested by connecting the WE to P(**E6E**) (or P(**P6P**)) and the CE (short cutted by the RE) to PEDOT. During a successive anodic scan, the cyclic voltammograms and UV-VIS spectra were monitored. Working range between -0.6 V and 0.8 V was found as suitable for both devices. The ECDs was deep blue color at 0.8 V and green at -0.6 V (Figure 3.25). As seen from the figure, during the application of 0.8 V, dual band of P(**E6E**) in its ECD and P(**P6P**) in its ECD losses intensity which is accompanied by the evolution of a new band at about 620 nm. The newly formed corresponds to the electronic absorption band of PEDOT in its neutral form.

Switching time, optical contrast and coloration efficiency features of ECDs were also investigated under square wave input of predetermined potential ranges with the residence times of 10, 5, and 3 s by monitoring the transmittance and the kinetic responses of the films at 417 and 816 nm for P(**E6E**), at 418 nm and 820 nm for P(**P6P**).

P(**E6E**) - PEDOT ECD exhibited 6.5 % transmittance in 10 second residence time with the potentials -0.6 V and 0.8 V at both wavelengths. The response time of ECD

at 95 % of full contrast was calculated as 1.4 s for oxidation and 1.5 s for reduction at 417 nm. The response time at 816 nm was calculated as 2.7 s for oxidation and 1.0 s for reduction. The ECD was switched between -0.6 V and 0.8 V for 10, 5 and 3 s intervals. The optical contrast was 6.5 %, 6.3 % and 6 % for 10 s, 5 s and 3 s switchings, respectively (Figure 3.26 (a)).

The coloration efficiency and the other optical results were given at Table 3.7. P(**P6P**) - PEDOT ECD exhibited 8.4 % and 6 % transmittance in 10 second residence time at 418 nm and 820 nm, respectively. The response times of ECD at 95 % of full contrast was calculated as 1.7 s for both oxidation and reduction at 418 nm. The response time at its longer wavelength was calculated as 2.6 s for oxidation and reduction. The ECD was switched between -0.6 V and 0.8 V for 10, 5 and 3 second intervals (Figure 3.26 (b)). The optical contrast, coloration efficiency and the other optical results were given at Table 3.7.

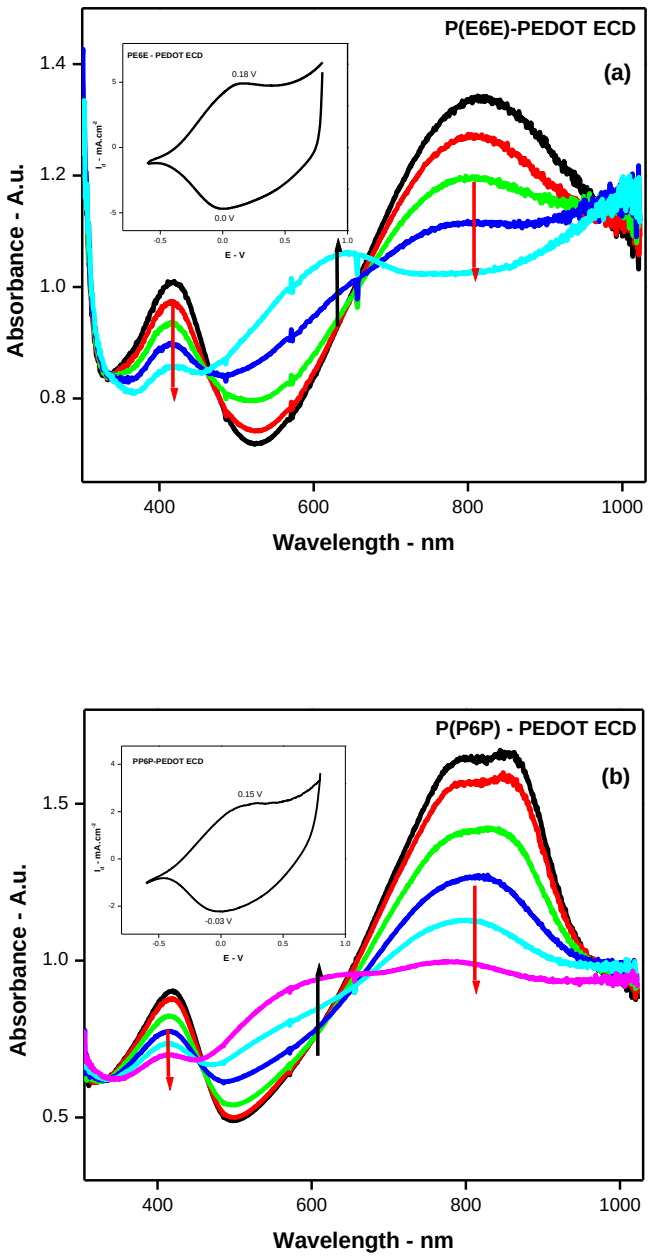

Figure 3.25. Spectroelectrochemical behaviour of P(**E6E**) - PEDOT ECD (**a**) and P(**P6P**) - PEDOT ECD (**b**) between -0.6 V and 0.8 V. Inset: Cyclic voltammograms of ECDs between -0.6 V and 0.8 V at scan rate of 100 $mV.s^{-1}$.

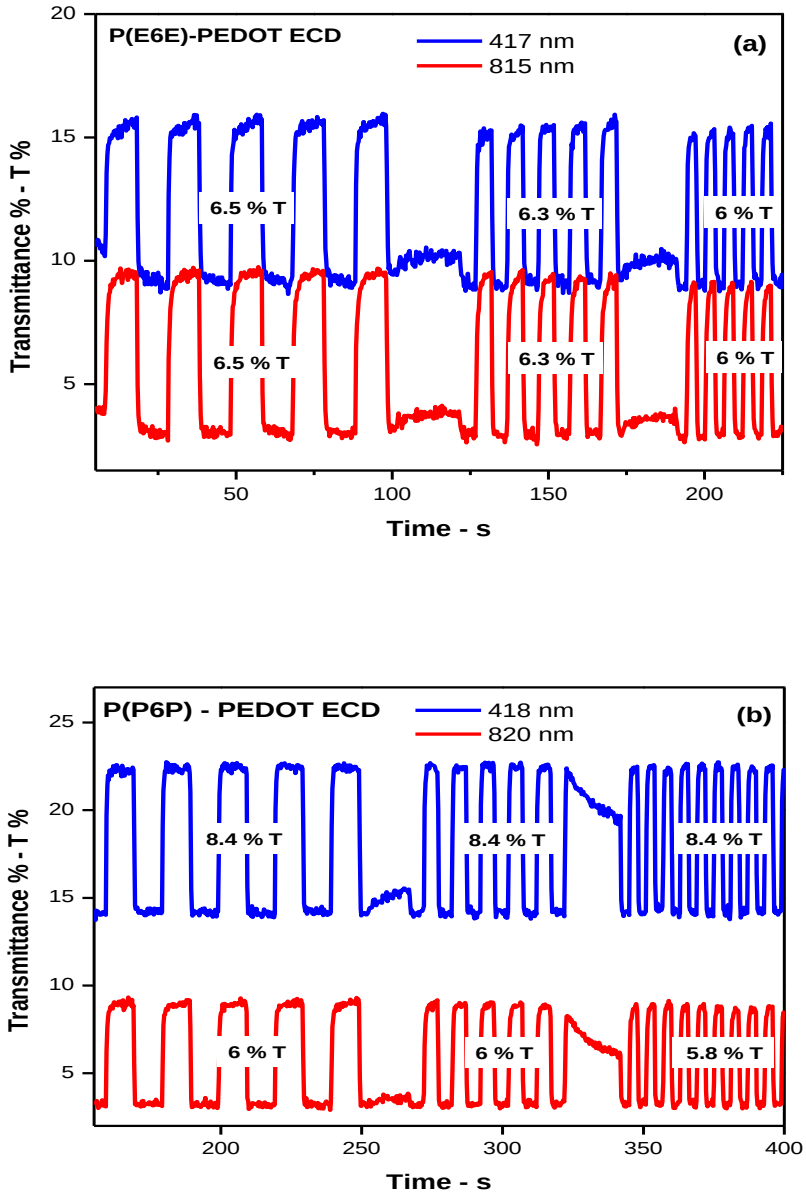

Figure 3.26. Percent transmittance change of P(**E6E**) – PEDOT ECD at 417 nm and 815 nm (**a**), P(**P6P**) - PEDOT ECD at 418 nm and 820 nm (**b**) switched between -0.6 V and 0.8 V with the residence times of 10, 5 and 3s.

Table 3.7. Spectroelectrochemical properties of P(**E6E**) - PEDOT and P(**P6P**) - PEDOT ECDs.

Optical Parameters		P(E6E) – PEDOT ECD		P(P6P) – PEDOT ECD	
λ_{max} (nm)		λ_{max1}	λ_{max2}	λ_{max1}	λ_{max2}
		417	816	418	820
t_{ox} (s) 95 % of full contrast		1.4	2.7	1.7	2.6
t_{red} (s) 95 % of full contrast		1.5	1	1.7	2.6
T %		6.5	6.5	8.4	6
CE at 100 % of full contrast	Ox	71	150	82	174
	Red	76	163	86	200
CE at 95 % of full contrast	Ox	75	151	87	189
	Red	76	162	90	282
Color at oxidized state			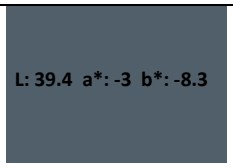		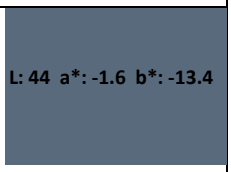
Color at reduced state		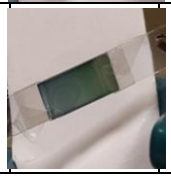	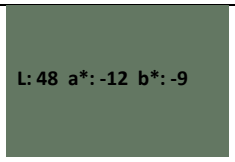	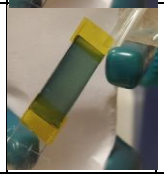	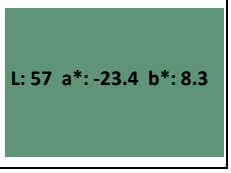

An inspection of Table 3.7 reveals that both electrochromic devices prepared utilizing P(**E6E**) and P(**P6P**) as anodically coloring part exhibit almost very similar properties. Mainly, P**(P6P) – PEDOT** ECD have slighty higher CE value at its longer wavelength than that of P(**E6E**) – PEDOT ECD and than the PEDOT itself (183 cm^2/C) [187]. When L*a*b* values are considered, P**(P6P) – PEDOT** ECD has higher L* values indicating brighter color for corresponding ECD.

3.4. Discussion

3.4.1. Comparison of EDOT Containing Polymers in Terms of Acceptor Unit

P(**E6E**), P(**E7E**), and P(**E8E**) have the absorption maxima in the range of 430 nm - 835 nm, and the average E_g value of 1.18 eV. Some other EDOT containing polymers with different acceptor groups (benzimidazole (**P1**), benzothiadiazole (**P2**), benzoselenadiazole (**P3**), benzoxadiazole (**P4**), benzotriazole (**P5**)) in the literature were examined and the results were tabulated in Table 3.8. **P1** to **P5** polymers have at least two absorption bands and the band gap values changes from 1.15 eV to 1.60 eV. The smallest band gap value was found for **P1** and the highest one was for **P5**. A comparison of these values with that of P(**EXE)**s synthesized in this work indicates that benzimidazole containing polymers have smaller E_g values. This shows that benzimidazole is a stronger acceptor unit causing better band gap compression and stronger ICT. Furthermore, all the polymers listed in Table 3.8 have quite low oxidation potentials due to the electron rich EDOT donor unit.

The P(**EXE**) films are green in their neutral states. The other polymers (**P1** to **P5**) are also green except **P5**. It can be concluded that benzotriazole acceptor results with the blue shift of the resulting polymer. Moreover, the P(**EXE**)s and **P1** exhibited transparent gray color when they are oxidized, but **P2**, **P3**, **P4** and **P5** showed transparent blue. Indeed, It was reported that **P1** also exhibits blue color in further oxidized state.

Table 3.8. The electrochemical-optical properties of the EDOT containing polymers from this work and of the similar polymers from the literature.

Polymers	λ_{max} (abs) nm	E_{ox} (onset) (V)	HOMO (eV)	LUMO (eV)	Eg^{UV} (eV)	Neut. Color	Ox. Color	Red. Color
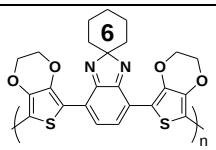 P(E6E)	433 835	-0.32	-4.48	-3.31	1.17	Green	Transparent Gray	Brick-red
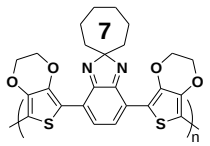 P(E7E)	430 820	-0.25	-4.55	-3.36	1.19	Green	Transparent Gray	Brick-red
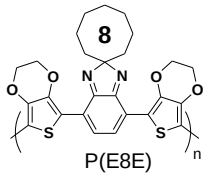 P(E8E)	431 828	-0.32	-4.48	-3.30	1.18	Green	Transparent Gray	Brick-red
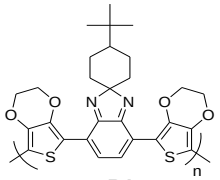 **P1** [147]	440 ~ 740	E_{ox}: 0.55 0.82 vs Ag wire	-5.31	-4.42	1.15	Green	Gray--blue	Brick-red
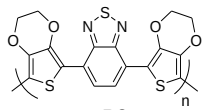 **P2** [95]	428 755	E_{ox}: -0.06 vs Ag wire	-3.94	-2.75	1.19	Green	Transparent Blue	Not Reported
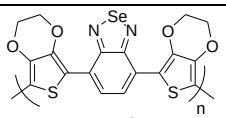 **P3** [190]	~ 420 830	-0.43	-3.97	-2.76	1.21	Green	Transparent Blue	Not Reported
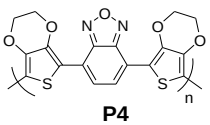 **P4** [190]	~ 400 767	-0.37	-4.03	-2.77	1.26	Green	Transparent Blue	Not Reported
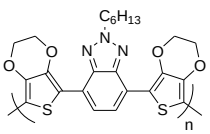 **P5** [190]	624 684	-0.30	-4.10	-2.50	1.60	Blue	Transparent Blue	Not Reported

3.4.2. Comparison of PRODOT Containing Polymers in Terms of Acceptor Unit

There are several reports on PRODOT containing DAD type polymers. It is already reported that alkyl chain length has pronounced effect on the properties of the resulting polymer [122]. Although increasing chain length improves the solubility, it also causes a decrease in planarity due to steric reasons. Therefore, PRODOT(C6) was selected as the donor group in synthesizing the target monomers in this work. Thus, due to limited number of examples present in the literature we compared our results with the reported values to get a general idea (see Table 3.9).

When it comes to PRODOT containing polymers, there are CPs in the literature that bear comparison. They include different acceptor units but the same donors, PRODOT(C10) [127]. In this work we preferred to use PRODOT(C6) in order to decrease the steric hindrance. It was demonstrated that; when PRODOT alkyl chain length increases, the planarity decreases and the steric hindrance increases but the absorption band exhibits red shift and solubility gets better. Although changing the alkyl size on PRODOT affects the properties of polymer, the including products can also give a general idea of comparison with our counterparts in this work.

Among **P1**-**P4**, n-doping behaviour was observed only in **P3**. This was explained due to the steric hindrance caused by long alkyl chains. On the other hand, presence of n-dopping property in **P3** was explained in terms of higher electronegativity of oxygen atom which overcame the steric hindrance problem of the polymer. In addition, when alkyl size is reduced to (C6), n-doping behaviour is observable like in **P5** due to the lower steric hindrance. However, all P(**PXP**)s synthesized in this study are n-dopable and exhibits brick-red color beyond the -1.25 V.

The E_g values of **P1**-**P4** lay between 1.37 eV (for **P2**) and 1.80 eV (for **P4**). The P(**PXP**)s in this work exhibited the E_g values around 1.30 eV which is lower than **P5**. It can be easily concluded that the **BIm** acceptor unit causes stronger ICT with PRODOT(C6) donor unit and reduced the band gap.

Table 3.9. The electrochemical-optical properties of the PRODOT containing polymers from this work and of the similar polymers from the literature.

Polymers	λ_{max} (abs) nm	E_{ox} (onset) (V)	HOMO (eV)	LUMO (eV)	Eg^{UV} (eV)	Neut. Color	Ox. color	Red. color
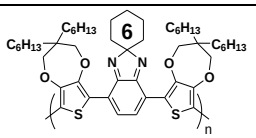 PP6P	410 768	-0.04	-4.76	-3.47	1.29	Green	Transparent Gray	Brick-red
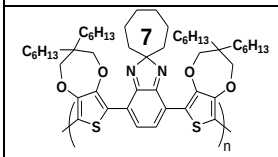 PP7P	410 766	-0.04	-4.76	-3.45	1.31	Green	Transparent Gray	Brick-red
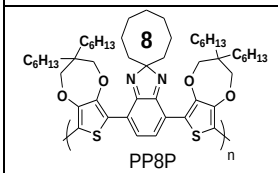 PP8P	410 769	0.04	-4.84	-3.53	1.31	Green	Transparent Gray	Brick-red
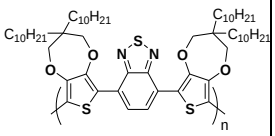 P1 [127]	408 685	0.33	-5.13	-3.63	1.48	Cyan	Transparent Blue	-
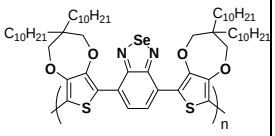 P2 [127]	419 700	0.48	-5.28	-3.91	1.37	Green	Transparent Gray	-
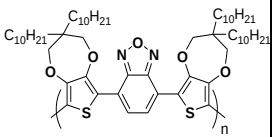 P3 [127]	400 697	0.48	-5.28	-3.88	1.40	Cyan	Transparent Gray	Yes but Not Reported
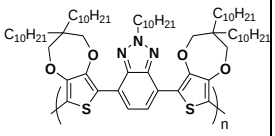 P4 [127]	585	0.46	-5.26	-3.46	1.80	Blue	Transparent Blue	-
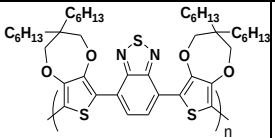 P5 [127]	417 665	0.27	-5.07	-3.57	1.50	Cyan	Transparent Gray	Dark Brown

3.4.3. Comparison of PRODOT and EDOT Containing Polymers in Terms of Donor Unit:

As it is mentioned in the introduction part, existence of ethylenedioxy bridge on the 3rd and 4th locations of thiophene (EDOT) results with highly electron rich structure (means lower oxidation potential) and more stable molecule as well. On the other hand, EDOT polymers were not soluble or very slightly soluble even if synthesized chemically [188,189].

Introducing PRODOT with different alkyl chain lengths overcame the solubility problem. Propylenedioxy bridge on the thiophene ring increases the electron density of the molecule as in PEDOT, therefore this molecule has also lower oxidation potential. However, the oxidation potentials of these two promising units are slightly different; 0.98 V for PRODOT [191] and 0.88 V for EDOT [192]. This difference is explained by the xylenedioxy bridges of the molecules. Propylenedioxy bridge on PRODOT unit has twisted conformation, decreasing the overlap between the lone pairs of oxygen atom and thiophene ring [193].

The same trend was observed for **EXE** and **PXP** monomers synthesized in this work. **E6E** and **P6P** oxidation potentials were measured as 0.46 V and 0.50 V vs Fc/Fc^{+}, respectively. Similar trend was also observed for the other monomers (**E7E**; 0.50 V, **P7P**; 0.56 V and **E8E**; 0.43 V, **P8P**; 0.54 V).

Due to stronger ICT between EDOT and acceptor units, the absorption maxima of the **EXE** monomers are red shifted as compared to **PXP** monomers. The largest difference in λ_{max} values was observed between **E6E** and **P6P** as about 20 nm. This may be due to having stronger ICT of **E6E** monomer among other **EXE**s.

The effect on ICT was also clearly observed in the case of polymers prepared from **EXE** and **PXP.** When considering the polymers, the E_g values of P(**EXE**)s were found to be about 0.12 eV lower than their P(**PXP**) counterparts. This is due to P(**EXE**)s having the absorption bands at lower energies because of the stronger

donor character of EDOT unit as compared to PRODOT unit. Due to the same reasoning, P(**EXE**)s have lower oxidation potentials and higher HOMO levels.

Although P(**EXE**)s and P(**EXE**)s bear the same acceptor unit, which is mainly responsible from the reduction of polymers, reduction onsets of P(**PXP)**s were found to be about 0.1 V higher than that of P(**EXE**)s polymers ($E_n^{red-onset}$ = -1.31 V for P**(E6E)**; $E_n^{red-onset}$ = -1.30 V for P**(E7E)** and $E_n^{red-onset}$ = -1.35 V for P**(E8E)**), ($E_n^{red-onset}$ = -1.23 V for P**(P6P)**; $E_n^{red-onset}$ = -1.22 V for P**(P7P)** and $E_n^{red-onset}$ = -1.20 V for P**(P8P)**). This indicates that donor units are also affecting the redox behaviour. The higher electron density on the EDOT unit may not allow inserting extra electron into the system as easy as in PRODOT unit.

When we consider the electronic absorption spectra of polymer thin films on ITO surface, they all have dual band absorption spectra due to their DAD characteristics. As in the case of their similar analogues, the absorption spectra were red shifted in P(**EXE**)s as compared to P(**PXP**)s (about 20 nm and 50 nm right shift in λ_{max} in the higher and lower energy bands, respectively). This also indicates better ICT between donor and acceptor units in P(**EXE**)s.

The colors of all six polymers were transparent gray in their oxidized state and brick-red in their reduced states. In neutral state, P(**EXE**)s exhibited higher L value than P(**PXP**)s, which was consistent with the observers view that P(**PXP**)s have darker green (The L* value indicates the lightness or brightness of the color which can take the value up to 100 at CIE color space).

The a* value depicts the color range between green and red. The negative a* values of the polymers indicate that their colors were greenish. More negative a*'s in P(**PXP**)s point the greener hue in their color. The b* value expresses the saturation of the color between blue and yellow.

All polymers have positive b* which indicates to the yellow region but greater b* values of P(**EXE**)s mark more yellowish saturation in their neutral colors. On the

other hand, L* values in P(**EXE**)s in their oxidized state are higher indicating the lighter gray. In their reduced form, L*a*b* values of the polymers almost the same except the greater b* values in P(**EXE**)s underlying more yellowish saturation in their brick-red color.

CHAPTER 4

CONCLUSION

In this study, three different benzimidazole based acceptor groups (bearing cyclohexane, cycloheptane and cyclooctane rings at 2-C position of benzimidazole) were synthesized and coupled with EDOT and PRODOT(C6) donor units. Six different DAD type monomers were obtained. The monomers were examined in terms of their electrochemical and optical behaviours. It was seen that changing the ring size on the acceptor group has an observable effect on intramolecular charge transfer on the monomers. In EDOT containing monomers, cyclohexane ring caused the best intramolecular charge transfer and this shows a decreasing trend with increasing the cycle size. Also the emission spectra of EDOT monomers showed blue shift with increasing the ring size.

On the other hand, for the PRODOT containing monomers, cyclooctane ring showed the best intramolecular charge transfer with the PRODOT donor. However, there was not revealed any trend in the properties by changing the ring size in PRODOT containing monomers. Moreover, the EDOT containing monomers were oxidized easier than their PRODOT counterparts.

The monomers were electrochemically polymerized and electro-optical properties were investigated. The optical properties of the same donor unit containing polymers did not exhibit a significant difference. Moreover, when compared the EDOT containing and the PRODOT containing CPs, they exhibited different optical behaviours. EDOT containing polymers showed a red shift in their optical absorption spectra and lower band gap values with respect to PRODOT analouges.

All the EDOT containing and PRODOT containing polymer films exhibited ambipolar (both anodically and cathodically dopable) property. The polymer films are green in their neutral states, gray in the oxidized states and the brick-red in their reduced states. The minor difference between the neutral and reduced colors of EDOT and PRODOT containing polymers illustrated in Figure 4.1. The EDOT polymers exhibited softer green in the neutral state and more brownish brick-red in the reduced state. The green of the PRODOT polymers were more bright (or cyanish) and the reduced state color was more reddish brick-red. They were matched with the autumn leaves in the figure for seeing the color difference between them.

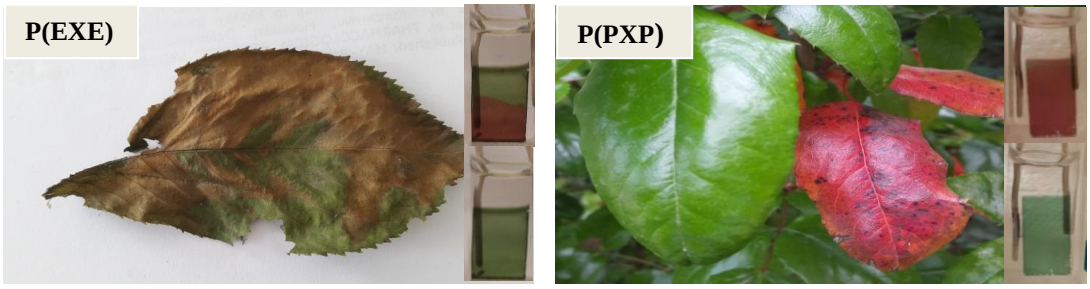

Figure 4.1. The neutral state and reduced state colors of the EDOT containing (left) and the PRODOT containing (right) polymer films.

The band gap values of all six polymers were found to be lower than the other same donor containing CPs in literature. This showed the efficient intramolecular charge transfer caused by the benzimidazole units that synthesized in this work.

Although dihexylated PRODOT donor unit was used in this study with the expectation of solubility, it could not be achieved for the electrochemically synthesized polymer films. Then the electrochromic devices were constructed with one of the EDOT polymers (with PEDOT) and one of the PRODOT polymers (with PEDOT). Both electrochromic devices exhibited similar optical behaviors. The

switching times of the devices were measured as around 2.7 s, with the percent transmittance change about 6 %. The coloration efficiency of the PRODOT containing electrochromic device was found to be higher (189 cm^2/C) than that of EDOT containing device (163 cm^2/ C) and also that of PEDOT itself (183 cm^2/C).

In this work, it was seen that changing the ring size on benzimidazole acceptor has no significant effect on the properties of the resulting monomers and the polymers. On the other hand, comparison of the polymers with their analogous in the literature showed that benzimidazole acceptor caused better intramolecular charge transfer with EDOT and the PRODOT donor unit, resulting with the red-shifted absorption and the lower band gap energy.

REFERENCES

[1] Staudinger, H.; Fritschi, J. *Helv. Chim. Acta* 1922, 5, 785.

[2] Staudinger, H. *Ber. Dtsch. Chem. Ges. B* 1920, 53, 1073.

[3] Chiang, C.K.; Fincher, C.R.; Park, Y.W.; Heeger, A.J.; Shirakawa, H.; Louis, E.J.; Gau, S.C.; MacDiarmid A.G. *Phys. Rev. Lett.* 1978, 40, 1472.

[4] Chiang, C.K.; Fincher, C.R.; Park, Y.W.; Heeger, A.J.; Shirakawa, H.; Louis, E.J.; Gau, S.C.; MacDiarmid, A.G. *Phys. Rev. Lett.* 1977, 39.

[5] Nalwa, H. S. *Handbook of Organic Conductive Molecules and Polymers*, Vol. 4 , Wiley, Chichester, UK, 1997.

[6] Feast, W. J.; Tsibouklis, J.; Pouwer, K. L.; Groenendaal, L.; Meijer, E. W. *Polymer* 1996, 37, 5017.

[7] Skotheim, T. A.; Elsenbaumer, R. L.; Reynolds, J. *Handbook of Conducting Polymers*, 2nd ed.; Marcel Dekker: New York, 1998.

[8] Farges, J. P. *Organic Conductors: Fundamentals and Applications*; Marcel Dekker: New York, 1994.

[9] Granqvist, C. G. *Sol. Energy Mater. Sol. Cells* 2000, 60, 201.

[10] Granqvist, C. G.; Avendano, E.; Azens, A. *Thin Solid Films* 2003,442, 201.

[11] Avendano, E.; Berggren, L.; Niklasson, G. A.; Granqvist, C. G.; Azens, A. *Thin Solid Films* 2006, 496, 30.

[12] Roncali, J. *Chem. Rev.* 1997, 97, 173.

[13] Arbizzani, C.; Mastragostino, M.; Soavi, F. *Electrochim. Acta* 2000 45, 2273.

[14] Barbarella, G.; Favaretto, L.; Sotgiu, G.; Zambianchi, M.; Arbizzani, C.; Bongini, A.; Mastragostino, M. *Chem. Mater.* 1999, 11, 2533.

[15] Bongini, A.; Barbarella, G.; Favaretto, L.; Zambianchi, M.; Mastragostino, M.; Arbizzani, C.; Soavi, F. *Synth. Met.* 1999, 101, 13.

[16] Suh, M. C.; Jiang, B.; Tilley, T. D. *Angew. Chem. Int. Ed.* 2000, 39, 2870.

[17] Pennisi, A.; Simone, F.; Barletta, G.; Di Marco, G.; Lanza, L. *Electrochim. Acta* 1999, 44, 3237.

[18] Rauh, R. *Electrochim. Acta* 1999, 44, 3165.

[19] Tang, C. W. *Appl. Phys. Lett.* 1986, *48*, 183.

[20] Song, S.; Park, S. H.; Jin, Y.; Goo, Y.; Kim, I.; Lee, H.; Lee, K.; Suh, H. *Synth. Met.* 2010, 160, 2618.

[21] Schmidt-Mende, L.; Fechtenkotter, A.; Mullen, K.; Moons, E.; Friend, R. H.; Mackenzie, J. D. *Science* 2001, 293, 1119.

[22] Liscio, A.; De Luca, G.; Nolde, F.; Palermo, V.; Müllen, K.; Samori, P. *J. Am. Chem. Soc*. 2008, 130, 780.

[23] Fréchet, J.M.J.; Thompson, B. C. *Angew. Chem., Int. Ed.* 2008, 47, 58.

[24] Dance, Z. E. X.; Ahrens, M. J.; Vega, A. M.; Ricks, A. B.; McCamant, D. W.; Ratner, M. A.; Wasielewski, M. R. *J. Am. Chem. Soc.* 2008, 130, 830.

[25] Hagberg, D. P.; Yum, J.-H.; Lee, H.; De Angelis, F.; Marinado, T.; Karlsson, K. M.; Humphry-Baker, R.; Sun, L.; Hagfeldt, A.; Grätzel, M.; Nazeeruddin, Md. K. *J. Am. Chem. Soc.* 2008, 130, 6259.

[26] Sonmez, G.; Sonmez, H. B.; Shen, C. K. F.; Jost, R.W.; Rubin, Y.; Wudl, F. *Macromolecules*, 2005, 38, 669–675.

[27] Zhou, H.; Yang, L.; Stuart, A. C.; Price, S. C.; Liu, S.; You, W. *Angewandte Chemie*, 2011, 123, 13, 3051-3054.

[28] Hong, Y.; Wong, H.; Moh, L. C. H.; Tan, H.; Chen, Z. *Chem. Commun.* 2011, 47, 4920–4922.

[29] Kim, J. Y.; Lee, K.; Coates, N. E.; Moses, D.; Nguyen, T.-Q.; Dante, M.; Heeger, *Science* 2007, 317, 222-225.

[30] Yu, G.; Gao, J.; Hummelen, J. C.; Wudl, F.; Heeger, *Science* 1995, 270, 1789-1791.

[31] Liu, M. S.; Luo, J.; Jen, A. K. Y. *Chem. Mater.* 2003**,** *15*, 3496-3500.

[32] Gunes, S.; Neugebauer, H. S.; Sariciftci, N. S. *Chem. Rev.* 2007, 107, 1324-1338.

[33] Coakley, K.; McGehee, M. D. *Chem. Mater.* 2004, *16*, 4533-4542.

[34] Brabec, C. J.; Sariciftci, N. S.; Hummelen, J. C. *Adv. Funct.Mater.* 2001, *11*, 15-26.

[35] Thompson, B. C.; Frechet, J. M. J. *Angew.Chem., Int. Ed.* 2008, *47*, 58-77.

[36] Li, Y.; Zou, Y. *Adv. Mater.* 2008, *20*, 2952–2958.

[37] Hoppe, H.; Sariciftci, N. S. *J. Mater. Chem.* 2006, *16*, 45–61.

[38] Shaheen, S.; Brabec, C. J.; Sariciftci, N. S.; Padinger, F.; Fromherz, T.; Hummelen, J. C. *Appl. Phys. Lett.* 2001, *78*, 841-843.

[39] Zheng, L.; Zhou, Q.; Deng, X.; Yuan, M.; Yu, G.; Cao, Y. *J. Phys. Chem. B* 2004, *108*, 11921-11926.

[40] Wang, L.; Liu, Y.; Jiang, X.; Qin, D.; Cao, Y. *J. Phys. Chem. C* 2007, *111*, 9538-9542.

[41] Ballantyne, A. M.; Chen, L. C.; Nelson, J.; Bradley, D. D. C.; Astuti, Y.; Maurano, A.; Shuttle, C. G.; Durrant, J. R.; Heeney, M.; Duffy, W.; McCulloch, I. *Adv. Matter.*2007, *19*, 4544–4547.

[42] Shi, C.; Yao, Y.; Yang, Y.; Pei, Q. *J. Am. Chem. Soc.* 2006, *128*, 8980-8986.

[43] Blouin, N.; Michaud, A.; Leclerc, M. *Adv. Mater.* 2007, *19*, 2295-2300.

[44] Liang, Y.; Wu, Y.; Feng, D.; Tsai, S. T.; Son, H. J.; Li, G.; Yu, L. *J. Am. Chem. Soc.* 2009, *131*, 56-57.

[45] Chan, S. H.; Chen, C. P.; Chao, T. C.; Ting, C.; Lin, C. S.; Ko, B. T. *Macromolecules* 2008, *41*, 5519-5526.

[46] Mammo, W.; Admassie, S.; Gadisa, A.; Zhang, F.; Inganas, O.; Andersson, M. R. *Sol. Energy Mater. Sol. Cells* 2007, *91*, 1010-1018.

[47] Song, S.; Jin, Y.; Kim, S. H.; Shim, J. Y.; Son, S.; Kim, I.; Lee, K.; Suh, H. *J. Polym. Sci. Polym. Chem.* 2009, 47, 6540.

[48] Froehlich, J. D.; Young, R.; Nakamura, T.; Ohmori, Y.; Li, S.; Mochizuk, A. *Chem. Mater.* 2007**,** *19*, 4991-4997.

[49] Jin, Y.; Kim, J.; Park, S. H.; Lee, K.; Suh, H. *Bull. Korean Chem. Soc.* 2005, 26, 795.

[50] Jin, Y.; Kim, K.; Song, S.; Kim, J.; Kim, J.; Park, S. H.; Lee, K.; Suh, H. *Bull. Korean Chem. Soc.* 2006, 27, 1043.

[51] Yang, Y.; Huang, Q.; Metz, A. W.; Ni, J.; Jin, S.; Marks, T. J.; Madsen, M. E.; DiVenere, A.; Ho, S-T. *Adv. Mater*. 2004, 16, 321-324.

[52] Jin, Y.; Kang, J. H.; Song, S.; Park, S. H.; Moon, J.; Woo, H. Y.; Lee, K.; Suh, *H. Bull. Korean Chem. Soc.* 2008, 29, 139.

[53] Tonzola, C. J.; Alam, M. M.; Bean, B. A.; Jenekhe, S. A. *Macromolecules* 2004, 37, 3554.

[54] Greenham, N. C.; Moratti, S.; Bradley, D. D. C.; Friend, R. H.; Holmes, A. B. *Nature* 1993, 365, 628.

[55] Friend, R. H.; Gymer, R. W.; Holmes, A. B.; Burroughes, J. H.; Marks, R. N.; Taliani, C.; Bradley, D. D. C.; Dos Santos, D. A.; Bredas, J. L; Logdlund, M.; Salaneck, W. R. *Nature* 1999, 397, 121.

[56] List, E. J. W.; Guentner, R.; De Freitas, P. S.; Scherf, U. *Adv. Mater.* 2002, 14, 374.

[57] Argun, A. A.; Aubert, P. H.; Thompson, B. C.; Schwendeman, I.; Gaupp, C.L.; Hwang, J.; Pinto, N.J.; Tanner, D. B.; MacDiarmid, A. G.; Reynolds, J. R. *Chem. Mater*. 2004,16, 4401–4412.

[58] Mortimer, R. J.; Dyer, A. L.; Reynolds, J.R. *Display*, 2006, 27, 2-18.

[59] Beaujuge, P.M.; Reynolds, J.R. *Chem. Rev.* 2010, 110, 268-320.

[60] Kelly, F.M.; Meunier, L.; Cochrane, C.; Koncar, V. *Displays* 2013, 34, 1-7.

[61] Muccini, M. *Nat. Mater*. 2006, 5, 605.

[62] Usta, H.; Facchetti, A.; Marks, T. J. *J. Am. Chem. Soc.* 2008, 130, 8580.

[63] Yang, C.; Kim, J. Y.; Cho, S.; Lee, J. K.; Heeger, A. J.; Wudl, F. *J. Am. Chem. Soc*. 2008, 130, 6444.

[64] Cho, S.; Seo, J. H.; Kim, S. H.; Song, S.; Jin, Y.; Lee, K.; Suh, H.; Heeger, A. *J. Appl. Phys. Lett.* 2008, 93, 263301.

[65] Burroughs, J. H. Et al. *Nature* 347, 539-541, 1990

[66] Braun, D.; Heeger, A. J. *Appl. Phys. Lett*. 1991, 58, 1982-1984.

[67] Chandrasekhar, P.; Zay, B. J.; Birur, G. C.; Rawal, S.; Pierson, E. A.; Kauder, L.; Swanson, T. *Adv. Funct. Mater.* 2002, 12, 95.

[68] Beaupré, S.; Breton, A.-C.; Dumas, J.; Leclerc, M. *Chem. Mater.* 2009, 21, 1504.

[69] Chandresekhar, P.; Zay, B. J.; McQueeney, T.; Scara, A.; Ross, D.; Birur, G. C.; Haapanen, S.; Kauder, L.; Swanson, T.; Douglas D. *Synth. Met.* 2003, 135-136, 23-24.

[70] Gerard, M.; Chaubey, A.; Malhotra, B. D. *Biosensors and Bioelectronics* 2002, 17, 5, 345-359.

[71] Arshak, K.; Velusamy, V.; Korostynska, O.; Oliwa-Stasiak, K.; Adley, C. *IEEE Sensors Journal,* 2009, 9, 12.

[72] Malitesta, C.; Losito, I.; Zambonin, P. G. *Anal. Chem.* 1999, 71, 1366 - 1370.

[73] John, R.; Spencer, M.; Wallace, G. G.; Smyth, M. R. *Anal. Chim. Acta* 1991, 249 381-385.

[74] Ng, K. K. *Complete Guide to Semiconductor Devices*, McGraw-Hill: New York, 1995.

[75] Kar, P. *Doping in Conjugated Polymers*, Ch. 1, pg 24, Wiley, 2013.

[76] Shirakawa, H.; Louis, E.J.; MacDiarmid, A.G.; Chiang C.K.; Heeger, A.J. *J Chem Soc Chem Comm* 1977, 579.

[77] Heeger, A. *Reviews of Modern Physics* 2001, 73**,** 3, 681.

[78] Rothberg, L.; Jedju, T. M.; Etemad S.; Baker, G. L. *Journal of Quantum Electronics* 1988, 24, 311-314.

[79] Bredas J. L.; Street, G. B. *Accounts of Chemical Research* 1985, 18, 309-315.

[80] Nigrey, P. J.; MacDiarmid, A. G.; Heeger, A. J. *J. Chem. Soc. Chem. Commun*. 1979, 594.

[81] Perepichka, F.; Perepichka, D. F.; Meng, H.; Wudl, F. *Adv. Mater*. 2005, 17, 1.

[82] S. Asavapiriyanont, G. K. Chandler, G. A. Gunawardena and D. Pletcher, *J. Electroanal. Chem.*, 1984, 177, 229.

[83] B. L. Funt and A. F. Diaz, *Organic Electrochemistry: an Introduction and a Guide*, Marcel Dekker, New York, 1991, 1337.

[84] Creager, S. *Solvents and Supporting Electrolytes in Handbook of Electrochemistry*. Zoski, C.G., Ed.; Elsevier: Amsterdam, 2007; pp. 51-64.

[85] Duan, C.; Huang, F.; Cao, Y. *J. Mater. Chem.* 2012, *22*, 10416.

[86] Zhou, H.; Yang, L.; You, W. *Macromolecules* 2012, *45*, 607.

[87] Jhuo, H. J.; Yeh, P. N.; Liao, S. H.; Li, Y. L.; Cheng, Y. S.; Chen, S. A. *J. Chin. Chem. Soc.* 2014, *61*, 115-126.

[88] Kularatne, R.-S.; Magurudeniya, H.-D.; Sista, P.; Biewer, M.-C.; Stefan, M.-C. *J. Polym. Sci. Part A: Polym. Chem.*2013, *51*, 743.

[89] Mortimer R.G. *Chem. Soc. Rev.* 1997, 26, 147.

[90] Abidin, T.; Zhang, Q.; Wang, K.; Liaw, D. *Polymer* 2014, 55, 21, 5293-5304.

[91] Sotzing G.A.; Reynolds J.R.; Steel P.J. *Chem. Mater.* 1996, 8, 882.

[92] Groenendaal L.B.; Friedrich J.; Freitag D.; Pielartzik H.; Reynolds J.R. *Adv. Mater.* 2000, 12, 481.

[93] Sonmez G.; Shen C.K.F.; Rubin Y.; Wudl F. *Angew. Chem. Int. Ed* 2004, 43, 1498.

[94] Sonmez G.; Sonmez H.B.; Shen C.K.F.; Jost R.W.; Rubin Y.; Wudl F. *Macromolecules*, 2005, 38, 669.

[95] Durmus A.; Gunbas G.; Camurlu P.; Toppare L. *Chem. Commun.* 2007, 3246.

[96] Durmus A.; Gunbas G.; Toppare L. *Chem. Mater.* 2007, 19, 6247.

[97] Durmus A.; Gunbas G.; Toppare L. *Adv. Mater.* 2008, 20, 691.

[98] Durmus A.; Gunbas G.E.; Toppare L. *Adv. Funct. Mater.* 2008, 18, 2026.

[99] Celebı S.; Balan A.; Epik B.; Baran D.; Toppare L. *Org. Electron.* 2009, 10, 631.

[100] Beaujuge P.M.; Ellinger S.; Reynolds J.R. *Adv. Mater.* 2008, 20, 2772.

[101] Cihaner A.; Algi F. *Adv. Func. Mater.* 2008, 18, 3583.

[102] Algı F.; Cihaner A.; *Org. Electron.* 2009, 10, 704.

[103] İçli M.; Pamuk M.; Algı F.; Cihaner A.; Önal A.M. *Chem. Mater.* 2010, 22, 4034.

[104] Beaujuge P.M.; Vasilyeva S.V.; Ellinger S.; McCarley T.D.; Reynolds J.R. *Macromolecules* 2009, 42, 3694.

[105] İçli-Özkut M.; Pamuk-Algi M.; Öztaş Z.; Algi F.; Önal A.M.;Cihaner A. *Macromolecules* 2012, 45, 729.

[106] İçli M.; Pamuk M.; Algi F.; Onal A.M.; Cihaner A. *Org. Electron.* 2010, 11, 1255.

[107] Beaujuge P.M.; Ellinger S.; Reynolds J. R. *Nat. Mater.* 2008, 7, 795.

[108] Oktem G.; Balan A.; Baran D.; Toppare, L. *Chem. Commun.* 2011, 47, 3933.

[109] Roncali, J.; Lemaire, M.; Garreau, R.; Garnier, F. *Synth. Met.* 1987, 18, 139.

[110] Chen, T. A.; Rieke, R. D. *J. Am. Chem. Soc*. 1992, 114, 10087.

[111] Chen, T. A.; Obrien, R. A.; Rieke, R. D. *Macromolecules*, 1993, 26, 3462.

[112] Chen, T. A.; Wu, X.; Rieke, R. D. *J. Am. Soc. Chem*. 1995, 117, 233.

[113] Bayer AG, Eur. Patent 339, 340, 1988.

[114] Dietrich, M.; Heinze, J.; Heywang, G.; Jonas, F. *J. Electroanal. Chem.*1994, 369, 87.

[115] Reynolds, J. R. *Chem. Mater.* 1998, 10, 896.

[116] Welsh, D. M.; Kumar, A.; Morvant, M. C.; Reynolds, J. R. *Synth. Met*. 1999, 102, 967.

[117] Stophan, O.; Schottland, P.; Le Gall, P.-Y.; Chevrot, C.; Mariet, C.; Carrier, M. J. *Electroanal. Chem.* 1998, 443, 217.

[118] Stophan, O.; Schottland, P.; Le Gall, P.-Y.; Chevrot, C. *J. Chim. Phys*. 1998, 95, 1168.

[119] Schottland, P.; Stophan, O.; Le Gall, P.-Y.; Chevrot, C. *J. Chim. Phys*. 1998, 95, 1258.

[120] Welsh, D. M.; Kumar, A.; Meijer, E. W.; Reynolds, J. R. *Adv. Mater.* 1999, 11, 1379.

[121] Welsh, D. M.; Kloeppner, L. J.; Madrigal, L.; Pinto, M. R.; Thompson, B. C.; Schanze, K. S.; Abboud, K. A.; Powell, D.; Reynolds, J. R. *Macromolecules*, 2002, 35, 6517.

[122] Reeves, B. D. Processable Disubstıtuted Poly(propylenedioxythiophenes, PhD Thesis, University of Florida, 2015, 202 pgs.

[123] Unver, E. K.; Tarkuc, S.; Udum, Y. A.; Tanyeli, C.; Toppare, L. *J. Polym. Sci. Part A: Polym. Chem.* 2010, 48, 1714-1720

[124] Unver, E. K.; Tarkuc, S.; Udum, Y. A.; Tanyeli, C.; Toppare, L. *Org. Electron*. 2011, 12, 1625-1631.

[125] Akbasoglu, N.; Balan, A.; Baran, D.; Cirpan, A.; Toppare, L. *J. Polym. Sci. Part A: Polym. Chem.* 2010, 48, 5603-5610;

[126] Sendur, M.; Balan, A.; Baran, D.; Karabay, B.; Toppare, L. *Org. Electron*. 2010, 11, 1877-1885.

[127] İçli Özkut, M. Color engineering of π-conjugated donor-acceptor systems: the role of donor and acceptor units on the neutral state color, Ph.D.thesis, Department of Chemistry, METU, July 2011, 179 pgs.

[128] Gibson, G. L.; McCormick, T. M.; Seferos, D. S. *J. Phys. Chem.* 2013**,** 117, 16606-16615.

[129] Duan, C.; Huang, F.; Cao, Y. *J. Mater. Chem*., 2012, 22, 10416-10434.

[130] Blouin, N.; Michaud A.; Leclerc, M. *Adv. Mater*. 2007, 19, 2295–2300.

[131] Nie, W.; MacNeill, C. M.; Li, Y.; Noftle, R. E.; Carroll D. L.; Coffin, R. C. *Macromol. Rapid Commun*. 2011, 32, 1163-1168.

[132] Yang, R.; Tian, R.; Yan, J.; Zhang, Y.; Yang, J.; Hou, Q.; Yang, W.; Zhang C.; Cao, Y. *Macromolecules*, 2005, 38, 244-253.

[133] Zhao, W.; Cai, W.; Xu, R.; Yang, W.; Gong, X.; Wu H.; Cao, Y. *Polymer* 2010, 51, 3196-3202.

[134] Zhang, L. J.; He, C.; Chen, J. W.; Yuan, P.; Huang, L. A.; Zhang, C.; Cai, W. Z.; Liu, Z. T., Cao, Y. *Macromolecules*, 2010, 43, 9771-9778.

[135] Song, S.; Jin, Y.; Park, S. H.; Cho, S.; Kim, I.; Lee, K.; Heeger A. J.; Suh, H. *J. Mater. Chem.* 2010, 20, 6517-6523.

[136] Ragno, G; Risoli, A.; Ioele, G.; Luca, M.; *Chem. Pharm. Bull.* 2006, 54, 6, 802-806.

[137] López-Rodríguez, M. L.; Benhamú, B.; Morcillo, M. J.; Tejada, I. D.; Orensanz, L.; Alfaro, M. J.; Martín, M. I. *J. Med. Chem.* 1999, 42, 5020-5028.

[138] Pérez-Villanueva, J.; Santos, R.; Hernández-Campos, A.; Giulianotti, M. A.; Castillo, R.; Medina-Franco, J. L. *Med. Chem. Commun*. 2011, 2, 44-49.

[139] Ahmadi, A. *Bulgarian Chemical Communications*, 2014, 46, 2, 245-252.

[140] Walia, R.; Hedaitullah, M.; Naaz, S. F.; Iqbal, K.; Lamba, H. *IJRPC* 2011, 1, 3, 575-578.

[141] Altıntop, M. D.; Mohsen, U. A.; Özkay, Y.; Demirel, R.; Kaplancıklı, Z. A. *Turk. J. Pharm. Sci.* 2015, 12, 1, 29-38.

[142] Yamamoto, T.; Sugiyama, K.; Kanbara, T.; Hayashi, H.; Etori, H. *Macromol. Chem. Phys.*1998, 199,1807-1813.

[143] Nurulla, I.; Morikita, T.; Fukumoto, H.; Yamamoto, T. *Macromol. Chem. Phys.* 2001, 202, 2335-2340.

[144] Akpinar H.; Balan, A.; Baran, D.; Unver, E. K.; Toppare, L. *Polymer* 2010, 51, 6123-6131.

[145] Akpinar, H.; Goycek Nurioglu, A.; Toppare, L. *J. of Electroanal. Chem.* 2012, 683, 62-69.

[146] Goycek Nurioglu, A.; Akpinar, H.; Ekiz Kanik, F.; Toffoli, D.; Toppare, L. *J. of Electroanal. Chem.* 2013, 693, 23-27.

[147] Ozelcaglayan, A. C.; Sendur, M.; Akbasoglu, N.; Apaydin, D. H.; Cirpan, A.; Toppare, L. *Electrochim. Acta* 2012, 67, 224-229.

[148] Zaifoglu, B.; Sendura, M.; Akbasoglu Unlu, N.; Toppare, L. *Electrochim. Acta* 2012, 85, 78-83.

[149] Song, S.; Park, S. H.; Jin, Y.; Kim, I.; Lee, K.; Suh, H. *Bull. Korean Chem. Soc.* 2011, 32, 8, 3045-3050.

[150] Song, S.; Park, S. H.; Jin, Y.; Kim, I.; Lee, K.; Suh, H. *Polymer* 2010, 51, 5385-5391.

[151] Song, S., Park, S. H.; Jin, Y.; Kim, J.; Shim, J. Y.; Goo, Y.; Jung, O.; Kim, I.; Leef, H.; Jeong, E. D.; Jin, J. S.; Lee, K.; Suh, H. *Synthetic Metals* 2011, 161, 307-312.

[152] Kim, J.; Park, S. H.; Kim, J.; Choc, S.; Kim, I.; Lee, K.; Suh, H. *Synthetic Metals* 2011, 161, 1336-1342.

[153] Song, S.; Kim, J.; Shim, J.; Kim, J.; Lee, B. H.; Jin, Y.; Kim, I.; Lee, K.; Suh, H. *Solar Energy Materials & Solar Cells* 2012, 98, 323–330.

[154] Kim, J.; Shim, J. Y.; Song, S.; Kim, J.; Kim, I.; Kim, J. Y.; Suh, H. *Macromolecular Research* 2015, 23, 2, 214-222.

[155] Emre, F. B.; Kesik, M.; Ekiz Kanik, F., Akpinar, H. Z.; Aslan-Gurel, E.; Rossi, R. M.; Toppare, L. *Synthetic Metals* 2015, 207, 102–109.

[156] Demirci Uzun, S.; Akbasoglu Unlu, N.; Sendur, M.; Ekiz Kanik, F.; Timur, S.; Toppare, L. *Colloids and Surfaces B: Biointerfaces* 2013, 112, 74-80.

[157] Tanimoto, A.; Shiraishi, K.; Yamamoto, T. *Bull. Chem. Soc. Jpn.* 2004, 77, 597-598.

[158] Nurulla, I.; Tanimoto, A.; Shraishi, K.; Sasaki, S.; Yamamoto, T.; *Polymer* 2002, 43, 1287-1293.

[159] Hedberg, F. L.; Marvel, C. S.; *J. Polym. Sci. Part A: Polym. Chem.* 1974, 12, 1823-1828.

[160] Kokelenberg, H.; Marvel, C. S. *J. Polym. Sci. Part A: Polym. Chem.* 1970, 8, 3199-3209.

[161] Higgins, J.; Marvel, C. S. *J. Polym. Sci. Part A: Polym. Chem.* 1970, 8, 171-177.

[162] Y. Tsubata, T. Suzuki, T. Miyashi, Y. Yamashita, *J. Org. Chem.* 1992, 57, 6749.

[163] Song, S.; Park, S. *Bull Korean Chem. Soc*. 2011, 32, 8, 3045.

[164] Q. Hou, Q. Zhou, Y. Zhang, W. Yang, R. Yang, Y. Cao, *Macromolecules* 2004, 37, 6299.

[165] Shin, W. S.; Kim, M.; Jin, S.; Shim, Y.; Lee, J.; Lee, J. W.; Gal, Y. *Mol. Cryst. Liq. Cryst.* 2006, 444, 129.

[166] Espinet, P.; Echavarren, A. M. *Angew. Chem. Int. Ed*. 2004, 43, 4704.

[167] Kosugi, M.; Sasazawa, K.; Shimizu, Y.; Migita, T. *Chem. Lett.* 1977, 301.

[168] Milstein, D.; Stille, J. K. *J. Am. Chem. Soc*. 1978, 100.

[169] Mabbott, G. A. *J. Chem. Educ.* 1983, 60, 9, 697.

[170] Zanello, P. *Inorganic Electrochemistry: Theory, Practice and Application*, 1st Ed., The Royal Society of Chemistry 2003, 606 pgs.

[171] Sanghavi, B. J.; Srivastava, A. K. *Electrochimica Acta* 2010, 55, 8638-8648.

[172] Dessie, Y.; Admassie, S. *Orient. J. Chem.* 2013, 29, 4, 1359-1369.

[173] Agudo, J. E.; Pardo, P. J.; Sánchez, H.; Pérez, A. L.; Suero, M. I. *Sensors* 2014, 14, 11943-11956.

[174] Beaujuge, P. M.; Reynolds, J. R. *Chemical Reviews* 2010, 110, 1, 268-320.

[175] Bechinger, C.; Burdis, M.S.; Zhang, J. G. *Solid State Commun.* 1997,101, 753-756.

[176] Wilson, H.R.; Raicu, A.; Nitz, P.; Ferber, J. *Proc. of Windows Innovation Conf.* 1995, Toronto, Canada, 5-6 June, 489.

[177] Lampert, C. M. *IEEE Circuits* and *Devices,* 1992, 19-26.

[178] Lampert, C.M. *Solar Energy Materials & Solar Cells* 2003,76, .489-499

[179] Lee, E.S.; Tavil, A. *Building and Environment* 2007, 42, 6, 2439-2449.

[180] Żmija, J.; Małachowski, M. J. *J. Of Achs. in Mat. And Man. Eng.* 2001, 48, 1, 14-23.

[181] Xu, L.Y.; Zhao, J.S.; Cui, C.S.; Liu, R.M.; Liu, J.F.; Wang, H.S. *Electrochim. Acta* 2011, 56, 2815 – 2822.

[182] Gibson, G. L.; McCormick, T. M.; Seferos, D. S. *J. Am. Chem. Soc.* 2012, 134, 1, 539–547.

[183] Kopczynski, M.; Ehlers, F.; Lenzer, T.; Oum, K. *J. Phys. Chem. A* 2007, 111, 5370-5381.

[184] Gibson, G. L.; McCormick, T. M.; Seferos, D. S. *Polym. Chem.* 2013, 4, 2457-2463.

[185] Pommerehne, J.; Vestweber, H.; Guss, W.; Mahrt, R. F.; Bässler, H.; Porsch, M.; Daub, J. *Adv. Mater.*1995, 7-6, 551–554.

[186] Tamilavan, V.; Song, M.; Agneeswari, R.; Kim, S.; Hyun, M. H. *Bull. Korean Chem. Soc.* 2014, 35, 4, 1098-1104.

[187] Sonmez, G.; Meng, H.; Wudl, F. *Chem. Mater*. 2004, 16, 574.

[188] Irvin, J. A.; Reynolds, J. R. *Polymer* 1998, *39*, 2339-2347.

[189] Sotzing, G. A.; Reynolds, J. R.; Steel, P. J. *Chem. Mater.* 1996, *8*, 882-889.

[190] Poverenov, E.; Zamoshchik, N.; Patra, A.; Ridelman, Y.; Bendikov, M. *J. Am. Chem. Soc.* 2014, 136, 5138−5149.

[191] Kumar, A.; Welsh, D. M.; Morvant, M. C.; Piroux, F.; Abboud, K. A.; Reynolds, J. R. *Chem. Mater.* 1998, 10, 896-902.

[192] Sankaran, B.; Reynolds, J. R. *Macromolecules* 1997, 30, 2582-2588.

[193] Galand, E. M.; Mwaura, J. K.; Argun, A. A.; Abboud, K. A.; McCarley, T. D.; Reynolds, J. R. *Macromolecules* 2006, 39, 7286-7294.

APPENDIX A

NMR DATA

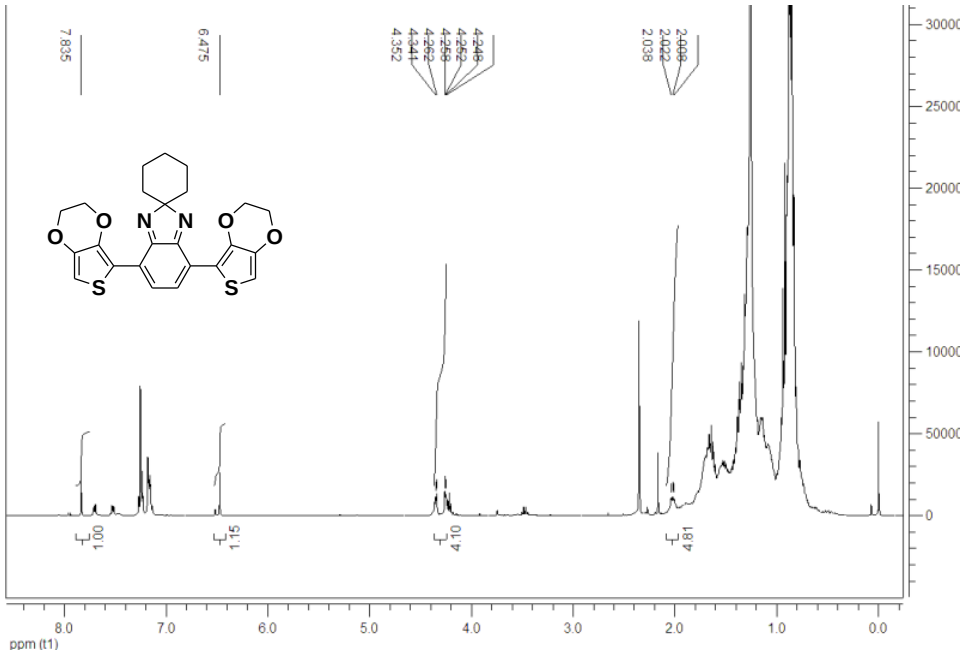

Figure A.1. [1]HNMR spectrum of E6E monomer.

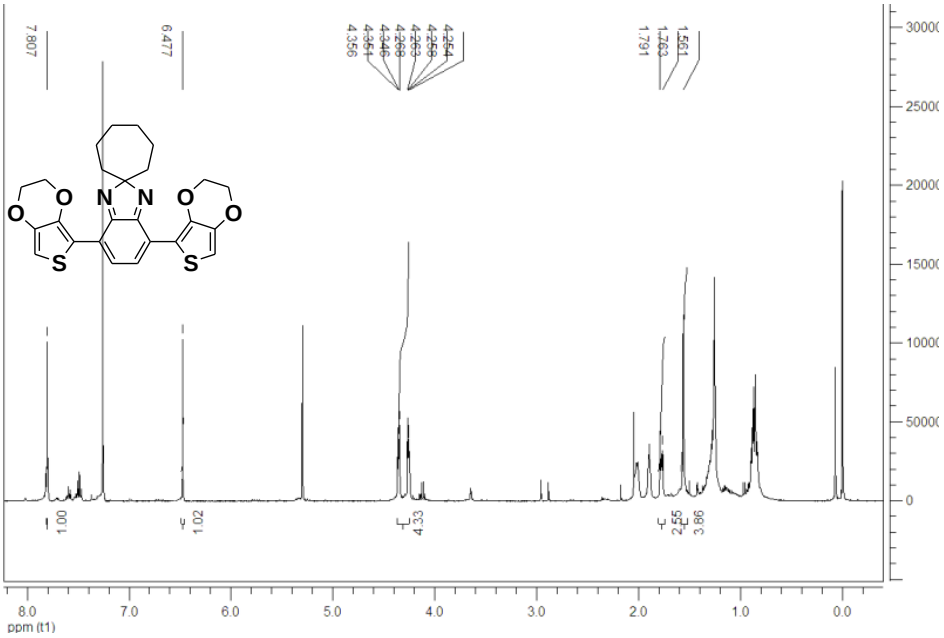

Figure A.2. [1]HNMR spectrum of E7E monomer.

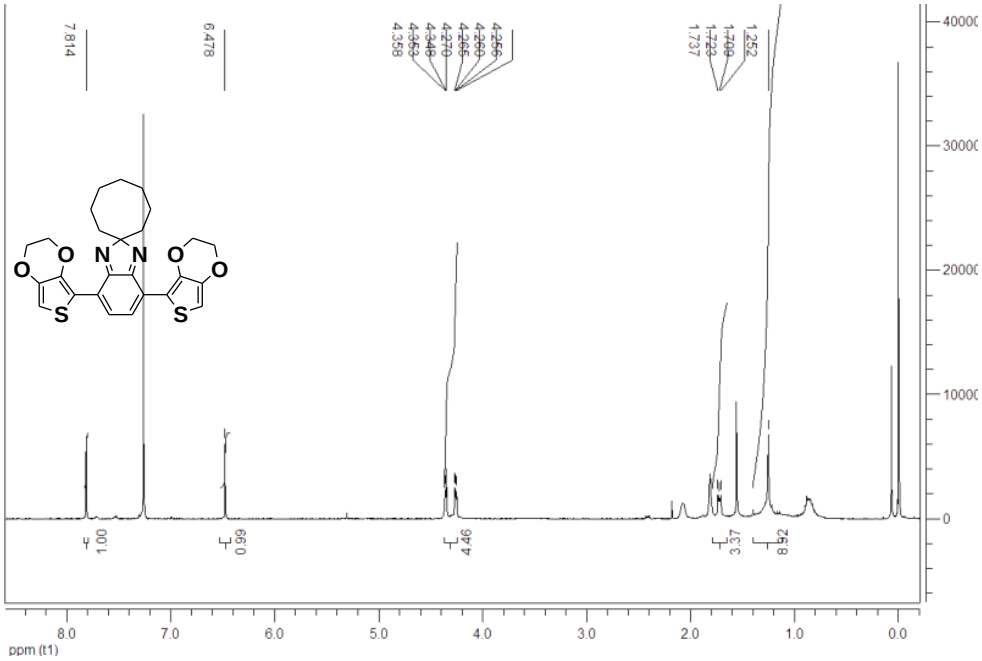

Figure A.3. [1]HNMR spectrum of E8E monomer.

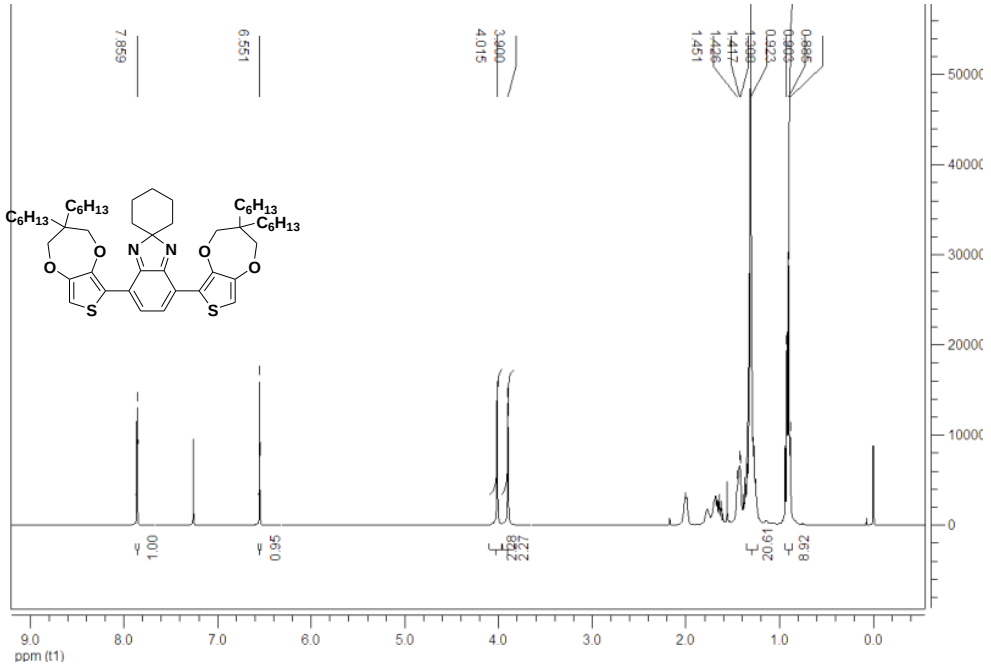

Figure A.4. [1]HNMR spectrum of P6P monomer.

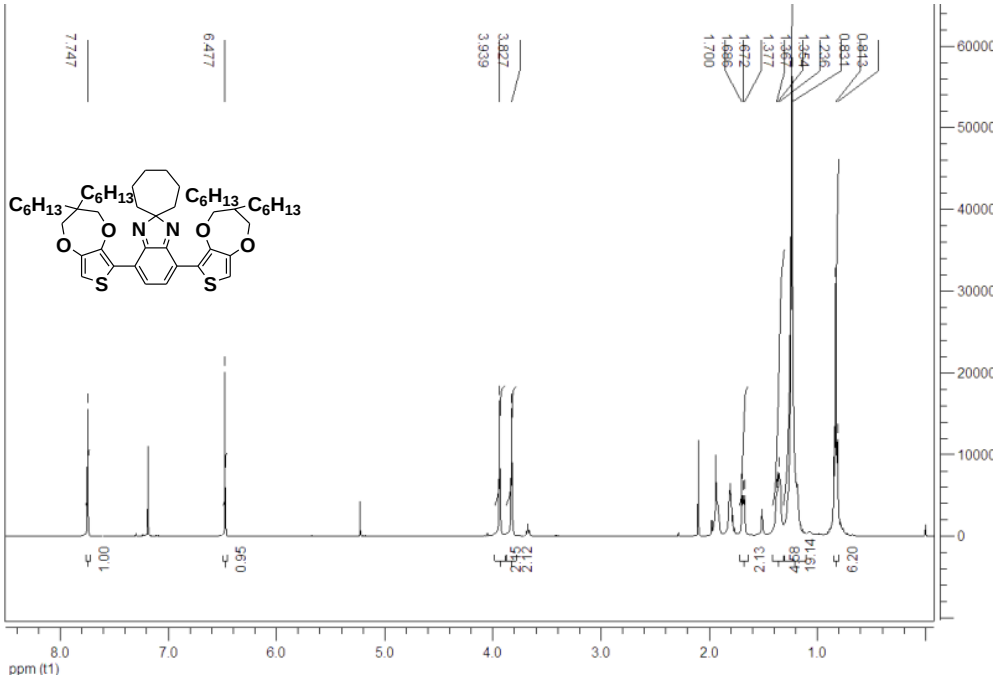

Figure A.5. [1]HNMR spectrum of P7P monomer.

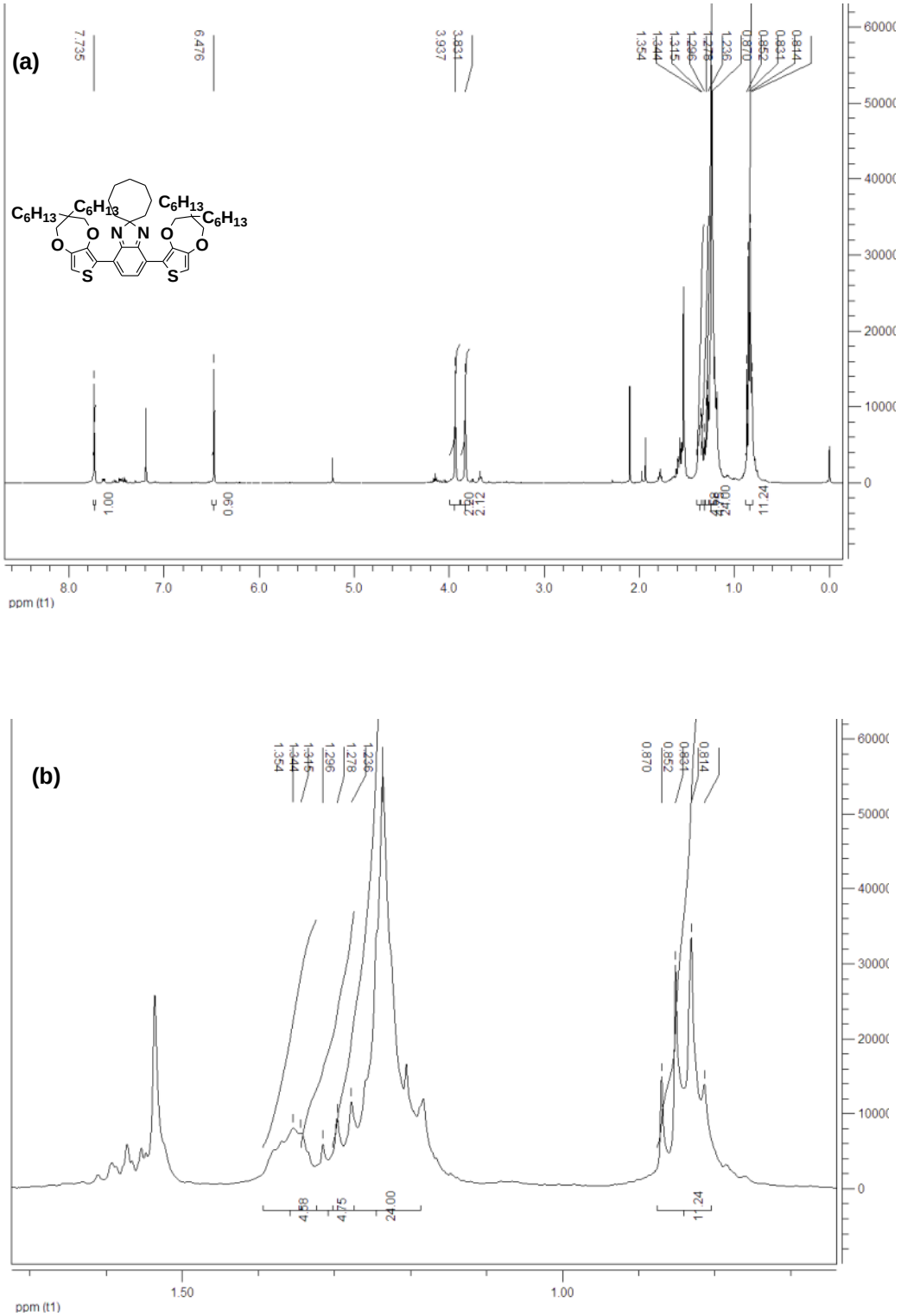

Figure A.6. [1]HNMR spectrum of P8P monomer **(a)** and the close look in the alkyl region of P8P **(b)**.

APPENDIX B

HRMS DATA

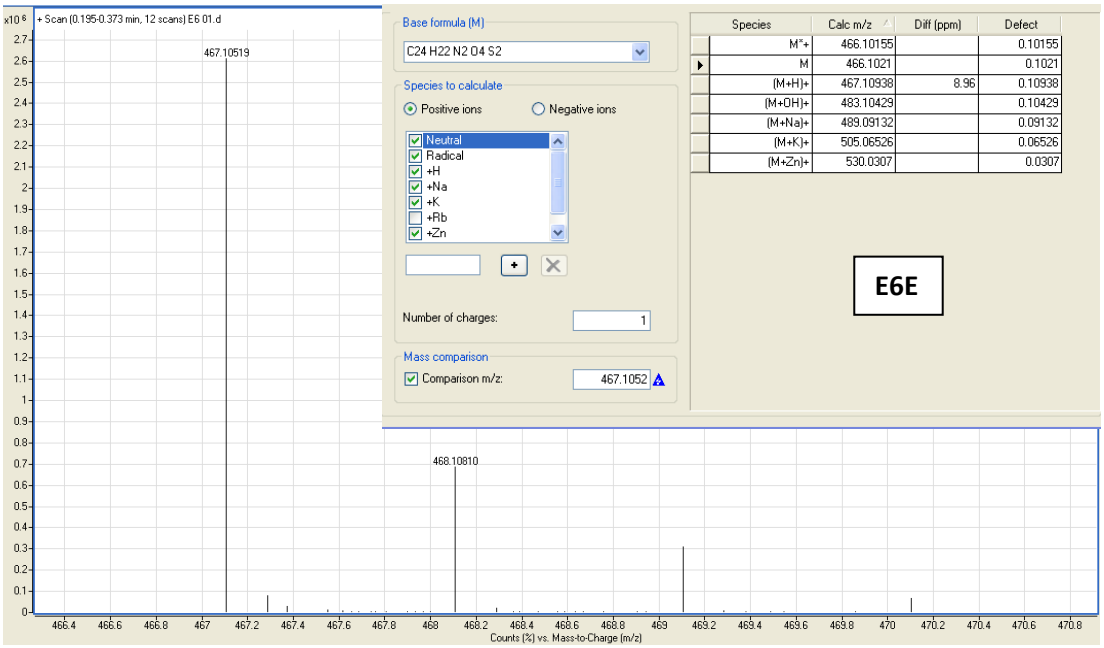

Figure B.1. HRMS report of E6E monomer.

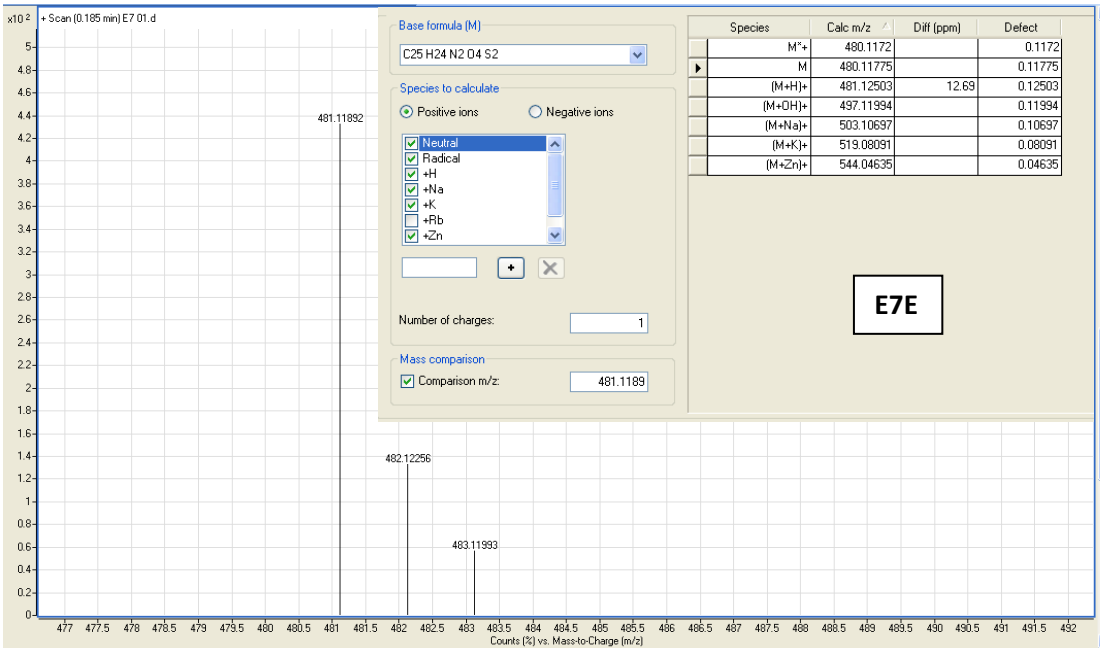

Figure B.2. HRMS report of E7E monomer.

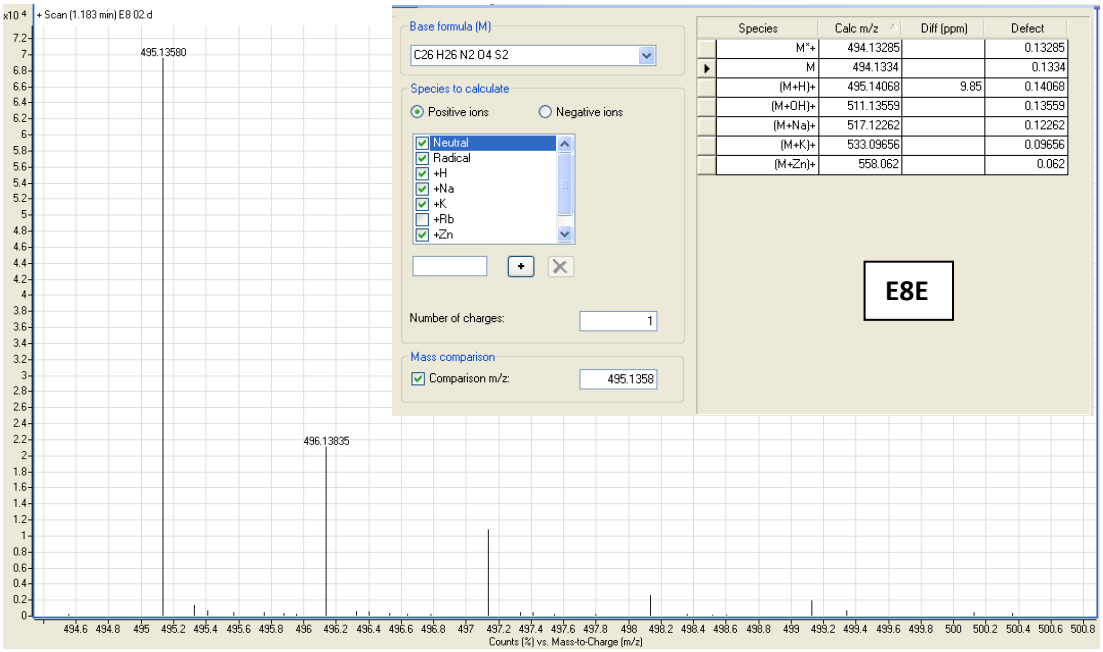

Figure B.3. HRMS report of E8E monomer.

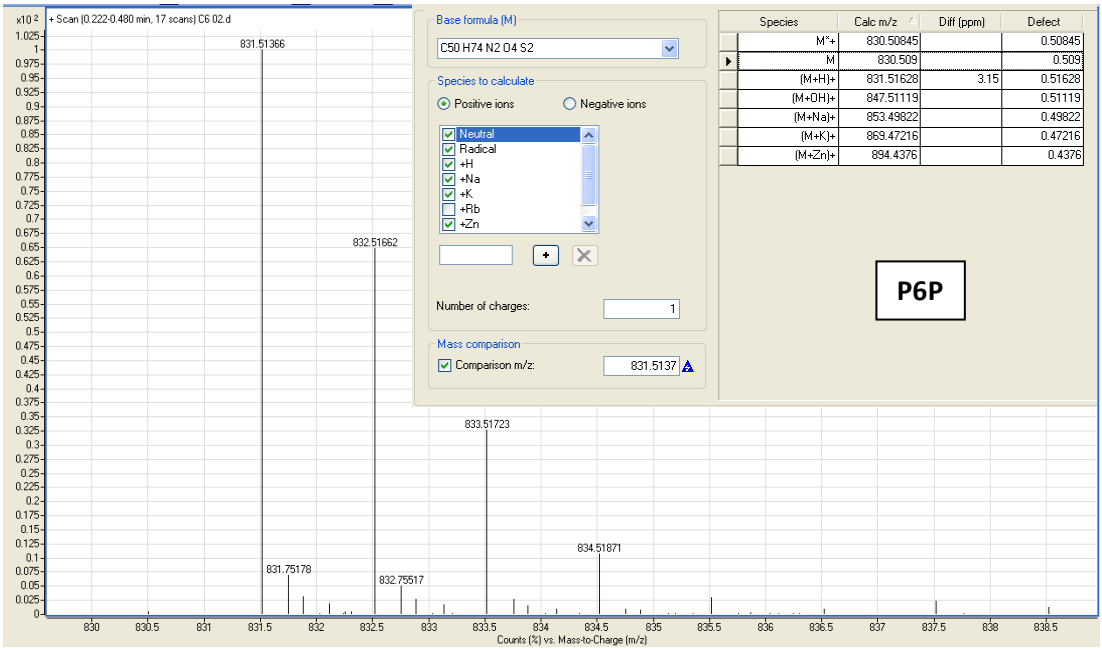

Figure B.4. HRMS report of P6P monomer.

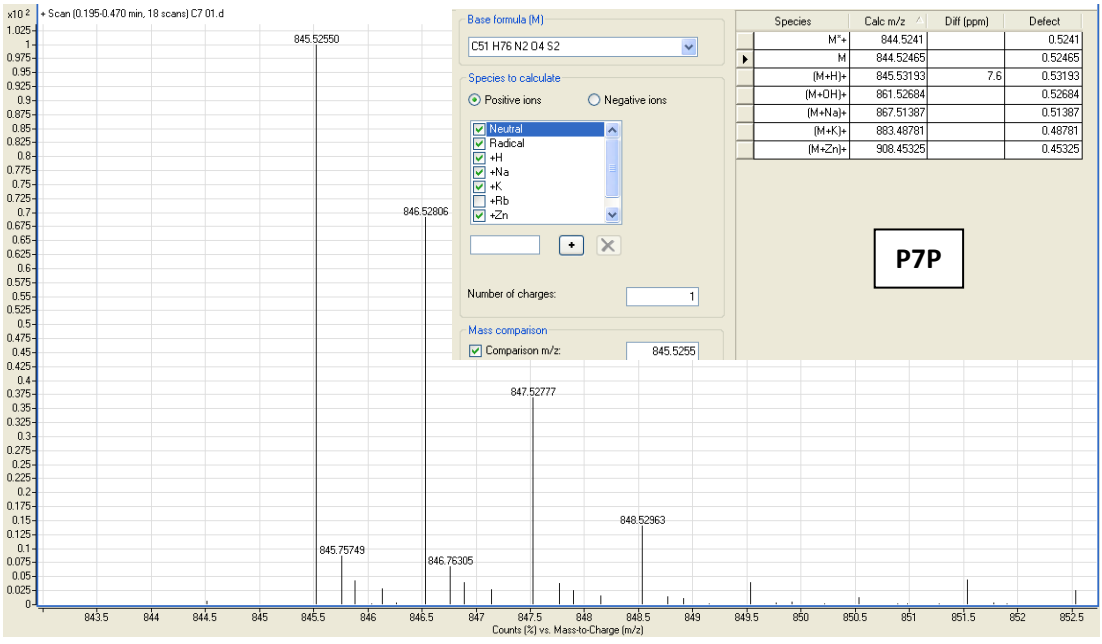

Figure B.5. HRMS report of P7P monomer.

APPENDIX C

UV-VIS SPECTRA OF THE ACCEPTORS

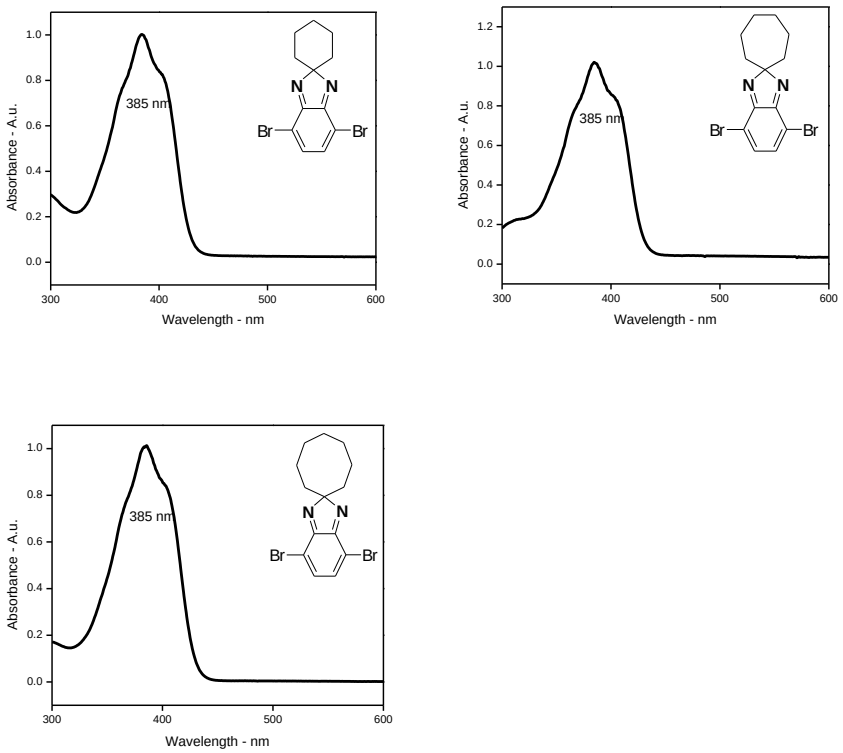

Figure C.1. Optical absorption spectra of the acceptor groups.

CURRICULUM VITAE

CANSU ERGÜN, EMİNE GÜL

PERSONAL INFORMATION

Date and Place of Birth : 05.03.1976 - BAFRA
Address : Atılım University, Department of Chemical Engineering and Applied Chemistry, 06836, Gölbaşı, ANKARA.

EDUCATION

- 2015 August – PhD degree in Polymer Science and Technology
  Middle East Technical University – METU
  Ankara, Turkey
- 2010 July – MSc degree in Chemistry
  Ankara University, Ankara, Turkey
- 1998 June – BSc degree in Chemistry Education
  Middle East Technical University – METU
  Ankara, Turkey

PROFFESSIONAL EXPERIENCE

- Research assistant at Atılım University (from 2009 – still working)

PUBLICATIONS

- Cansu-Ergun, E. G.; Cihaner, A. New carborane based polymeric electrochrome *Journal of Electroanalytical Chemistry* 2013, 707, 78-84.
- Algi, M. P.; Tirkes, S.; Ertan, S.; Cansu Ergun, E. G.; Cihaner, A.; Algi, F. Design and synthesis of new 4,4_-difluoro-4-bora-3a,4a-diaza-s-indacene based electrochromic polymers *Electrochimica Acta* 2013, 109, 766-774.
- Cansu-Ergun, E. G.; Cihaner, A. Electro-optical properties of poly[di(2-thiophenyl)carborane] and its opto-electronic application *Materials Chemistry and Physics* 2013, 143, 387-392.

CONFERENCES

- A Carborane Based New Electrochromic Polymer, 4th National Polymer Science and Technology Congress (Oral Presentation), 2012, Çanakkale, Turkey.
- Properties Of A New Conjugated Copolymer With Different Feed Ratios, (Oral Presentation), 10th International Electrochemistry Meeting, 2013, Konya, Turkey.
- A new Carborane Based Conjugated Copolymer, IUPAC-44th Word Chemistry Congress (Poster Presentation), 2013, Istanbul, Turkey.
- Dithienosilole Type Electrochromic Copolymer: Synthesis and Characterization, 5th National Polymer Science and Technology Congress (Oral Presentation), 2014, Konya, Turkey.